TUNABLE-Q WAVELET TRANSFORM BASED METHODOLOGIES FOR ANALYSIS AND CLASSIFICATION OF CARDIAC SIGNALS

Ph.D. Thesis

By

SHIVNARAYAN PATIDAR

DISCIPLINE OF ELECTRICAL ENGINEERING

INDIAN INSTITUTE OF TECHNOLOGY INDORE

NOVEMBER 2014

TUNABLE-Q WAVELET TRANSFORM BASED METHODOLOGIES FOR ANALYSIS AND CLASSIFICATION OF CARDIAC SIGNALS

A THESIS

Submitted in partial fulfillment of the

requirements for the degree

of

DOCTOR OF PHILOSOPHY

by

SHIVNARAYAN PATIDAR

DISCIPLINE OF ELECTRICAL ENGINEERING

INDIAN INSTITUTE OF TECHNOLOGY INDORE

NOVEMBER 2014

INDIAN INSTITUTE OF TECHNOLOGY INDORE

CANDIDATE'S DECLARATION

I hereby certify that the work which is being presented in the thesis entitled " **TUNABLE-Q WAVELET TRANSFORM BASED METHODOLOGIES FOR ANALYSIS AND CLASSIFICATION OF CARDIAC SIGNALS**" in the partial fulfillment of the requirements for the award of the degree of DOCTOR OF PHILOSOPHY and submitted in the DISCIPLINE OF ELECTRICAL ENGINEERING, Indian Institute of Technology Indore, is an authentic record of my own work carried out during the time period from July 2011 to November 2014 under the supervision of Dr. Ram Bilas Pachori, Associate Professor, Indian Institute of Technology Indore, India.

The matter presented in this thesis has not been submitted by me for the award of any other degree of this or any other institute.

Signature of the student with date

(SHIVNARAYAN PATIDAR)

This is to certify that the above statement made by the candidate is correct to the best of my knowledge.

Signature of Thesis Supervisor with date

(DR. RAM BILAS PACHORI)

SHIVNARAYAN PATIDAR has successfully given his Ph.D. Oral Examination held on

Signature(s) of Thesis Supervisor(s) Convener, DPGC

Date: Date:

Signature of PSPC Member:1 Signature of PSPC Member:2 Signature of External Examiner

Date: Date: Date:

Dedicated to my family

Acknowledgements

I am immensely grateful to my supervisor Dr. Ram Bilas Pachori for his invaluable guidance, encouragement and direction throughout this work. Working with him ultimately resulted into a great deal of enjoyment in my dissertation research.

I would like to thank Dr. Niranjan Garg from Department of Cardiology, RD Gardi Medical College Ujjain, India for his helpful discussions, encouragement and directions throughout this work. I would also like to thank Prof. U.R. Acharya, Ngee Ann Polytechnic, Singapore, for providing dataset and valuable suggestions to successfully conduct research work on coronary artery disease. I would like to express my heartfelt gratitude towards my PSPC committee members Dr. Srivathsan Vasudevan and Dr. Anand Parey for their interesting discussions and suggestions towards my research.

I am truly thankful to Dr. Santosh Kumar Vishvakarma and Dr. Amod C. Umarikar for their helpful discussions and invaluable support. Finally, I want to thank everyone who have, in one way or another, helped me to conduct this research. I express my appreciation and indebtedness to my friends Keshav Patidar, Dheeraj Sharma, Varun Bajaj, Hari Mohan Kushwaha, Suneel Yadav, Abhay Upadhyay, Rajeev Sharma, Vikas Vijayvargiya, Pooran Singh, and Pooja Jain who helped me in many ways during my thesis work.

My daughter's birth was auspicious sign of my immediate selection to PhD program. Moreover, whatever little I have achieved in my life, the credit goes to my family members: grand parents, parents, my wife and my daughter to whom I take great pride in dedicating this thesis. They have always been a source of inspiration for me and have kept trust and faith in whatever I did. Last but not the least, I would also like to thank God for showering me his blessings since my childhood.

SHIVNARAYAN PATIDAR

Abstract

After cancer, heart disorders are the second major cause of mortality and morbidity around the globe. The heart valve disorders, septal defects and coronary artery disease are the most commonly occurring heart disorders. Timely diagnosis of heart disorders is generally required for prevention and treatment of these disorders to ensure contented, happier and longer life of patients.

The cardiac auscultation and electrocardiogram (ECG) are the important means of assessing the activity of cardiovascular system. These procedures are commonly used for reliable diagnosis of heart disorders. Heart disorders especially heart valves cause changes or additional sounds to normal heart sounds that can be useful for diagnosis. These heart sounds can be analysed non-invasively using traditional cardiac auscultation with conventional stethoscope. However, analysing these heart sounds by listening, requires sophisticated interpretive skills and expertise in diagnosis. Moreover, the heart sounds often last for a short period of time and pathological splitting of the heart sound is difficult to judge because human ears lack desired sensitivity towards heart sounds and murmurs. The cardiac sound signals represent digital recording of the heart sounds by placing an electronic stethoscope at the appropriate location on the subject's chest. These signals can be used to extract valuable diagnostic features for diagnosis of the heart valve disorders.

Electrocardiography is also a non-invasive measure of the electrical activity of the heart against time. It records electrical potentials of the contractile heart cells by placing electrodes on the surface of the chest and on the limb. Generally, electrocardiography involves recording of ECG waveform onto a graph paper that runs at a constant speed or visual display on a screen. ECG waveform analysis is carried out by evaluating the morphological changes in shape, amplitude, period, segments, and intervals. The subtle changes in these features of ECG waveforms cannot be deciphered precisely on visual inspection. Moreover, the clinical interpretations of ECG waveform are based on observation or experimental knowledge. On the other hand, the digitally recorded ECG signals can provide valuable diagnostic features for automatic diagnosis of the CAD.

In recent years, with the development of many advanced signal processing and medical artificial intelligence technologies, a huge potential exist for development of efficient, informative and accurate state of the art computer-aided diagnostic tool for heart valve and other heart disorders. Therefore, cardiac signals based computer aided diagnosis can be a promising and cost effective technology for prompt, noninvasive, convenient and efficient diagnosis of heart disorders.

The aim of this thesis work has been to develop advanced signal processing based methods for automatic diagnosis of heart disorders using cardiac sound signals and ECG signals. Implementation of such diagnostic systems based on cardiac sound signals involves the primary stage of segmentation of cardiac sound signals into heart beat cycles. This is then followed by analysis and extraction of suitable diagnostic features from the segmented heart beat cycles for final development of pattern classification process to classify a set of cardiac sound signals. In case of diagnostic systems based on ECG signals, pre-processing involving removal of noises, artifacts like baseline wondering etc., feature extraction and classification are general steps to implement.

The compression of cardiac sound signals can further help in data archiving and telemedicine application for convenient diagnosis of heart disorders. The compression algorithm can reduce the power consumption in wireless sensor networks for better long term monitoring intended for telemedicine applications.

In particular, the work in this thesis, focuses on development of advanced signal processing based methodologies for segmentation and classification of cardiac sound signals to automatically diagnose the heart valve and septal defects. The development of methodology for automatic diagnosis of CAD using ECG based heart rate signals is the centre of interest. Moreover, this work also focuses on the compression of cardiac sound signals for data archiving and telemedicine application to improve the bandwidth and the storage efficiency for convenient diagnosis of heart disorders. The details of these proposed methodologies in this work can be described as follows:

The automatic segmentation of cardiac sound signals into heart beat cycles is generally

required for the diagnosis of heart valve disorders. As the first main part of this thesis, the segmentation of the cardiac sound signals using tunable-Q wavelet transform (TQWT) has been performed as follows. The murmurs from cardiac sound signals have been removed by suitably constraining TQWT based decomposition and reconstruction. The Q-factor, redundancy parameter and number of stages of decomposition of the TQWT have been adapted to the desired statistical properties of the murmur-free reconstructed cardiac sound signals. The envelope based on cardiac sound characteristic waveform (CSCW) has been extracted after the removal of low energy components from the reconstructed cardiac sound signals. Then the heart beat cycles have been derived from the original cardiac sound signals by mapping the required timing information of CSCW which is obtained using established methods. The experimental results are included in order to show the effectiveness of the proposed method for segmentation of cardiac sound signals in comparison with other existing methods for various clinical cases.

The features extracted from the cardiac sound signals are commonly used for detection and identification of heart valve disorders. As the second main part of this thesis, a new method for classification of cardiac sound signals using constrained tunable-Q wavelet transform (TQWT) has been proposed. The proposed method begins with a constrained TQWT based segmentation of cardiac sound signals into heart beat cycles. The features obtained from heart beat cycles of separately reconstructed heart sounds and murmur can better represent the various types of cardiac sound signals than that from containing both. Therefore, heart sounds and murmur have been separated using constrained TQWT. Then the proposed novel raw feature set has been created by the parameters that have been optimized while constraining the output of TQWT and that of extracted by using time-domain representation and Fourier-Bessel (FB) expansion of separated heart sounds and murmur. However, the adaptively selected features have been used to obtain the final feature set for subsequent classification of cardiac sound signals using least squares support vector machine (LS-SVM) with various kernel functions. The performance of the proposed method has been validated with publicly available datasets and the results have been compared with the existing short-time

Fourier transform (STFT) based method. The proposed method shows higher percentage classification accuracy of 94.01 as compared to 93.53 of STFT based method. In comparison with STFT based method, it is noteworthy that the proposed method uses well defined and lower dimensionality of feature vector that can reduce the computational complexity.

In view of accurate and quick diagnosis of septal defects, automatic analyses of cardiac sound signals can be performed by using advanced signal processing methods. Therefore, as a third main part of this thesis, a new method for diagnosis of septal defects from cardiac sound signals using TQWT based features has been proposed. To start with, the established constrained TQWT based approach has been used in this study to derive the heart beat cycles from cardiac sound signals. Then the TQWT based decomposition of segmented heart beat cycles have been performed up to a certain level. The combinations of sub-bands obtained during TQWT based decomposition can be used to extract the diagnostic features. The correlation between sub-bands can characterize the various types of murmurs in cardiac sound signals. Therefore, in order to represent the murmurs in cardiac sound signals, proposed feature set was created with sum of average magnitude difference function (SAMDF) that have been computed from reconstruction of decomposed sub-bands. In search of effective feature set based on SAMDF, various decomposition levels have been examined that could provide significant classification performance. Moreover, in order to establish the usefulness of the proposed method for diagnosis of septal defects, besides cardiac sound signals for septal defects and normal, this study covers signals to be detected for valvular defects and other defects like ventricular hypertrophy, constrictive pericarditis etc as available from publicly available datasets. The classification has been performed using LS-SVM with different kernel functions. At each decomposition level under study, the effect of quality-factor (Q) of the TQWT from 1 to 50 on classification performance has been evaluated. The experimental results show that the proposed method has provided significant classification performance with tenth levels of decomposition for all the values of Q in the given range using Morlet wavelet kernel function. The test results demonstrate classification accuracy of 98.92% with sensitivity of 98.80% specificity of 99.29% and Matthews correlation coefficient

of 0.9684 at tenth levels of decomposition for $Q = 6$. Moreover, in order to show the effectiveness of the proposed method, results have been compared with existing method.

Analysis of ECG based heart rate signals using advanced signal processing methods can lead to efficient automatic diagnosis of CAD. In view of this, the fourth main part of this thesis present a new method for diagnosis of CAD using TQWT based features from heart rate signals obtained from ECG signals. The time-frequency/scale domain can provide more insightful view of the subtle changes in heart rate signals that are indicative of any particular heart disorder. Hence, the heart rate signals have been decomposed into various sub-bands using TQWT for better diagnostic feature extraction. The nonlinear and nonstationary biomedical signals can be successfully analysed and classified using nonlinear parameters. The correntropy is a nonlinear correlation function that can transforms the sub-band signals into high dimensional space using kernel function in turn providing useful feature space. Therefore, in order to represent the heart rate signals of normal and CAD conditions, proposed raw feature set was created with centered correntropy (CCo) that has been computed from particular decomposed detail sub-band. The principal component analysis (PCA) has been applied to obtain the final feature set using the linear combination of the raw features. This features set has been used to perform classification using LS-SVM with different kernel functions. In search of effective feature set based on CCo, various values of Q have been examined that could provide significant classification performance. The experimental results demonstrate highest classification accuracy, sensitivity, specificity and Matthews correlation coefficient for $Q = 24$ using Morlet wavelet kernel function with optimized kernel and regularization parameters. In addition, the proposed methodology has been found more suitable in classification of normal and CAD heart rate signals in comparison to other previous methods.

As the last main part of this thesis, a new method for compression of cardiac sound signals using TQWT to improve the bandwidth and the storage efficiency for convenient diagnosis of heart disorders. In the proposed method, the cardiac sound signals have been compressed using TQWT, linear quantization, Huffman and run length coding (RLC) techniques. As the

compression depends on various parameters, therefore the optimal values of these parameters have been found using genetic algorithm (GA) with a subset of dataset. The proposed compression method has provided significant performance with lower distortion when evaluated using a test set. Moreover, the obtained results have been found comparatively better than that of an existing wavelet (WT) based method due to the properties of TQWT and the resulting increased number of compression parameters for optimization. The proposed algorithm can reduce the power consumption in wireless sensor networks for better long term monitoring intended for telemedicine applications.

Contents

List of Figures

List of Tables

List of Abbreviations and Symbols

TQWT: Tunable-Q wavelet transform

FHS: Fundamental/primary heart sounds

SDOF: Single-degree-of-freedom

ECG: Electrocardiogram

WT: Wavelet transform

GA: Genetic algorithm

SSA: Adaptive singular spectrum

CSCW: Cardiac sound characteristic waveform

STFT: Short-time Fourier transform

DCT: Discrete cosine transform

SVM: Support vector machine

HMM: Hidden Markov model

MFCC: Mel-frequency cepstral coefficient

SVD: Singular value decomposition

FB: Fourier-Bessel

LS-SVM: Least squares support vector machine

OAO: One-against-one

RBF: Radial basis function

CWT: Continuous wavelet transform

KNN: k-nearest neighbors classifier

ANN: Artificial neural network

db: Daubechies

EEG: Electroencephalogram

TQWD: TQWT based decomposition

PRD: Percentage root mean square difference

WPT: Wavelet packets transform

RLC: Run length coding

Q: Q-factor

r: Over-sampling rate or redundancy of TQWT

j: Number of levels of TQWT based decomposition

THV: Threshold

C_{rate}: Compression rate

CAD: Coronary artery disease

CCo: Centered correntropy

PCA: Principal component analysis

CTA: Computed tomography angiogram

PSD: Power spectral density

Chapter 1

Introduction

The heart sounds and ECG are widely used for cardiac examination. The stethoscope has been a symbol of medical profession for a long time since its invention in 1816 by René Laennec, a French physician [2]. Physicians have relied on stethoscope based cardiac auscultation as a non-invasive primary diagnostic procedure for detection and characterization of heart disorders. However, the recent advances in cardiac imaging have led to the use of sophisticated technologies like echocardiography, magnetic resonance imaging etc. for diagnosis of heart disorders. Irrespective of their higher cost, these modalities have become so dominating in cardiac assessment that the use of traditional cardiac auscultation has shown a marked declining trend because of the following aspects. Traditional cardiac auscultation requires sophisticated skills and long-term experience. The human ear is far more sensitive to the speech having frequencies in the range 1000-2000 Hz than to higher and lower frequencies. It lacks desired sensitivity towards heart sounds and murmurs [3, 4, 5]. In addition, the short period of heart sounds and pathological splitting of the heart sound make it difficult to produce any decision on presence of heart disorders [6]. The poor auscultatory skills of the primary care clinicians have been documented in the primary screen examination due to lack of effective educational support [7]. Consequently, traditional cardiac auscultation is not performed properly in the primary health care and all the subjects showing symptoms other than normal auscultatory findings are sent to a cardiologist for further investigations [8, 9].

ECG has become a common diagnostic procedure for heart disorder since the 1940s [10]. It was first realised by an English physiologist August Waller in 1887. However, it was W. Einthoven, who recorded the first ECG waveform with a string galvanometer in 1902 [10]. There has been a significant development on ECG based diagnosis such as exercise test ECG, Holter ECG, monitoring of patients in intensive care, high resolution electrocardiography etc. The ECG based diagnosis is quite promising and requires minor changes in the ECG recordings to detect specific heart disorders. However, in many cases, visual analysis of ECG recordings for detecting CAD is not reliable because it is difficult to notice the differences in recordings. The presence of noises and artifacts like baseline wondering make it complex to accurately analyse the small morphological changes in the ECG recordings due to heart disorders. While undergoing tread mill stress tests, patients are at risk of developing tachycardia and eventual heart failure. The cardiac catheterization is performed invasively and takes an average time of thirty minutes. However, overall time including the preparation and recovery time amounts to several hours. This leads to almost whole day for patients to do this test. Most of the imaging modalities can be operated only by trained physicians or radiologists. Some of the above mentioned diagnostic tools are quite expensive and their availability is limited to health care centers in urban areas.

In a world where modern health care is striving for cost effective point-of-care medical technology, it is now time to upgrade the traditional cardiac auscultation and ECG interpretation. Therefore, the automatic heart sound and ECG analysis using advanced signal processing techniques based on digital acquisition of these signals has a lot of potential in cardiac health care [11].

1.1 Background

1.1.1 The Nature of Cardiac Signals

The properties of nonlinear and non-stationary cardiac sound signals and ECG signals can be described as follows:

1.1.1.1 The Nature of Cardiac Sound Signals

The cardiac sound signals are the traditional biomedical signals that carry a lot of information about the structure and functioning of cardiovascular system [12]. These signals are basically caused by the contractile activity of the cardiohemic system that consists of the heart and blood together [12, 13, 14, 15]. The recording of cardiac sound signals involves placement of sensor on the chest that converts the heart sound into electronic signal. The cardiac sound signals may consist of two types of components, the heart sounds and the murmur. The heart sounds and murmur are low frequency and high frequency components respectively. However, the intensity, frequency content and timings of the heart sounds and murmur vary with affected type of heart valves and other parts of heart, type of defect, degree of defect, heart rate and blood velocity. The heart beat cycles of normal cardiac sound signals are mostly composed of two types of sound: S1 and S2 heart sounds which are referred as primary heart sounds. The S1 and S2 heart sounds exhibit predominant frequencies in the range 20-150 Hz [15]. The presences of other sounds that may be indicative of cardiac pathology are murmurs, two feeble S3 and S4 heart sounds and other irregularities due to different pathologies of the cardiovascular system. The average murmurs have frequencies in the range 100-600 Hz [16]. The frequencies of S3 and S4 heart sounds lie in the range 20-70 Hz [15]. These heart sounds have comparatively lower amplitude to that of primary heart sounds. The presence of S3 heart sound could be a sign of heart disorder. Generally, S4 heart sound is always considered to be associated with cardiac abnormality.

In spite of the heart sounds and murmur, cardiac sound signals may contain the ambient noise, respiratory sounds, bowel sounds and other undesired noises such as rubbing of stethoscope on the subjects chest surface, voices etc. These undesired components needs to be dealt properly in carrying out accurate analysis of cardiac sound signals [17, 18, 19]. The respiratory artifacts occupy frequencies less than 100 Hz to over 300 Hz [20].

1.1.1.2 The Nature of ECG Signals

The ECG signal carries potential information about chemical, electrical and mechanical events of the heart that generally occurs during pumping action of the heart. Many commonly occurring cardiovascular diseases manifest themselves in the altered shape of ECG signal. The medical experts consider the diagnostic morphological features of the ECG signal to assess the functioning of the heart and its muscles. The pumping action of the heart in terms of beats per minute (bpm) can be measured by counting the easily identifiable repeating waves in ECG signals. Generally, the ECG based cardiovascular assessment is done in an empirical manner based on the existing knowledge and acquired experience. Some defined characteristic segments or waves, points, and parameters of the ECG signal are used for diagnostic evaluation of the heart. In medical diagnostic decision making, the relationships between morphological features of ECG signal and the functioning of the heart are often expressed with some logical clinical terms or expressions. The terms such as "extended R wave," "shortened QT interval," "unclear Q wave," elevated ST segment," "low T wave," etc. are very common. These terms can be used as fuzzy logics. For example, in myocardial infarction, the QRS complexes and T wave change as heart muscle tissue progresses from early to late infarction. In the beginning, ischemia is first reflected in ST segment depression. The elevation of ST segment in ECG waveform is a sign of an early infarction. Late infarction causes to T wave inversion. The deep QRS complex is the evidence of an old resolved infarction [21]. The analysis of ECG signals for diagnostic purpose generally lacks detailed numeric relationships or formulas and it rather relies on these logical clinical terms. The expert's opinion depends on the cardiologist's own model of the diagnostic process, which is mainly described in a linguistic fashion based on the acquired knowledge and experience.

Registration, processing and analysis of ECG signals constitute the main steps of diagnostic decision making. The ECG signals are due to nonlinear and nonstationary phenomena and exhibit noise susceptibility together with variability among individuals. The main sources of noise and artifacts in ECG signals include: low frequency interferences, muscle artifacts, power-line interferences and impulsive electromagnetic interferences. The body-electrode

impedance varies due to underlying physical and chemical processes at the site of contact region as well as the movement of the subjects. These phenomena results into slow-varying distortions in the form of baseline wandering effect in ECG signals [22, 23]. Respiratory movements also change position of the electrodes relative to the heart in turn causing some slow-changing disturbances in ECG recordings. The contraction of skeletal muscles due to subjects body movement or unsuitable ambient temperature leads to muscle artifacts. The muscle artifacts are very difficult to deal without affecting important diagnostic information in ECG signals because they have broad frequency spectrum that overlaps with the frequencies of the ECG signals [24]. Interference due to power sources are electromagnetic in nature and are referred to as power-line interferences [25]. High power devices like diathermy cause to impulsive electromagnetic interferences [26, 24].

Depending upon the type of the ECG test, the points of electrode placement for signal acquisition vary in turn affecting the quality of ECG recordings. The ECG signals recorded from various points exhibit diversity in amplitude with usually a very low signal-to-noise ratio (SNR). Typically, the amplitudes of ECG signals measured non-invasively from the body surface have amplitude in the range 10 μV to 5mV with normal peak reading of 1mV [27]. The maximum bandwidth of ECG signals is up to 1 kHz. Higher signal amplitudes in mV are mainly caused by the contraction and relaxation of ventricular muscles of the heart. On the other hand, fetal ECG signals and heart micro potentials have amplitudes in the range of μV accompanying highly undesirable SNR of about 20dB [28, 29, 30] .

1.1.2 The Anatomy and Physiology of Heart

The heart pumps to move the blood through the blood vessels. Anatomically, the heart has two sides that serve as two separate pumps: the right side and the left side, which are separated by a wall of tissue called the septum. Each side of the heart has two chambers: the atrium and the ventricle. Atrium receives the blood and ventricle forces the blood away from the heart. The right side of the heart pumps deoxygenated blood containing carbon dioxide from the body to the lungs, and the left side receives oxygenated blood with its carbon

dioxide being ventilated from the lungs to pumps it to the body. Related figure showing the schematic representation of chambers, valves, major blood vessels and other connective tissues of heart can be found in [31].

The blood vessels that circulates the blood to and from the lungs constitute the pulmonary circulation, and those that circulates to and from the rest of the tissues in the body constitute the systemic circulation as demonstrated in [31]. The blood vessels that move blood away from the heart are called arteries and those that move blood toward the heart are called veins. The only exceptions are the pulmonary artery and the pulmonary vein that carry deoxygenated blood and oxygenated blood respectively.

There are four heart valves that lie between the atria and the ventricles, and between the ventricles and the major arteries from the heart. The figure showing the anterior view of the heart indicating the positions of four valves can be seen in [31]. These valves facilitate flow of blood in one particular direction. These valves are the tricuspid valve, the mitral valve, the pulmonic valve, and the aortic valve. The atrioventricular valves (AV) namely tricuspid and mitral valves direct the flow of blood from the atria to the ventricles. The efficiency of these valves depends on working of the valve leaflets, papillary muscles and chordae tendineae that are strong tendons that connect the papillary muscles to these valves. The papillary muscles are the finger-like projections of the muscle tissue from the endocardium of the heart. The semilunar valves namely the aortic and the pulmonary valves are half-moon-shaped structure that prevent the back flow of blood from the aorta or the pulmonary artery into the ventricles. Blood supply to the myocardium of the heart is provided by the right and left coronary arteries as demonstrated in [21]. If a branch of a coronary artery becomes narrow or obstructed by an embolus (clot), the myocardial cells it supplies may deprive of blood causing condition called ischemia. Angina pectoris or the chest pain accompanies ischemia. Death of a portion of the heart muscle from ischemia is called myocardial infarction (heart attack).

In general, the cardiac cycle consists of repeating actions of contraction (systole) and relaxation (diastole) of the chambers of the heart as demonstrated in [31]. These activities

are caused basically in response to an electrochemical stimulus by the group of cells present as the sinoatrial node. In the beginning of a cardiac cycle, the atria contract to move the blood into the ventricles. During this time, the atrioventricular valves get open to allow the flow of blood into the ventricles. As soon as the atria begin to relax, the ventricles contract to push the blood into the aorta and the pulmonary artery. Meanwhile, the semilunar valves get open to allow the flow of blood out of the heart and the atrioventricular valves get close thereby preventing backwards flow of blood from the ventricles to the atria. Subsequently, the ventricular relaxation occurs after which both the atria and the ventricles remain relaxed until atrial contraction occurs again at the onset of next cardiac cycle. During this stage, the semilunar valves prevent blood from flowing back from the pulmonary artery and aorta into the right and left ventricles, respectively. The figure showing the correlation of the four heart sounds with the electrical and the mechanical events of the cardiac cycle can be seen in [32]. It represents the left atrial, aortic, and left ventricular pressure pulses correlated in time with aortic flow, ventricular volume, heart sounds, venous pulse, and ECG for one complete cardiac cycle.

1.1.3 The Genesis of Cardiac Signals

The cardiac sound signals and ECG signals are produced by the rhythmic activity of the heart. The generation of these signals can be described as follows:

1.1.3.1 The Genesis of Cardiac Sound Signals

The pressure gradients cause to the vibration of the cardiohemic system that consists of the heart and blood together. These vibrations are externally recorded as cardiac sound signals. The mechanism of generation of these signals is based on the fact that cardiohemic system acts like fluid-filled balloon. This system, when simulated at any location, produces the vibrations.

The underlying physiological causes for the generation of various heart sounds have been well demonstrated in [31]. The generation of heart sounds and the murmur that are the

main components of cardiac sound signals and can be described as follows [17, 33]:

The S1 heart sound : The S1 heart sound contains four components [34]. The first component of S1 heart sound is caused by the onset of myocardial contraction in the ventricles and is related to the closing of the AV valves. At this phase of systole, blood is forced to move towards atria while sealing the AV valves. Abrupt tension of the AV valves causes deceleration of the blood that in turn manifest as second component of S1 heart sound. Subsequently, the semilunar valves namely the aortic and pulmonary valves get open and blood is moved out of the ventricles. The oscillations of the blood between the root of the aorta and the ventricle walls generate the third component of the S1 heart sound.

The turbulence caused by the ejected blood moving rapidly through the ascending aorta and the pulmonary artery generates the fourth component of S1 heart sound. The S1 heart sound is the loudest in intensity and persists for longest duration among all the heart sounds. As it originates from mitral and tricuspid valve, it is best heard at the apex of the heart [35]. The acoustic properties of components of S1 heart sound can reveal the strength of the myocardial systole and the status of the functioning of tricuspid and mitral valves. The two components (M1 and T1) of S1 heart sound corresponding to these valves are often separated by a time delay of 20–30 ms [36]. This splitting of S1 heart sound carry significant diagnostic information. An abnormally large splitting is often a sign of heart disorder. The duration of S1 heart sound ranges from 100ms to 200ms [36]. The frequency spectrum of the first heart sound has frequency components that lie in the range of 10–200 Hz [36].

The S2 heart sound: It is generated by the closure of the semilunar valves when the interventricular pressure begins to drop. The primary vibrations associated with S2 heart sound occur in the arteries due to deceleration of blood. The ventricles and atria also vibrate due to transmission of vibrations through the blood and the valves. The S2 heart sound has two components: one is related to the aortic valve (A2) and another one is related to closure of pulmonary valve (P2).

Generally, since aortic valve closes before pulmonary valve, therefore A2 is ahead of P2 by a few milliseconds [34]. During expiration, the separation between A2 and P2 is small,

generally, less than 30 ms. However, during inspiration, the splitting of the two components is quite evident [36]. In pathological conditions, the duration between A2 and P2 may get widen and order of occurrence of A2 and P2 may also get reverse. As compared to S1 heart sound, the S2 heart sound has lower intensity and persists for shorter duration of about 110ms. The reason for the shorter duration is due to the fact that the semilunar valves are much rigid than the AV valves and that makes them to close faster. As the S2 heart sound originates from aortic and pulmonary valve, it is best heard at the base of the heart [35].

The S3 heart sound: This heart sound is also referred as the "ventricular gallop". It occurs just after S2 heart sound due to abrupt termination of the rapid-filling of blood in ventricles. The spectrum of S3 heart sound consists of very low frequencies because it occurs when the ventricles are filled with blood and the walls are relaxed. The S3 heart sound is actually heard due to the large amount of blood striking a very compliant left ventricle. The occupancy of S3 heart sound can be a normal auscultatory finding in children, pregnant females, and well trained athletes. However, it can be an important sign of systolic heart failure as the over compliant myocardium can result in a dilated left ventricle. The S3 heart sound may be pathological if heard in over aged individuals.

The S4 heart sound: This heart sound is also known as the "atrial gallop". The S4 heart sound is heard just before the S1 heart sound and spectrum consists of lower frequencies. It occurs in late diastolic phase when the atria contract to displace the blood into the distended ventricles. The non-compliant left ventricle produces S4 heart sound. The left ventricular hypertrophy causes impaired relaxation of the myocardium of left ventricle generating S4 heart sound. The presence of S4 heart sound is rarely a normal finding. The frequencies of S3 and S4 heart sounds lie in the range 20 -70 Hz [15].

Murmurs: The murmurs are noise-like sounds that are audible during the systole and diastole phases. They are caused due to various cardiovascular diseases and defects. The spectrum of murmurs consists of high frequency components. The murmurs occur when blood flows through irregularities such as leaking and narrowed or deformed valves. Typically, they are produced by the turbulence due to the valvular stenosis and regurgitation. In case

of valvular stenosis, valve leaflets becomes stiffer may be due to calcium deposition and fails to open completely thereby hindering the flow of ejected blood. In case of valvular regurgitation, valve can not close properly and cause to leakage of blood through narrow opening. A dysfunction of the chordae tendineae and papillary muscles and stretching of the leaflets of the valve in pathological conditions may cause regurgitation or leakage. The murmurs may also arise due to high rate of blood flow that in turn cause turbulent flow through a normal or defective valve and vibrations of loose structures within the heart. The average murmurs have frequencies in the range 100-600 Hz [16].

In additions to the above mentioned sounds, ejection clicks and opening snaps occasionally appear as auscultatory findings that can be briefly described as follows.

Ejection clicks/sounds: They are basically high-pitched sounds that appear at the instant of maximal opening of the aortic or pulmonary valves in pathological cases. They occur shortly after the S1 heart sound. The sounds occur in the presence of a dilated aorta or pulmonary artery or in the presence of a bicuspid or flexible stenotic aortic or pulmonary valve.

Opening sounds: As compared to ejection click, opening snaps arise in diastolic phase at the instant of maximal opening of a flexibly stenotic mitral or tricuspid valve. They are most frequently caused by sudden pathological arrest of the opening of the mitral or tricuspid valve. These sounds occur after the S2 heart sound in early diastole and represent short high frequency sounds.

1.1.3.2 The Genesis of ECG Signals

The electrical system of the heart is the main source of rhythmic contractile activity of the heart. The cells of myocardium and the SA node are the main component of the electrical system of the heart. These cells produce co-ordinate electrical events and form a specialized conduction system intrinsic and unique to the heart. The SA node is the natural cardiac pacemaker that spontaneously generates the electrical activity in the form of action potentials. This action potential of the SA node travel through the heart thereby causing heart

to beat in a particular pattern of excitation, contraction and relaxation. The myocardium contracts after stimulation. In response to the propagating action potentials, myocardium gets stimulated that allows it to contract for pumping the blood throughout the body. The occurrence of sequence of electrical events and the associated waves in a cardiac cycle of ECG trace on the surface of the body has been shown in [37, 38]. It can be described as follows [13]:

The SA node shoots the electrical impulses in the form of action potentials. The electrical activity is propagated through the muscles of atria via the right atrium, and through Bachmann's bundle to the left atrium, triggering the myocardium of the atria to contract. The conduction of the action potential throughout the atria is seen on the ECG waveform as the P wave. The speed of propagation is relatively low causing slow depolarization (contraction) of the atria. The small size of atria and lower speed of propagation of action potentials make the P wave lower in amplitude and slow wave. The P wave exhibit amplitude in the range 0.1 - 0.2 mV with a time duration falling in the range 60 - 80 ms. Then the electrical activity spreads from the SA node to the AV node via specialized pathways, known as internodal tracts. At the AV node, there occurs a propagation delay in the electrical excitation, which results in a normally iso-electric segment having time duration of about 60 - 80 ms. This iso-electric segment (base line) appears after the P wave in the ECG recording as the PQ segment. The delay helps in completion of the transfer of blood from the atria to the ventricles in a proper way.

The bundle of His, the bundle branches, and the Purkinje system forms the specialized conduction pathways that helps to propagate the electrical excitation to the ventricles at a high rate. The Bundle of His splits into two branches, the left bundle branch and the right bundle branch that in turn activates the left and the right ventricles respectively. The left bundle branch is short and bifurcate into the left anterior fascicle and the left posterior fascicle. The left posterior fascicle is relatively short and broad and it transmits impulses to the papillary muscles leading to mitral valve closure prior to ventricular contraction by longer right bundle branch. This creates pre-tension in the chordae tendinae for increased

resistance to the blood flow through the mitral valve during systole. The left and right bundle branches get thinner forming Purkinje fibers which stimulate individual groups of muscle cells to contract. The action potential spreads rapidly from the apex of the heart towards upward causing the ventricles to contract. This activity appears as QRS wave in the ECG waveform which is a sharp biphasic or triphasic wave of about 1 mV in amplitude and 80 ms in time duration. The ventricular muscle cells have comparatively long action potential duration in the range 300 - 350 ms.

The last event of the cardiac cycle is the repolarization (relaxation) of the ventricles that restores the resting state. In the ECG waveform, repolarization activity appears as ST-segment and T wave [39]. After the QRS wave, iso-electric segment of about 100 - 120 ms occurs as the ST segment in ECG waveform. Generally, a slow T wave, having amplitude of about 0.1 - 0.3 mV and time duration of 120 - 160 ms occurs during the repolarization of the ventricles. The other rare waves in ECG waveforms associated with repolarization are J wave and U waves [39].

1.1.4 The Recording of Cardiac Signals

The data acquisition procedure for cardiac sound and ECG signals can be described well under the following subsection.

1.1.4.1 The Recording of Cardiac Sound Signals

The acoustical path of the heart sounds begins with the vibrating structures of cardiohemic system which includes the heart and the blood. Then these vibrations propagate through the body tissues along different paths toward the body surface. However, the energy of heart sounds get heavily attenuated while they reaches the surface of body because of the phenomena of spreading, absorption, scattering, reflection, and refraction. The compressible tissues comprising the lung and the fat layers attenuate most of the transmitted heart sounds. The components of heart sounds having low frequencies are relatively less attenuated than that of high frequencies. Ipso facto, the consequences of the attenuation are complex

to determine. Therefore, in order to reduce the effect of attenuations and clearly perceive the heart sounds, certain areas on the chest surface have been defined to perform cardiac auscultation as demonstrated in [40]. These locations have been determined such that transition of heart sound is through solid tissues or through a minimal thickness of interfering tissues. The radiated sound intensity from each of the four heart valves is maximum at these locations. Therefore, the auscultation of heart sounds is generally preferred on specific areas on the chest surface namely aortic area, pulmonic area, tricuspid area and mitral area. The corresponding valves are best heard at these locations [34].

- Mitral area: The cardiac apex.
- Tricuspid area: The fourth and fifth intercostal space along the left sternal border.
- Aortic area: The second intercostal space along the right sternal border.
- Pulmonic area: The second intercostal space along the left sternal border.

Moreover, the cardiac sound signals are recorded in a quiet environment to reduce interference from the ambient noise. The subject can be asked to perform various maneuvers in different postures for improved auscultation. For example, generally the subject is asked to be in supine position and completely relaxed. Holding breaths may reduce effect of noise due to respiration and the baseline wandering caused by movement can be minimized.

Fig. 1.1 shows the schematic of the cardiac sound acquisition and analysis system which can be used for automatic analysis of heart disorders. In order to record the cardiac sound signals, the chestpiece has to be placed on to the four standard auscultatory locations on the chest. The chestpiece and sensor together convert the acoustic waveforms into electrical signals. These electrical signals can be processed for listening and transmission to computer for automatic analysis using software based on advanced signal processing techniques.

1.1.4.2 The Recording of ECG Signals

The 12-lead scalar ECG is the most commonly used procedure in clinical practice. It is obtained using four limb leads and chest leads in six positions [41, 13]. The lead attachment

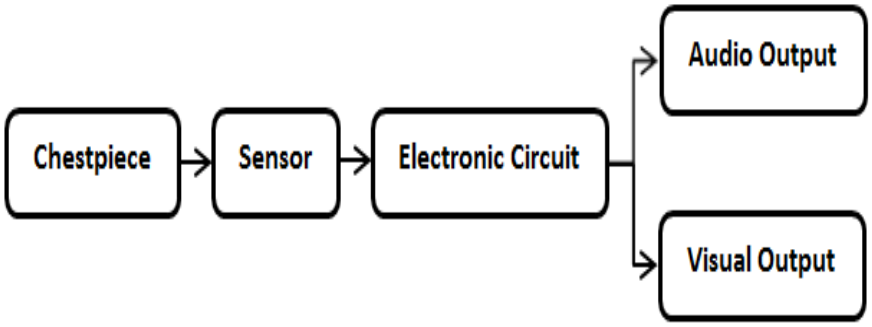

Figure 1.1. The schematic of the cardiac sound acquisition and analysis system for heart disorders.

on right leg serves as one of the reference signal. The ECG recordings from leads I, II and III are obtained using left arm, right arm, and left leg as demonstrated in [41, 13]. One more reference is obtained by combining output from the lead attached to the left arm, right arm, and left leg leads. This reference is termed as Wilsons central terminal and used as the reference for ECG recordings from chest leads.

The aVR, aVL, and aVF limb leads form the augmented limb leads. Where, 'a' stands for the augmented lead, R for the right arm, L for the left arm, and F for the left foot. The augmented leads are recorded using the exploring limb leads as indicated by the lead name, with the reference being Wilson's central terminal. The aVR, aVL, and aVF leads can be derived from lead I and II.

The directions of the axes of the six ECG leads formed by four limbs are depicted in [42]. The leads I, II and III can be hypothetically envisaged in the form of equilateral triangle known as Einthoven 's triangle. The center of this triangle is the reference or Wilson's central terminal. Thematically, the heart is assumed to be present at the center of the Einthoven 's triangle. The six leads project the electrical activity of the heart as three-dimensional (3D) cardiac electrical vector as depicted in [42]. These six axes sample the 0^0 - 180^0 range with a resolution of nearly 30^0. This 3D cardiac electrical vector facilitates viewing and analysis

of the electrical activity of the heart and from different angles in the frontal plane [34] .

The leads from V1 to V6 form the six precordial (chest) leads that are recorded from six standardized positions on the surface of the chest as demonstrated in [13]. The Wilson's central terminal is used as the reference. The precordial leads help analysis of the heart's electrical activity from different orientations in the horizontal plane. The electrodes for V1 and V2 leads are placed at the fourth intercostal space just to the right and left of the sternum, respectively. The lead V4 is attached at the fifth intercostal space at the left midclavicular line on the chest. The V3 lead is mounted at the center of V2 and V4 leads. The V5 and V6 leads are aligned at the same level as that of V4 lead. They are placed at the anterior axillary line and the midaxillary line, respectively. The V1 and V2 leads lie directly over the right ventricle and reflect its activity very well. The V3 and V4 leads lie directly over the inter ventricular septum and depict the septa1 activity in a best manner. The V5 and V6 leads are most sensitive to left ventricular activity. Heart disorder, if any, can be localized by analyzing the shapes of ECG wave in these six chest leads. However, clinical interpretation of ECG recordings is commonly performed empirically with experimental knowledge.

Another compact and efficient ECG system commonly used is Vectorcardiography (VCG) [43]. It involves recording the magnitude and direction of the 3D cardiac electrical vector in the form of loops. This loops are plotted and analyzed using three mutually orthogonal planes, namely, the frontal, horizontal, and sagittal planes, It uses three leads derived using the basic leads I, II and III which are: right-left axis (X), head-to-feet axis (Y) and front-back (anteroposterior) axis (Z).

Some of the main specifications of the standard clinical ECG include the following aspects: Normally, the ECG signal exhibit maximum amplitude of 1 mV. Therefore, graphical recording on a paper is obtained by operating the stylus at a speed of 25 mm/s. This speed results in a graphical scale of 0.04 s/mm. The amplitude and time calibration is achieved using a rectangular pulse of 1 mV amplitude and 200 ms of time duration. The corresponding calibration pulse width on time axis and amplitude axis are 5 mm and 1 cm. The morphological distortions in the calibration pulse are used to reset the ECG signal acquisition

system for normal operation. The amplification of 1,000 is commonly applied. A bandwidth of about 0.05 - 100 Hz, with a recommended sampling frequency of 500 Hz is generally used for reduced noises and artifacts in Clinical ECG for diagnostic purpose. The long term monitoring is prone to low frequency noises or artifacts, therefore a reduced bandwidth of 0.5 - 50 Hz is usually recommended for measuring heart rate in that scenario. For obtaining high-resolution ECG a greater bandwidth of 0.05 - 500 Hz is generally used.

1.1.5 The Analysis of Cardiac Signals

The analysis of cardiac sound signals and ECG signals for clinical applications can be described as follows:

1.1.5.1 The Analysis of Cardiac Sound Signals

The heart sounds contain useful diagnostic information about the status of cardiovascular system. However, the components of the heart sounds have extremely small amplitudes and therefore they are difficult to interpret by listening.

Moreover, the human ear is far more sensitive to the speech having frequencies in the range 1000-2000 Hz than to higher and lower frequencies. It lacks desired sensitivity towards heart sounds and murmurs [3, 3, 5] and most of the diagnostic information conveyed by the heart sounds are too weak to be identified by the human ear. In addition, the heart sounds often last for a short period of time and pathological splitting of the heart sound is also short which is difficult to interpret to make any decision on presence of heart disorders [3]. From the above mentioned facts and the the figure as demonstrated in [44], it can be inferred that an important part of the intensity and frequency distribution of the heart sounds and murmurs is not properly audible to the human ear for diagnostic decision making.

The cardiac auscultation has been a traditional means of early diagnosis of cardiovascular disorders. In recent years, with the development of new cardiac sound transducers or sensors and many advanced signal processing and medical artificial intelligence technologies, it is now possible to analyze cardiac sounds signals in the audible and inaudible ranges. These

technologies are quite potential to pave the way for development of efficient, informative and accurate state of the art computer-aided diagnostic tool for heart disorders. Much more diagnostic information can be extracted from heart sounds than before using advanced signal processing techniques that have helped us to gain new insight into normal and pathological cardiac sound signals. Therefore, a cardiac sound signals based expert system can be envisaged as a promising and cost effective technology for prompt, noninvasive, convenient and efficient diagnosis of heart disorders. Implementation of such systems involves analysis and extraction of suitable diagnostic features from the cardiac sound signals for final development of pattern classification process to classify a set of cardiac sounds signals.

After the stage of data acquisition, the application of cardiac sound signals for diagnosis involves five basic stages [45, 33, 46]: (1) signal conditioning, (2) segmentation, (4) signal analysis and feature extraction, and (5) classification. These steps can be briefly described as follows:

The aim of data acquisition is to acquire the signal without losing information and encode in a form suitable for computer based analysis. The stage of signal conditioning eliminates or reduces extraneous components such as noise from the cardiac sound signals. The stage of segmentation of cardiac sound signals aims to derive the heart beat cycles to facilitate feature extraction. Even this stage can serve as the measures of heart rate. At the stage of feature extraction, small number of parameters that could serve as diagnostic features are identified and measured that can best represent the information of interest in the cardiac sound signals. The last stage of cardiac sound signal processing is the decision making that is particularly important in clinical applications where a course of action needs to be performed. It aims at answering questions such as "Does the subject have a heart disorder based on cardiac sound signal analysis ? " or "Does patient show a specific heart disorder in the heart based on cardiac sound signal analysis ?" This stage basically involves development of pattern classification process to classify a set of cardiac sound signals. Specifically, the work in this thesis, focuses on automatic diagnosis of the heart valve and septal defects. The recorded heart sounds can be classified into different groups that represent different types of

cardiovascular diseases.

1.1.5.2 The Analysis of ECG signals

ECG signals are the valuable source of diagnostic information in cardiology. ECG signals are basically quasi-periodic signals having weak amplitude. They are often prone to contaminated by noise and artifacts. The ECG signal registration generally requires the amplification and proper removal of noise and artifacts for effective diagnostic applications. The complete ECG signal processing and analysis comprises the similar steps as that of cardiac sound signals. The important steps include: signal amplification, A/C conversion, noise reduction, data compression, feature selection, classification or interpretation. The details about these steps can be found in [10].

1.1.6 Heart Valve Disorders

The mitral and aortic valves are more prone to disorders since the left side of the heart confronts higher pressure gradients and greater workloads. Typically, there are two major clinical issues with these valves: stenosis and insufficiency [17, 47, 48]. In case of valvular stenosis, valve leaflets become stiffer may be due to calcium deposition and fails to open completely thereby hindering the flow of ejected blood. Even thickened or fused valve leaflets may reduce the opening through which the blood passes from one chamber to another. The occluded flow of blood leads to an accumulation of blood in the chamber, compelling the heart to work harder in order to pump the blood.

Murmurs: The murmurs are noise-like sounds that are audible during the systole and diastole phases. They are caused due to various cardiovascular diseases and defects. The spectrum of murmurs consists of high frequency components. The murmurs occur when blood flows through irregularities such as leaking and narrowed or deformed valves. Typically, they are produced by the turbulence due to the valvular stenosis and regurgitation. In case of valvular stenosis, valve leaflets becomes stiffer may be due to calcium deposition and fails to open completely thereby hindering the flow of ejected blood. In case of valvular

regurgitation, valve can not close properly and cause to leakage of blood through narrow opening. A dysfunction of the chordae tendineae and papillary muscles and stretching of the leaflets of the valve in pathological conditions may cause regurgitation or leakage. The murmurs may also arise due to high rate of blood flow that in turn cause turbulent flow through a normal or defective valve and vibrations of loose structures within the heart.

In case of valvular regurgitation as demonstrated in [49], valve can not close properly and cause to leakage of blood through narrow opening. A dysfunction of the chordae tendineae and papillary muscles and stretching of the leaflets of the valve in pathological conditions may cause regurgitation or leakage. The murmurs may also arise due to high rate of blood flow that in sequence cause turbulent flow through a normal or defective valve and vibrations of loose structures within the heart. Valvular stenosis and regurgitation cause to turbulent flow of blood that may gradually wear out the heart tissues. In the beginning, it causes the heart muscle to grow abnormally stronger and thicker which is called hypertrophy. It also cause to unusual enlargement of heart ventricles which is called dilatation. The hypertrophy and dilation try to compensate for the extra workload and allow the heart to supply an adequate amount of blood to the body. However, over the period of time, the overdeveloped heart muscle may wear out gradually leading to functional degradation and heart failure.

Aortic stenosis occurs between the left ventricle and the aorta. The obstruction of aortic stenosis may be present in the valve as: above the valve and below the valve. It is mainly caused by congenital abnormality, rheumatic fever, and calcific degeneration or deposits of calcium on the valve. Due to the obstruction, the left ventricular pressure increases that gradually develop into hypertrophy. The left ventricular hypertrophy increase resistance to filling in turn elevating the preload with strong atrial contractions. Consequently, the increased left atrial pressure may results into increased pressures in the right side of the heart, increased systemic venous pressure and peripheral edema [48]. Pulmonary edema is the pathological condition which refers to accumulation of fluid in the air spaces of lungs and alveolar tissues. It causes to impaired gas exchange that may lead to respiratory failure.

Mitral regurgitation is an abnormal leaking of blood from the left ventricle into the

left atrium of the heart through narrow opening. It is mainly caused due to myxomatous degeneration of the valve which refers to the abnormal weakening of the connective tissues, annulus dilatation, dysfunction of the papillary muscles and rupture of the chordae tendineae. Figures showing the stretching or tearing of chordae tendineae or papillary muscles and dilatation of the valve annulus respectively can be found at [49]. In order to compensate the reduced supply of blood due to leakage, the heart rate increases and hypertrophy occurs. The atrium increases its force of contraction in order to maintain ventricular filling. With increase in atrial pressure, the left ventricle of the heart fails to adequately remove blood from the pulmonary circulation that may lead to cardiogenic pulmonary edema.

Mitral valve stenosis is typically caused by rheumatic fever. It usually occurs during childhood due to body's immune response to an infection with the streptococcal bacteria. The infection includes strep throat or scarlet fever. Besides heart, the most affected parts of the body are the joints of the body that can lead to temporary and sometimes chronic disability. In rare clinical cases, calcium deposition may cause narrowing of the mitral valve. Other rare causes for mitral valve stenosis include: tumors (less commonly), blood clots, radiation treatments and congenital heart defects.

Aortic regurgitation refers to the leaking of the aortic valve of the heart that causes back flow of blood during ventricular diastole, from the aorta into the left ventricle. It may involve the abnormalities of either the aortic valve or the aortic root. The rheumatic fever is the common cause of this disorder. The other causes include: congenital valve defects, infections of the heart tissue, high blood pressure, genetic conditions such as Marfan syndrome that affects the connective tissues, untreated syphilis, systemic lupus erythematosus that is an autoimmune disease, heart aneurysms, ankylosing spondylitis that is a form of inflammatory arthritis.

Tricuspid or pulmonic stenosis and regurgitation constitute a small part of the heart valve disorders. The abnormalities of the tricuspid valve are commonly caused by rheumatic fever or metabolic abnormalities. The major symptoms of tricuspid valve dysfunction include edema and fatigue. Pulmonary valve dysfunction is primarily caused due to congenital

defects. Pulmonary stenosis is the second most common congenital heart disease.

In some clinical cases, it is difficult to find the cause of heart valve disorder. The main causes of heart valve disorders may include but not limited to the following [50]:

Rheumatic Fever: It is basically an inflammatory condition that is mainly caused by strep throat or scarlet fever. It involves autoimmune response in which the body starts attacking its own tissues in response to infection with the strep throat bacteria. The acute inflammation is hardly fatal but chronic and progressive inflammation may cause cardiac disability or death many years after its inception.

Infective Endocarditis: It refers to an inflammation of the inner tissue of the heart caused by infectious agents usually bacterial. However, it may be due to other microorganisms. The heart valves lack dedicated blood supply, as a result of which defensive immune mechanisms such as white blood cells do not have direct access to the valves. The microbial infection can cause vegetation on the heart valves in turn weakening the host immune response. These germs or microorganisms can enter the blood pathways during: dental procedures, surgery, intravenous drug use and severe infections. In case of treatment, the lack of blood supply to the valves also inhibits the flow of drugs to reach the infected valves.

Myxomatous degeneration: It refers to the pathological weakening of the connective tissues, annulus dilatation, dysfunction of the papillary muscles or stretching or tearing of the chordae tendineae. It commonly affects the mitral valve. It originates from a series of metabolic changes that leads to reduced elasticity of the valvular tissue while becoming weak and covered by deposits.

Congenital heart valve disorders: They refer to an abnormality of heart valves that develops before birth. It may be pertaining to improper valve size, malformed leaflets, septal defects and irregular attachment of leaflets. The condition mostly affects the aortic or pulmonic valve. In most cases, bicuspid aortic valves develop two leaflets instead of three as demonstrated in [49]. The cause of congenital heart valve disorders may be either genetic or environmental, but is usually a combination of both.

Fibro-calcific degeneration: It mostly affects the aortic valve as demonstrated in [49].

The condition predominantly occurs in adults over the age of 65. The heart valve leaflets become fibrotic and calcified leading to thickening and hardening of underlying tissue. This cause to narrowed valve opening of aortic valve. The risk factors for this type of valve disease include: increased age, low body weight and high blood pressure.

Other causes of heart valve disorders include coronary artery disease or myocardial infarction. These diseases can cause damage to the papillary muscles that acts as support to the valves, or annulus dilatation, so that the valve does not close properly.

1.1.7 Septal Defects

The most common pediatric cardiac disorders result from defects in the wall of tissue separating the right and left chambers of the human heart. The wall is termed as the septum and the associated defects are referred to as septal defects. The wall of tissue between the right and left atria is called the atrial septum and that of between the ventricles is called the ventricular septum. The cardiac septal defects are generally fall into two groups: ventricular septal defects (VSDs) and atrial septal defects (ASDs) as demonstrated in [49]. The septal defects are congenital heart defects that can range from a small hole in the septum to a significant portion of the septum actually being absent. These defects can cause to shunting that enables undesired flow of blood between two compartments of the heart. Moreover, the septal defects can be categorized with the help of defect diameter as small, medium and large defects [51]. The early diagnosis of the septal defects is crucial to ensure sooner treatment in turn saving many lives.

A VSD refers to a hole in the septum that separates ventricles. They usually occur by themselves in absence of other birth defects of any kind. VSDs forms about 30 percent of all congenital heart defects, occurring with a frequency of 1 out of every 500 babies [49]. The size of the defect determines its effects on the functioning of heart. When the defect is large, oxygenated blood flows back into the right ventricle instead of moving out to the body. From the right ventricle, this oxygenated blood is pumped back to the lungs. This displaces the blood in the pulmonary circulation that needs oxygen. Consequently, in order

to compensate this inefficient blood flow, the heart works harder. As a result of which the heart becomes large and high blood pressure gets develop in the arteries of the lungs that is called pulmonary hypertension. A subject with a large VSD may show the following symptoms: shortness of breath, fatigue and weakness. In case of smaller defect, the only symptom is often a loud murmur, caused by the blood flowing backwards into the right ventricle [49].

An ASD represents the hole in the septum that separates atria. It occurs when part of the atrial septum does not develop properly. They are classified by means of their place of occurrence and size. The various types of ASD include: secundum ASD, patent foramen ovale (PFO), sinus venosus, primum ASD etc. A secundum ASD is a hole in the middle of the atrial septum and a PFO is a "flap" that is present when the atrial septum does not close properly at birth. This PFO defects generally allow flow of blood only when there is more pressure inside the chest, such as straining during a bowel movement, coughing or sneezing. The sinus venosus and primum ASD refers to different parts of the septum and also involve abnormal blood return from the lungs or heart valve abnormalities. They are quite complicated in nature and are rare types of ASD. ASD is the third most common type of disorder after mitral valve prolapse and bicuspid aortic valve [52] that forms about 7 percent of all congenital heart defects. They are most common in adults and are more common among women than men.

1.1.8 Coronary Artery Disease

The coronary artery disease (CAD) is a common and the leading cause of death in the developed countries of the world [53]. The other commonly used term for CAD are atherosclerotic heart disease, atherosclerotic cardiovascular disease, coronary heart disease or ischemic heart disease (IHD) [54, 55, 56]. The CAD is a condition characterized by the deposition of atherosclerotic plaques or fibro-fatty deposits within the inner wall of the coronary arteries of the heart. The affected artery wall thickens as a result of invasion and accumulation of white blood cells. The deposition of plaque can block the required flow of blood to the heart

muscles [57]. In other words, the advanced plaque manifest into clinical symptoms. Under the condition of increased amount of plaque deposition, the blood vessels become narrow and allow lesser amount of blood supply to the heart muscle thereby making it deprived of adequate nutrients and oxygen it requires to work properly. This condition becomes progressively worse affecting the metabolic activity of the heart muscles. Over a period of time, the heart muscles become weak that may lead to heart failure and arrhythmias [58]. Even more, often the deposited plaques erode or rupture resulting into thrombus formation that can restricts the flow of blood to the heart muscles causing sudden cardiac death. The four major risk factors of CAD, in order of significance, are dyslipidemia, hypertension, tobacco smoking [59] and increasing age. The other risk factors include obesity, family history of premature CAD, physical inactivity and environmental pollution [60]. Depending on the symptoms and risk of complications in CAD, the following treatments are usually prescribed: medication, percutaneous coronary intervention (angioplasty) or coronary artery bypass surgery. Timely diagnosis and treating of CAD is important to reduce the risk of occurrence of heart attack or stroke and to save many lives.

The physicians often evaluate the presence and extent of CAD by observing common symptoms, reviewing the medical history and risk factors, performing physical examination and diagnostic laboratory tests, including blood tests, an ECG and tread mill stress tests [61]. The diagnosis of CAD depends largely on the nature of the symptoms. Often the first clinical investigation is an ECG test, both for stable angina and acute coronary syndrome. It usually follows an X-ray of the chest and blood tests. The imaging modalities like echocardiogram, coronary computed tomography angiogram (CTA) and coronary angiography or cardiac catheterization are also used to detect the presence of CAD. The ECG based diagnosis is quite promising and it requires minor changes in the ECG recordings to be get detected that may be indicative of any specific heart disorders. However, in many cases, visual analysis of ECG recordings for detecting CAD is not reliable because it is difficult to notice the differences in recordings [62]. The presence of noises and artifacts like baseline wondering make it complex to accurately analyse the small morphological changes

in the ECG recordings due to heart disorders. While undergoing tread mill stress tests, patients are at risk of developing tachycardia and eventual heart failure [63]. The cardiac catheterization is performed invasively and the average time it takes is about thirty minutes. However, overall time including the preparation and recovery time amounts to several hours. This leads to almost whole day for patients to do this test. Most of the imaging modalities can be operated only by trained physicians or radiologist and they involve lot of experience, time and effort. Some of the above mentioned diagnostic tools are quite expensive and their availability is limited to health care centers in urban areas.

In many cases CAD remains asymptomatic, however it may cause to the following coronary events: angina (stable or unstable), Acute myocardial infarction, silent ischemia (no pain), arrhythmias, heart failure or left ventricular dysfunction, ischemic cardiomyopathy (weakness of heart muscle) and sudden death. The two common types of clear symptoms of CAD are stable and unstable angina or chest pain. In case of stable angina, the chest pain occurs consistently with activity, after heavy meals, or at other predictable instances. The stable angina is correlated to high degree of narrowing of the coronary arteries. The chest pain that occurs at rest or minimal exertion lasting less than 20 minutes and occurring again within a month with more intensity, prolonged, or increased frequency than previously is termed as unstable angina. Unstable angina may be a sign of myocardial infarction.

In case of myocardial infarction, the QRS complexes and T wave change as heart muscle tissue progresses from early to late infarction. In the beginning, ischemia is first reflected in ST segment depression. The elevation of ST segment in ECG waveform is a sign of an early infarction. Late infarction causes to T wave inversion. The deep QRS complex is the evidence of an old resolved infarction [21].

1.2 Motivation

The heart disorders are the second leading cause of death and disability worldwide. They are mostly predominant in the developing countries. The heart valve disorders, septal defects

and coronary artery disease (CAD) are the most commonly occurring heart disorders. Early diagnosis and immediate treatment of these heart disorders can ensure contented, happier and longer life of patients. However, diagnosis at desired time is quite challenging because of absence of experienced physicians and lack of affordable investigations.

Cardiac auscultation, phonocardiography and ECG are the traditional means of diagnosis of the heart disorders. However, they depend on subjective assessment by the physicians involving variability in the perception and interpretation of the heart sounds and ECG waveforms respectively, thereby affecting the competence of diagnosis. The digital version of these techniques provide cardiac signals: cardiac sound signals and ECG signals. Small changes in the cardiac signals indicate a particular disease. It is very difficult to decipher these minute changes in the cardiac signal, as it is prone to artifacts and noise. The manual inspection of these cardiac signals is time consuming, taxing and prone to errors due to fatigue. Hence, a decision support system independent of human intervention can yield accurate repeatable results.

The recent advancement in the area of analog and digital electronics has paved the way for the development of portable electronic ECG machines and other gadgets like mobile. These instruments can facilitates the medical professional to apply auscultation, phonocardiography and ECG more conveniently and in a more versatile way. Nevertheless, these devices have also opened the possibilities for the application of advanced signal processing and medical artificial intelligence technologies for the diagnosis of heart disorders. With this, the practice of cardiac examination marks the beginning of a new era that will promote the development of efficient, informative and accurate computer-aided diagnostic tool for heart disorders.

In fact, heart disorders cause changes or additional features to normal cardiac signals and therefore they can be useful for diagnosis. These signals can be used to extract valuable diagnostic features for diagnosis of the heart disorders. However, these cardiac Signals are nonlinear and non-stationary signals and involve a great deal of complexity when intended to be used for extracting diagnostic information. It is challenging to improve the performance of the various stages of cardiac signal processing for diagnosis of heart disorders that involves:

feature extraction, and classification based decision making with or without segmentation.

The heart beat cycles of cardiac sound signals can represent all the information about the functioning of heart valves and hemodynamics. Therefore, segmentation of cardiac sound signals into heart beat cycles is required for diagnosis. However, the automatic segmentation of cardiac sound signals is a challenging task due to inconsistent lengths of the heart beat cycles, variation of the number of heart sound components inside individual heart beat cycles, the unpredictable existence of murmurs and the presence of various types of noises like lung sounds, rubbing of stethoscope on the chest, etc. These constrains can cause to inaccurate segmentation in turn limiting the performance of the next stages of algorithm for automatic identification of heart disorders. In view of the above mentioned facts and limitations, a non-stationary signal processing based accurate methodology for segmentation can be developed for effective diagnosis of heart disorders.

The stage of feature extraction is intended to identify and measure optimal feature set that can represent all the useful information in the raw cardiac signals thereby reducing the dimensionality. The reduced feature set can avoid storage problem and improve computational speed. In literature, much effort has been devoted in search of these effective diagnostic feature set using time-domain, frequency-domain, and time–frequency or scale domain. Recent research suggests that WT based features are quite effective for diagnosis of heart disorders. It is noteworthy that the TQWT has been recently proposed as a powerful technique for analysis and processing of oscillatory signals. As compared to other wavelet architectures, the TQWT has the ability to tune itself with more input parameter according to the behavior of the signal under study. In view of these, the feature based on TQWT can be explored to represent the cardiac signals. These features can be used for classification of cardiac signals for detection and identification of heart valve disorder, septal defects and CAD.

Diagnosis of heart disorders can be performed remotely using telemedicine which basically involves the use of telecommunication and information technologies. Telemedicine improves access to medical services for distant rural communities and reduces the overall cost of

medical care. It is also used to save lives in critical care and emergency situations. The compression algorithm can reduce the power consumption in wireless sensor networks for better long term monitoring intended for telemedicine applications. Therefore, advanced signal processing based method can be developed for compression of cardiac sound signals that can facilitate data archiving and telemedicine procedures for convenient diagnosis.

1.3 Objectives

The phonocardiography, cardiac auscultation and ECG are noninvasive, cost-effective, accurate and convenient methods for diagnosis of heart disorders. However, diagnosis using these methods needs experience and they suffer from various other limitations such as inter-observer variation. The cardiac sound and ECG signals based methodologies can be used for automatic diagnosis of heart disorders that surpass the limitations of the above mentioned methods.

The advanced signal processing methods can be developed to detect signs of heart disorders using cardiac sound and ECG signals in turn having a significant impact on cardiac health care industry. Therefore, the primary aim of this work is therefore to develop methods that can facilitates analysis and diagnosis of heart disorders which hardly involve basic professional medical assistance not necessarily from a cardiologist. More specifically, the aims of this thesis work are as follows:

- To develop an advanced signal processing based new method for automatic envelop based segmentation of cardiac sound signals into heart beat cycles by removing murmur. The resulting segmented heart beat cycles of the original cardiac sound signals or measured heart rates can be used for the diagnosis of heart disorders.
- To develop an advanced signal processing based new methodology for separation of heart sounds and murmur from the heart beat cycles. The intended separation may results into extraction of better and more diagnostic features with same parameters to eventually classify the cardiac sound signals effectively.

- To develop a new method for classification of cardiac sound signals to diagnose the heart valve disorders by identifying and measuring non-stationary signal decomposition based effective diagnostic features.
- To develop a new method to detect septal defects by identifying and measuring non-stationary signal decomposition based effective diagnostic features from cardiac sound signals.
- To develop a new method for diagnosis of CAD using non-stationary signal decomposition based effective diagnostic features for classification of heart rate signals.
- To develop a novel methodology for compression of cardiac sound signals using advanced signal processing methods that can improve the bandwidth and the storage efficiency for telemedicine based convenient diagnosis of heart disorders.

1.4 Research Contributions

The work in this thesis contributes in a number of ways to facilitate the diagnosis of heart valves and other heart disorders using cardiac sound and ECG signals. The main contributions of this work are summarized as follows:

- A TQWT based method for automatic segmentation of cardiac sound signals has been developed for the diagnosis of heart disorders. In order to accomplish this task effectively, the murmurs from cardiac sound signals have been removed by suitably constraining TQWT based decomposition and reconstruction.

  The envelope based on cardiac sound characteristic waveform (CSCW) has been extracted after the removal of low energy components from the murmur-free reconstructed cardiac sound signals. Then the heart beat cycles have been derived from the original cardiac sound signals. The proposed segmentation has achieved better segmentation performance as compared with existing methods. The following two methodologies use this method for segmentation of cardiac sound signals into heart beat cycles for feature extraction.

- A new method has been developed for diagnosis of heart valve disorders using constrained TQWT and FB expansion based features. The first main contribution of this work is the extraction of features during the separation of heart sounds and murmur from the segmented heart beat cycles. In fact, during separation optimized values of TQWT parameters are obtained that vary with nature and severity of murmurs in different clinical cases. Secondly, this separation has been intended for extracting better and more diagnostic features with same parameters to eventually classify the cardiac sound signals. Finally, as the FB expansion can model the perceptual hearing analogous to auscultation and can prevent undesired effect of windowing, therefore the features based on FB expansion are used to represent the spectral properties of cardiac sound signals.

  The novel raw feature set has been created by the parameters that has been optimized during constraining the output of TQWT and that of extracted by using time-domain representation and FB expansion of separately reconstructed heart sounds and murmur. The adaptively selected features have been used for least squares support vector machine (LS-SVM) based classification with various kernel functions. In comparison to one recent similar method, the proposed diagnostic framework has provided higher classification performance.
- A new method has been developed for diagnosis of septal defects by classification of cardiac sound signals using TQWT based features. The main contribution of this work was the extraction of sum of average magnitude difference function (SAMDF) based features from TQWT based decomposition of segmented heart beat cycles. The correlation between sub-bands can characterize the various types of murmurs in cardiac sound signals. Therefore, the proposed feature set was created with SAMDF that have been computed from reconstruction of decomposed sub-bands.

  In search of effective feature set based on SAMDF, various decomposition levels have been examined that could provide significant classification performance. The classification has been performed using LS-SVM with different kernel functions at ten

decomposition levels for various values of quality- factor (Q) of the TQWT. The proposed method has provided significant classification performance with tenth levels of decomposition irrespective of the value of Q in the specified range using Morlet wavelet kernel function.

- A novel method for detection of CAD using centered correntropy (CCo) based feature set derived from TQWT has been developed. The correntropy can characterize the heart rate signals by nonlinearly projecting the sub-band signals into high dimensional space using kernel function. The projected feature space can provide useful diagnostic features. Therefore, in this work, the proposed raw features are formed with CCo that are computed from third level detail sub-band. The principal component analysis (PCA) is applied to obtain the significant features.

  The transformed features are used to classify heart rate signals of normal and CAD subjects using LS-SVM with various kernel functions. The effect of Q on classification performance is studied to find the optimal value of Q. The experimental results of this work have provided higher classification performance using Morlet wavelet kernel function as compared to existing methods.
- A new method for compression of cardiac sound signals using TQWT has been developed to improve the bandwidth and the storage efficiency for telemedicine based convenient diagnosis of heart disorders. The cardiac sound signals have been compressed using TQWT, linear quantization, Huffman and run length coding (RLC) techniques.

  As the compression depends on various parameters, therefore the optimal values of these parameters have been found using genetic algorithm (GA) with a subset of dataset. The experimental results of the proposed work demonstrate higher compression performance as compared to one recent method.

1.5 Outline of Thesis

In this thesis, we have developed advanced signal processing based methods to assist diagnosis of heart disorders using cardiac signals namely cardiac sound signals and ECG signals. After the stages of data acquisition and signal conditioning, the signal processing for diagnosis may include the following basic stages: feature extraction, and classification based decision making with or without segmentation. The aim of data acquisition is to acquire the signal without losing information and encode in a form suitable for computer based analysis. The stage of signal conditioning eliminates or reduces extraneous components such as noise from the cardiac signals. The stage of segmentation aims to derive the heart beat cycles to facilitate feature extraction. Even this stage can serve as the measures of heart rate. At the stage of feature extraction, small number of parameters that could serve as diagnostic features are identified and measured that best represent the information of interest in the cardiac sound signals or ECG signals. The last stage of cardiac signal processing is the decision making that is particularly important in clinical applications where a course of action needs to be performed. It aims at answering questions such as "Does the subject have a heart disorder based on cardiac sound signal analysis ?" or "Does patient show a specific heart disorder in the heart based on cardiac sound signal analysis ?" This stage basically involves development of pattern classification process to classify a set of cardiac signals. Specifically, the work in this thesis, focuses on automatic diagnosis of the heart valve, septal defects and CAD.

Diagnosis of heart disorders can be performed remotely using telemedicine which basically involves the use of telecommunication and information technologies. Telemedicine improves access to medical services for distant rural communities and reduces the overall cost of medical care [64, 65, 66, 67]. It is also used to save lives in critical care and emergency situations. The compression algorithm can reduce the power consumption in wireless sensor networks for better long term monitoring intended for telemedicine applications. Therefore, in this work, advanced signal processing based method for compression of cardiac sound signals has been developed that can facilitate data archiving and telemedicine procedures

for convenient diagnosis.

In this thesis, the mathematical background on TQWT has been presented in chapter 2. The details of the proposed methodologies in this work have been described from chapter 3 to chapter 7 as follows:

In chapter 3, automatic segmentation of cardiac sound signals into heart beat cycles has been proposed which is normally required for the diagnosis of heart disorders. The segmentation of the cardiac sound signals has been performed using TQWT as follows. The murmurs from cardiac sound signals have been removed by suitably constraining TQWT based decomposition and reconstruction. The Q-factor, redundancy parameter and number of stages of decomposition of the TQWT have been adapted to the desired statistical properties of the murmur-free reconstructed cardiac sound signals. The envelope based on CSCW has been extracted after the removal of low energy components from the reconstructed cardiac sound signals. Then the heart beat cycles have been derived from the original cardiac sound signals by mapping the required timing information of CSCW which is obtained using established methods. The experimental results are included in order to show the effectiveness of the proposed method for segmentation of cardiac sound signals in comparison with other existing methods for various clinical cases.

The chapter 4 of this thesis presents a newly proposed method for classification of cardiac sound signals using constrained TQWT. The proposed method begins with a constrained TQWT based segmentation of cardiac sound signals into heart beat cycles. The features obtained from heart beat cycles of separately reconstructed heart sounds and murmur can better represent the various types of cardiac sound signals than that from containing both. Therefore, heart sounds and murmur have been separated using constrained TQWT. Then the proposed novel raw feature set has been created by the parameters that have been optimized while constraining the output of TQWT and that of extracted by using time-domain representation and Fourier–Bessel (FB) expansion of separated heart sounds and murmur. However, the adaptively selected features have been used to obtain the final feature set for subsequent classification of cardiac sound signals using LS-SVM with various kernel func-

tions. The performance of the proposed method has been validated with publicly available datasets and the results have been compared with the existing short-time Fourier transform (STFT) based method.

The chapter 5 presents a new method for accurate and quick diagnosis of septal defects by automatic analysis of cardiac sound signals using TQWT based features. To start with, the established constrained TQWT based approach has been used in this study to derive the heart beat cycles from cardiac sound signals. Then the TQWT based decomposition of segmented heart beat cycles have been performed up to certain level. The combinations of sub-bands obtained during TQWT based decomposition has been used to extract the time-frequency domain based proposed features. The combinations of sub-bands obtained during TQWT based decomposition can be used to extract the diagnostic features. The correlation between sub-bands can characterize the various types of murmurs in cardiac sound signals. Therefore, in order to represent the murmurs in cardiac sound signals, proposed feature set was created with SAMDF that have been computed from reconstruction of decomposed sub-bands. In search of effective feature set based on SAMDF, various decomposition levels have been examined that could provide significant classification performance. Moreover, in order to establish the usefulness of the proposed method for diagnosis of septal defects, besides cardiac sound signals for septal defects and normal, this study covers signals to be detected for valvular defects and other defects like ventricular hypertrophy, constrictive pericarditis etc. as available from publicly available datasets. The classification has been performed using LS-SVM with different kernel functions. At each decomposition level under study, the effect of quality- factor (Q) of the TQWT from 1 to 50 on classification performance has been evaluated. The experimental results show that the proposed method has provided significant classification performance with tenth levels of decomposition for all the values of Q in the given range using Morlet wavelet kernel function. The test results demonstrate classification accuracy of 98.92% with sensitivity of 98.80% specificity of 99.29% and Matthews correlation coefficient of 0.9684 at tenth levels of decomposition for $Q = 6$. Moreover, in order to show the effectiveness of the proposed method, results have been compared with

existing method. The chapter 6 describes a new method for diagnosis of CAD using TQWT based features extracted from heart rate signals. The heart rate signals are decomposed into various sub-bands using TQWT for better diagnostic feature extraction. The nonlinear feature called centered correntropy (CCo) is computed on decomposed detail sub-band. Then the principal component analysis (PCA) is applied on these CCo to transform the number of features. These features are subjected to LS-SVM with different kernel functions for automated diagnosis. The experimental results demonstrate highest classification accuracy, sensitivity, specificity and Matthews correlation coefficient for Q=24 using Morlet wavelet kernel function with optimized kernel and regularization parameters. The proposed methodology is more suitable in classification of normal and CAD heart rate signals and aids the clinicians while screening the CAD patients.

The chapter 7 covers a new method for compression of cardiac sound signals using TQWT to improve the bandwidth and the storage efficiency for convenient diagnosis of heart disorders. In the proposed method, the cardiac sound signals have been compressed using TQWT, linear quantization, Huffman and RLC techniques. As the compression depends on various parameters, therefore the optimal values of these parameters have been found using GA with a subset of dataset. The proposed algorithm can reduce the power consumption in wireless sensor networks for better long term monitoring intended for telemedicine applications.

Chapter 8 concludes the work in this thesis and it discusses the possible future work.

Chapter 2

Mathematical Background Related to TQWT

2.1 Introduction

In the areas of applied mathematics, statistics, science, and engineering, the time-frequency methods or transforms are commonly applied to design specialized algorithms for processing, analyzing, and storing signals and image. Most of the signals under study belong to biomedical, speech, radar, sonar and telecommunications that exhibit non-stationary in nature. The short-time Fourier transform (STFT) and wavelet based methods such as discrete wavelet transform (DWT), continuous wavelet transform (CWT), Rational- dilation Wavelet Transform (RDWT), and Wavelet Packet transform (WPT) are the widely used time-frequency methods that are suitable for the analysis of nonstationary signals. The most appropriate time-frequency methods to apply depend on the type of signal being processed. The STFT is one of the first time-frequency methods used for the analysis of nonstationary signals. The STFT provides fixed resolution. The width of the windowing function used in STFT determines the time and frequency resolution. The choice of wider window provides better frequency resolution but poor time resolution. The selection of narrower window provides good time resolution but poor frequency resolution [68]. As compared to STFT, the wavelet

transforms can provide good time resolution for high-frequency events and good frequency resolution for low-frequency events, the joint property requisite for many real signals.

Recently, the TQWT has been proposed as a powerful transform for the analysis of oscillatory signals [1]. Most of the wavelet transforms other than CWT exhibit little ability to tune Q-factor. The CWT involves continuous time wavelet which cause to higher computational cost and it approximately satisfy reconstruction property. However, TQWT is quite flexible and efficient to use for desired analysis of signal under study by adjusting its input parameters like Q-factor. The TQWT is based on real valued scaling factors and the main input parameters of TQWT that are easily specified are Q-factor denoted as Q, total over-sampling rate or redundancy denoted as r and number of levels of decomposition denoted as j. The parameter Q controls the number of oscillations of the wavelet and the parameter r controls the undesired excessive ringing in order to localize the wavelet in time without affecting its shape. With increased value of Q, each frequency response becomes narrower resulting into more levels of decompositions to span the same frequency range. For fixed Q, increasing the value of r leads to increase in overlap between adjacent frequency responses resulting into more levels of decomposition to cover the same frequency range. The filters of TQWT are non-rational transfer functions which are conceptually easier to implement in frequency domain. In addition, the TQWT inherits the perfect reconstruction property of wavelet transform. The two forms of TQWT have been defined one for discrete time signal and other for finite length discrete time signal. The later is meant for efficient implementation using radix-2 FFT based structure of DWT.

2.2 TQWT based Decomposition and Reconstruction

The implementation of j^{th} level TQWT based decomposition is achieved by iteratively applying two channel filters banks to the low-pass sub-band signal as shown in Fig. 2.1. At each stage of TQWT based decomposition, the input signal $s[n]$ with sampling rate f_s is decomposed into low-pass sub-band signal $c^0[n]$ and high-pass sub-band signal $d^1[n]$ having

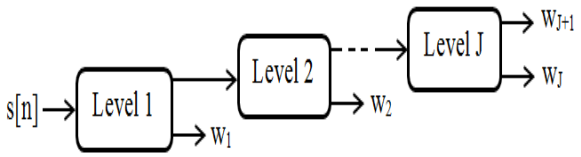

Figure 2.1. TQWT based J-level decomposition.

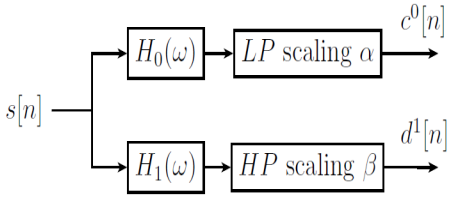

Figure 2.2. The single level TQWT based decomposition filter bank.

sampling frequencies αf_s and βf_s respectively as illustrated in Fig. 2.2. The generation of low-pass sub-band $c^0[n]$ uses low-pass filter $H_o(\omega)$ followed by low-pass scaling which is denoted as LP scaling α, and similarly the generation of high-pass sub-band $d^1[n]$ uses $H_1(\omega)$ and HP scaling β. The low-pass scaling preserves the low-frequency components of the signal and it depends on scaling parameter α. Similarly, the high-pass scaling preserves the high-frequency components of the signal and it depends on scaling parameter β. It has been shown that for perfect reconstruction $\alpha + \beta > 1$. In case if $\alpha + \beta = 1$, then the filter bank of TQWT is critically sampled with zero transition width and the $H_0(\omega)$ and $H_1(\omega)$ becomes ideal filter. The time-domain responses of these filters then changes to sampled sinc functions which are poorly localized and this is not the sought behavior. In order to prevent excessive redundancy $0 < \alpha < 1$ and $0 < \beta \leq 1$ [1]. The original signal can be reconstructed using the synthesis filter banks as illustrated in Fig. 2.3.

2.3 Scaling Functions

For $0 < \alpha \leq 1$, low-pass scaling which is denoted as LP scaling α is defined as [1]:

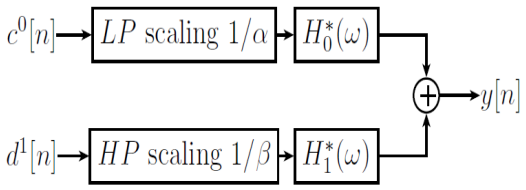

Figure 2.3. The single level TQWT based decomposition filter bank.

$$Y(\omega) = S(\alpha\omega), |\omega| \leq \pi, \tag{2.1}$$

For $0 < \beta \leq 1$, high-pass scaling which is denoted as HP scaling β is defined as [1]:

$$Y(\omega) = \begin{cases} S(\beta\omega + (1-\beta)\pi), 0 < \omega < \pi \\ S(\beta\omega - (1-\beta)\pi), -\pi < \omega < 0, \end{cases} \tag{2.2}$$

where $S(\omega)$ and $Y(\omega)$ are the discrete-time Fourier transforms of input signal $s[n]$ and output signal $y[n]$ respectively.

2.4 Non-rational Filter Banks

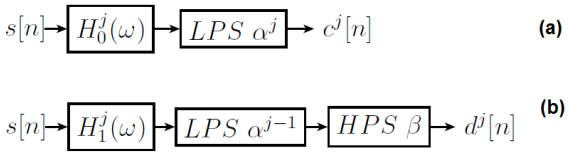

Figure 2.4. The equivalent system for j^{th} level TQWT based decomposition of input signal $s[n]$ to generate (a) the low-pass sub-band signal $c^j[n]$ and (b) the high-pass sub-band signal $d^j[n]$ [1].

The equivalent system for j^{th} level TQWT based decomposition of input signal $s[n]$ to generate the low-pass sub-band signal $c^j[n]$ and the high-pass sub-band signal $d^j[n]$ is shown in Fig. 2.4. The equivalent frequency response for low-pass and high pass sub-band signals

generated after j level is given by $H_o^{(j)}(\omega)$ and $H_1^{(j)}(\omega)$ respectively which are defined as[1]:

$$H_o^{(j)}(\omega) := \begin{cases} \prod_{m=0}^{j-1} H_o(\omega/\alpha^m), |\omega| \leq \alpha^j \pi \\ 0, \quad \alpha^j \pi < |\omega| \leq \pi, \end{cases} \tag{2.3}$$

$$H_1^{(j)}(\omega) := \begin{cases} H_1(\omega/\alpha^{j-1}) \prod_{m=0}^{j-2} H_o(\omega/\alpha^m), \\ \text{for} \quad (1-\beta)\alpha^{j-1}\pi \leq |\omega| \leq \alpha^{j-1}\pi \\ \\ 0, \text{for other } \omega \in [-\pi, \pi]. \end{cases} \tag{2.4}$$

where,

$$H_0(\omega) = \theta\left(\frac{\omega + (\beta-1)\pi}{\alpha+\beta-1}\right), \tag{2.5}$$

$$H_1(\omega) = \theta\left(\frac{\alpha\pi - \omega}{\alpha+\beta-1}\right), \tag{2.6}$$

It is to be noted that $\theta(\omega)$ is the frequency response of the Daubechies filter having two vanishing moments. $\theta(\omega)$ can be defined as follows:

$$\theta(\omega) = 0.5(1+\cos(\omega))\sqrt{2-\cos(\omega)}, |\omega| \leq \pi \tag{2.7}$$

2.5 Parameters of TQWT

The TQWT facilitates analysis of oscillatory signals with easily adjustable parameters [1]. The three input parameters of TQWT can be briefly described as follows.

For analysis of oscillatory signals, the value of Q is specified higher such that the underlying wavelets consist of more oscillations with narrower frequency responses relative to their center frequencies. Therefore, it requires more levels of decompositions to cover the spectrum of the signal under study. The property of high Q makes TQWT suitable for effective sparse representation and processing of oscillatory signals. For analysis of piecewise smooth signals like transients, Q is specified lower such that the underlying wavelets consist of fewer oscillations with wider frequency responses relative to their center frequencies that

necessitate relatively fewer levels to cover the spectral content of the signal under study. The property of low value of Q makes TQWT more suitable for the extraction of the transient components. At some level of decomposition, say j, the Q of TQWT can be defined in terms of center frequency and bandwidth as follows:

$$Q = \frac{f_c(j)}{BW(j)} \tag{2.8}$$

where, $f_c(j)$ and $BW(j)$ represent the center frequency and bandwidth respectively and,

$$f_c(j) = \alpha^j \frac{2-\beta}{4\alpha}, j = 1, 2, ..., J. \tag{2.9}$$

$$BW(j) = \frac{1}{2}\beta\alpha^{j-1}\pi, j = 1, 2, ..., J. \tag{2.10}$$

The parameter r helps localize the wavelet in time without affecting its shape. As shown in equations (2.9) and (2.10), for a certain Q, with increase in j, the value of $f_c(j)$ decreases and the associated BW also get reduces. Moreover, the time-domain duration of the wavelets becomes wider as shown in Fig. 2.5. With increased value of Q, each frequency response becomes narrower resulting into more levels of decomposition to span the same frequency range as shown in Fig. 2.6. For fixed Q, increasing the value of r leads to increase the overlap between adjacent frequency responses resulting into more levels of decomposition to cover the same frequency range as shown in Fig. 2.7.

The values of r and Q can be expressed in terms of filter bank parameters α and β as follows [1]:

$$r = \frac{\beta}{1-\alpha}, \qquad Q = \frac{2-\beta}{\beta}. \tag{2.11}$$

Considering the J-stage TQWT based decomposition, J+1 sub-band signals are obtained. These sub-band signals can be arranged in a cell array C as follows [1]:

$$C = \{w_1, w_2, w_3, ..., w_J, w_{J+1}\}, \tag{2.12}$$

where, w_{J+1} is the sub-band signal having lowest frequency and the sub-band signals from w_1 to w_J are high frequency signals. The number of samples in each of these sub-band signals

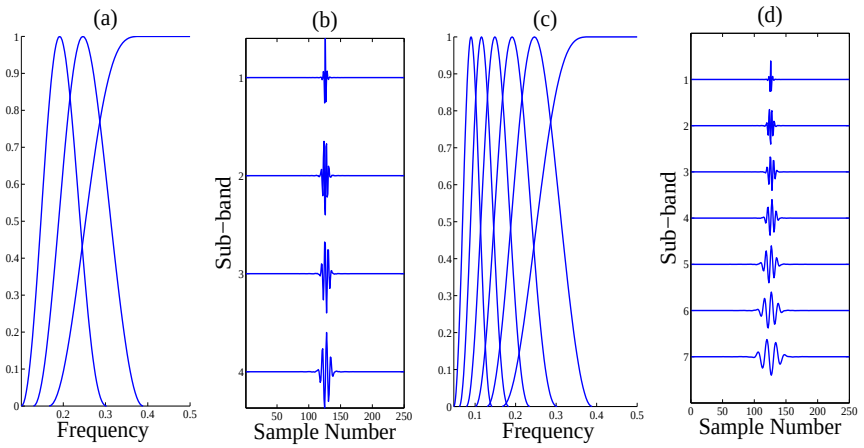

Figure 2.5. The effect of TQWT parameter J on normalized frequency responses (a, c) and sub-bands (b, d) : (a, b) for Q=2 and J=3 with r=3 and (c, d) for Q=2 and J=6 with r=3.

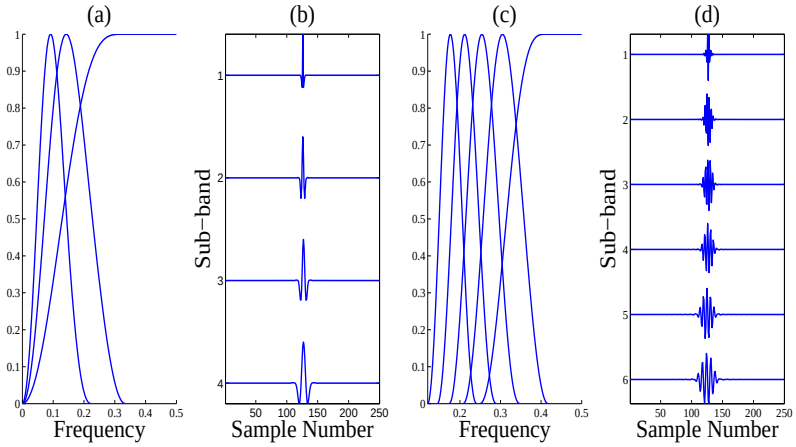

Figure 2.6. The effect of TQWT parameter Q on normalized frequency responses (a, c) and sub-bands (b, d) : (a, b) for Q=1 and J=3 with r=3 and (c, d) for Q=3 and J=5 with r=3.

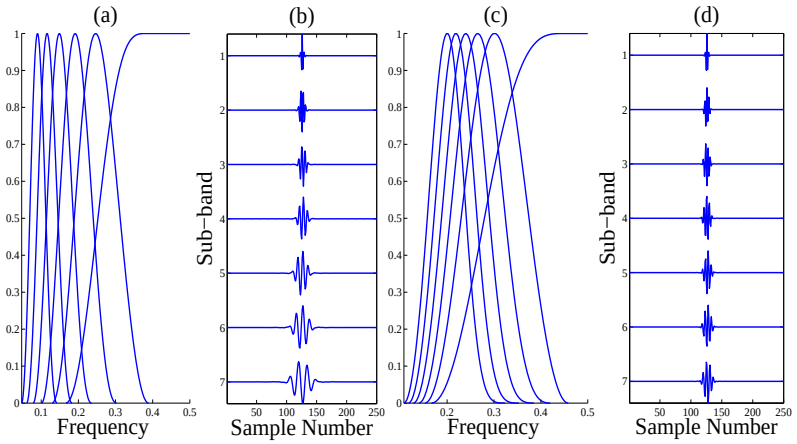

Figure 2.7. The effect of TQWT parameter r on normalized frequency responses (a, c) and sub-bands (b, d) : (a, b) for Q=2 and J=6 with r=3 and (c, d) for Q=2 and J=6 with r=8.

can be obtained using the values of scaling parameters as follows [1]:

$$C_l = [\beta f_s N, \alpha\beta f_s N, \alpha^2\beta f_s N, ..., \alpha^{J-1}\beta f_s N, \alpha^J f_s N], \tag{2.13}$$

where, N is the number of samples in $s[n]$.

In the conventional TQWT, it is difficult to automatically change the values of the input parameters depending upon the input signal for obtaining the desired signal component in the output reconstructed signal. Therefore, in this work, constrained TQWT has been proposed that can adaptively choose the input parameter such that required signal component of interest appear in the reconstructed output. The proposed system uses the relative knowledge of the signal components, one that needs to be retained and other that needs to be removed, known in advance to constrain the output. The more details about this method are described in section 3.3.3.

Chapter 3

Segmentation of Cardiac Sound Signals using Constrained TQWT

3.1 Introduction

All the cardiac events take place during a heart beat cycle of cardiac sound signal and it can provide the information about the functioning of heart valves and hemodynamics. Therefore segmentation of cardiac sound signals into heart beat cycles is required for diagnosis. The normal heart beat cycles contain the S1 and S2 heart sounds which are referred to as primary heart sounds. However, the abnormal heart beat cycles may contain murmurs, S3 and S4 heart sounds, and other aberrations due to different pathologies of the cardiovascular system [12]. The automatic segmentation of cardiac sound signals is a challenging task due to inconsistent lengths of the heart beat cycles, variation of the number of heart sound components inside individual heart beat cycles, the unpredictable existence of murmurs and the presence of various types of noises like lung sounds, rubbing of stethoscope on the chest etc. These constrains can cause to inaccurate segmentation in turn limiting the performance of the next stages of algorithm for automatic identification of heart valve disorders [45, 69, 70, 71, 72].

The automatic segmentation of cardiac sound signals can be achieved either by using

reference signal or without using any reference signal. The subsequent discussed methods use ECG signal as a reference signal for segmentation. Instantaneous energy of the ECG signal has been used to segment the cardiac sound signals in [73]. Segmentation based on the time-domain and frequency-domain characteristics of the components of the heart beat cycles have been proposed in [74, 75] and [76] respectively. These methods can achieve high performance but diagnostic procedure may become cumbersome for patient and even for a medical expert at massive medical camps as attaching and removing ECG electrodes to the patient may take long time. Therefore, recent segmentation algorithms use only cardiac sound signals for convenient diagnosis [77, 78].

The method for segmentation using the envelope of cardiac sound signal has been developed in [79]. Energy and simplicity-based segmentation with wavelet decomposition coefficients has been proposed in [80]. The segmentation based on wavelet transform (WT) involving the extraction of CSCW is provided in [81]. Due to inherent limitations these methods are incapable of significantly removing murmurs in turn affecting the efficacy of segmentation. Moreover, these methods require evaluation of the segmentation performance for exhaustive number of clinical cases. The segmentation algorithm employing high frequency signatures is provided in [82]. However, some murmurs having high frequency signatures may affect the results. Information regarding the popular envelope based segmentation methods along with their relative comparison has been presented in [83]. The method for detecting boundaries of primary heart sounds for available heart beat cycles has been used in [77, 84].

The ergodic hidden Markov model (HMM) for classification of a cardiac sound signals into four components: S1 heart sound, systolic phase, S2 heart sound, diastolic phase has been proposed in [85]. In several HMM based methods there is no user input requirement and the training process is required for system development [86, 87]. The moment-based algorithm has been presented to be simpler and faster than conventional WT based method [88]. However, the algorithm assumes cardiac sound signals to be approximate cyclical signals and it is not easy to vary the value of the used scale parameter in different clinical cases. The performance of the autocorrelation and instantaneous cycle frequency based

segmentation [89, 45] depends largely on variability of heart rate as these methods assume the cardiac sound signals to be stationary. The homomorphic envelogram and self-organizing probabilistic model have been applied for detection and identification of heart sounds in [90]. Recently, adaptive singular spectrum (SSA) analysis to detect murmur or primary heart sounds has been proposed in [91].

In this chapter, we present a new method for removing murmurs based on TQWT for efficient envelope based segmentation of cardiac sound signals. The TQWT is powerful technique for analysis and processing of oscillatory signals [1]. The method is based on constraining TQWT based decomposition and reconstruction with adaptive selection of its input variables. The experimental results of the proposed method for removal of murmurs can provide better results because by varying the Q-factor the shape of wavelet can be matched with primary heart sounds and redundancy parameter can reduce the ringing effects in turn improving the localization of primary heart sounds with respect to overlapping murmurs. Furthermore, the proposed method incorporates the advantage of CSCW extraction in order to improve the performance of the overall segmentation of cardiac sound signals. The rest of the chapter is organized as follows: The decimation and amplitude normalization, the constrained TQWT based decomposition and reconstruction for removing murmurs, low energy component removal, the extraction of CSCW, peak detection and boundary estimation of the methodology are presented in section 3.2. The experimental results and comparative study of the proposed method are given in section 3.3 and section 3.4 respectively. Finally, section 3.5 summarises the chapter.

3.2 Methodology

The subsections of the proposed method for segmentation of the cardiac sound signals into heart beat cycles are depicted in Fig. 3.1. The subsections include: decimation and amplitude normalization, constrained TQWT based decomposition and reconstruction, low energy component removal, CSCW extraction, peak detection and boundary estimation. The details

of each subsection are described as follows:

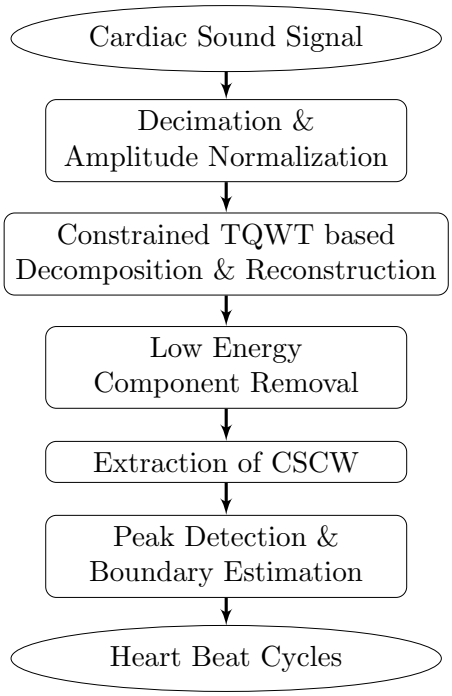

Figure 3.1. The signal processing flow of the proposed method for segmentation of the cardiac sound signals into heart beat cycles.

3.2.1 Decimation and Amplitude Normalization

In order to reduce the time of execution of the algorithm, the input signal is decimated by a factor of 32 from sampling frequency of 44.100 kHz to sampling frequency of 1378.125 Hz [45, 92]. This process may not significantly affect the primary heart sounds containing low frequency components. Even the diagnostic murmurs containing high frequency components may not be get affected significantly because the average murmurs have frequency range between 100 Hz to 600 Hz [16]. The decimation is followed by amplitude normalization which takes into account the variations in the recordings due to changes in pressure applied on the chest surface and the amplifier setting.

3.2.2 Constrained TQWT based Decomposition and Reconstruction

Generally, the primary heart sounds are limited in time duration and have relatively larger magnitude as compared to murmurs. Therefore, the distribution of primary heart sounds is super-Gaussian having sharper peak and often skewed toward left with relatively larger value of the kurtosis as compared to murmurs. On the other hand, the distribution is nearly Gaussian or sub-Gaussian for the murmurs [91]. This knowledge about statistical properties of primary heart sounds and murmurs can be used to constrain the TQWT during decomposition stages such that the reconstructed signal contains only the desired signal component of interest.

In order to remove murmurs, the input parameters of TQWT based decomposition are adaptively selected such that primary heart sounds having maximum kurtosis are obtained in the reconstructed signal. The primary heart sounds are low frequency component therefore the low pass sub-band at last output stage of TQWT based decomposition is used for signal reconstruction. The constrained TQWT based decomposition and reconstruction is effective in enhancing primary heart sounds because by varying the Q-factor the shape of wavelet can be matched with primary heart sounds and redundancy parameter can reduce the ringing effects in turn improving the localization of primary heart sounds with respect to overlapping murmurs.

During constraining the TQWT based decomposition and reconstruction, the input parameters can be adapted by using any suitable optimization method. Many optimization methods have been proposed in the literature but genetic algorithms are found to be more effective in global optimization [93]. Therefore, in this study genetic algorithm has been used to optimize the TQWT based decomposition for maximizing information of the desired signal component in the reconstructed signal.

3.2.3 Low Energy Component Removal

The signal processing at this stage involves the removal of low energy components from the reconstructed cardiac signal $x_r[n]$. The presence of these components may affect the performance of the peak detection stage for determining the heart beat cycles. The extent of removal of these low amplitude components in the noise attenuated signal $x[n]$ can be decided by analyzing the histogram $h(i)$ and cumulative histogram $c(i)$ which can be obtained as follows [45]:

$$h(i) = \sum_{n} d(x_r[n], i); \quad d(k_1, k_2) = \begin{cases} 1, k_1 = k_2 \\ 0, k_1 \neq k_2 \end{cases} \quad , 0 \leq i \leq A, \tag{3.1}$$

$$c(i) = \sum_{x_r=0}^{i} h(x_r), \quad 0 \leq i \leq A, \tag{3.2}$$

where A denotes the maximum amplitude of the signal $x_r[n]$. The threshold for removing low energy components can be decided by using the parameter λ which is obtained by $c(j) = c(A) \times \lambda$. For current experimental analysis λ is set to 0.93, which is found to be effective for removing the low energy components. The noise attenuated signal can be obtained as:

$$x[n] = \begin{cases} x_r[n], |x_r[n]| \geq j \\ 0, \text{otherwise.} \end{cases} \tag{3.3}$$

3.2.4 Extraction of CSCW

An analytical model based on single-degree-of-freedom (SDOF) system can be used for extracting CSCW of the cardiac sound signals [83, 81]. The model assumes the presence of the mass, spring, and the damper to represent the phenomena. The relationship between the input signal $X(t) = |x_{\text{norm}}(t)|$ and the output response $Y(t)$ of this system can be expressed as [94]:

$$M\ddot{Y}(t) + D\dot{Y}(t) + KY(t) = X(t), \tag{3.4}$$

where M, K, and D represent the mass, the spring coefficient, and the damping coefficient respectively. The above equation can also be expressed as:

$$\ddot{Y}(t) + 2\omega\zeta\dot{Y}(t) + \omega^2 Y(t) = \bar{X}(t), \tag{3.5}$$

where $\bar{X}(t) = \pm|X(t)/M|$, resonant angular frequency is $\omega = \sqrt{K/M}$ rad/s and the damping parameter is $\zeta = D/2\sqrt{MK} \times 100$ %. The default values of ω and ζ used in this analysis are set to 62.832 rad/s and 70.7 % respectively. In order to compensate for time delay between input signal $X(t)$ and above obtained waveform $Y(t)$ the cross correlation $XC[i]$ is used which is calculated as follows [83, 81]:

$$XC[i] = \frac{\sum_{n=0}^{N-1} \left(X[n] - \mu_X\right)\left(Y[n-i] - \mu_Y\right)}{\sqrt{\sum_{n=0}^{N-1} \left(X[n] - \mu_X\right)^2}\sqrt{\sum_{n=0}^{N-1} \left(Y[n-i] - \mu_Y\right)^2}}, \tag{3.6}$$

where delay $i = 1, 2, ..., N$. N is the number of samples, and μ_X and μ_Y are the average values of $X[n]$ and $Y[n]$ respectively. Finally, the CSCW which is represented as $W[n]$ can be obtained by using peak location (XC_p) of the cross correlation curve with the following formula:

$$W[n] = Y\left[n + \left|XC_p - \frac{N}{2}\right|\right]. \tag{3.7}$$

3.2.5 Peak Detection and Boundary Estimation

The peak detection method includes the picking up of the required peaks of primary heart sounds and rejecting the extra peaks as described in [79]. In order to separate the peaks of primary heart sounds from the background proper threshold can be applied either manually or automatically by fuzzy c-means clustering as suggested in [83, 81, 79, 95, 96, 97]. The more details about clustering of primary heart sounds can be obtained from [89, 98, 99]. The peak identification method facilitates the recognition of S1 and S2 heart sound based on the general fact that the diastolic interval is greater than the systolic interval. Moreover, the systolic interval is relatively constant as compared with diastolic interval. A segmented

heart beat cycle begins and ends with either S1 heart sound or S2 heart sound of the two consecutive heart beat cycles. Therefore, after the identification of peaks of primary heart sounds, the approximate boundaries of either S1 heart sound or S2 heart sound can be used to extract the timing information of the heart beat cycles as described in [79, 76]. Finally, the heart beat cycles can be derived by mapping this timing information of CSCW to the original cardiac sound signals.

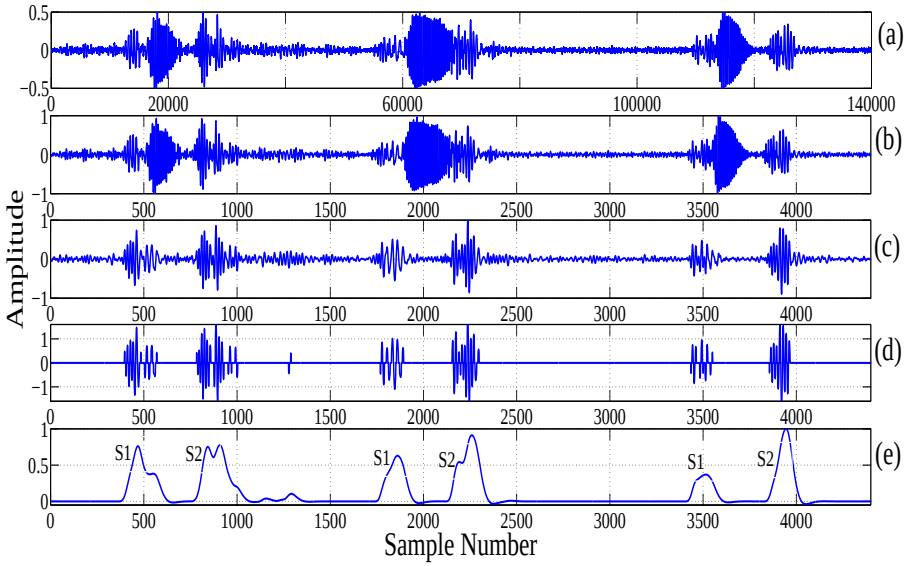

Figure 3.2. An example of cardiac sound signal processing using proposed method: (a) original tricuspid regurgitation signal, (b) the decimated signal, (c) reconstructed signal, (d) the noise attenuated signal, (e) CSCW based envelope showing detected primary heart sounds which can be used to derive the heart beat cycles.

3.3 Experimental Results

The dataset used in this work is the heart sounds pod cast series (2011) produced by the Robert J. Hall Heart Sounds Laboratory of Texas Heart Institute at St. Luke's Episcopal Hospital. The dataset contains 50 abnormal cardiac sound signals acquired from variety

of subjects with relevant chest positions with different patient maneuver. The sampling frequency of most of the data is 44.100 kHz except for few cases. Some of the recordings in the dataset were corrupted by the human voice, rubbing sound due to stethoscope and other lung sounds. Also, the duration of the heart beat cycles are inconsistent. For more information regarding the dataset, this series is available at [100].

An example of the proposed method is shown for two heart beat cycles of tricuspid regurgitation in Fig. 3.2. The reconstructed signal is obtained after adaptively selecting following values of the parameters $r = 11$ and $j = 11$ at $Q = 1$. The example demonstrates the output at main stages of the proposed method for segmentation of cardiac sound signals using constrained TQWT based removal of murmurs.

In order to remove murmurs, the input parameters of TQWT based decomposition are adaptively changed such that primary heart sounds having maximum kurtosis are obtained in the reconstructed signal. The primary heart sounds are low frequency component therefore the low pass sub-band at last output stage of TQWT based decomposition is used for signal reconstruction. The silent feature of constraining TQWT based decomposition and reconstruction is that it not only helps in identifying primary heart sounds with low Q but facilitates in localizing primary heart sounds with respect to overlapping murmur with high value of r. The experiment has been conducted with all possible values of Q and obtained results are found to be better when its value is one which is accompanied usually with high value of r. One possible reason for this could be that the wavelet at this Q better matches with primary heart sounds. Obviously the significant contribution of the proposed method is that it automatically adjusts to the severity of the murmurs. When murmurs are severe the required levels of the TQWT based decomposition (j) would be more and if they overlap with primary heart sounds the required redundancy would be more so that the primary heart sounds are well localized in time. The method is found very efficient in extracting primary heart sounds overlapping with murmur. Moreover, it performs well even when amplitude of murmur is comparable to primary heart sounds.

During constraining, the optimized values of r and j are adaptively selected using genetic

algorithm with following settings. The range of values of r and j are set to integer with stall generations=5, generation=10 and population=10 for reducing the time of execution of the algorithm. Moreover, by using trial and error approach it has been found that suitable bound for r is from 12 to 18 and for j is from 1 to 20.

In order to evaluate the performance of the proposed method in removing murmur the correct segmentation has been defined in terms of segmentation rate (denoted as SR) as the ratio of correctly segmented heart beat cycles (SB) to the actual total number of heart beat cycles (TB). Moreover, the method has been tested for a variety of clinical cases which are comprised in the dataset. Table 3.1 depicts the statistics concerning the effectiveness of segmentation achieved by our method. In this study, automatic threshold using fuzzy c-means clustering is used as described in [83, 81]. The duration between peaks and width of peaks obtained in sequence after applying threshold are used as input to the fuzzy c-means clustering to determine the clusters. The minimum value of objective function used for fuzzy c-means clustering with variable threshold corresponds to the required threshold. In order to reduce the time of execution, the required threshold (THV) is determined by varying the threshold in steps of 5 percent of the range of amplitude of the extracted CSCW based envelope. The results are discouraging in case of Austin flint rumble due to presence of multiple peaks corresponding to third heart sound and severe murmur with rumble. Moreover, in this case manual setting of parameters is required for constrained TQWT based murmur removal and segmentation. For other cases, the adjustments are automatic. For reference, the actual number of heart beat cycles comprised in each clinical case of the tabulated results is manually labeled by an experienced cardiologist.

3.4 Comparison with other Existing Methods

In this section, the results of murmur removal for segmentation of cardiac sound signals using the proposed method with constrained TQWT based decomposition and reconstruction are compared to two other popular methods based on conventional WT and adaptive SSA. In

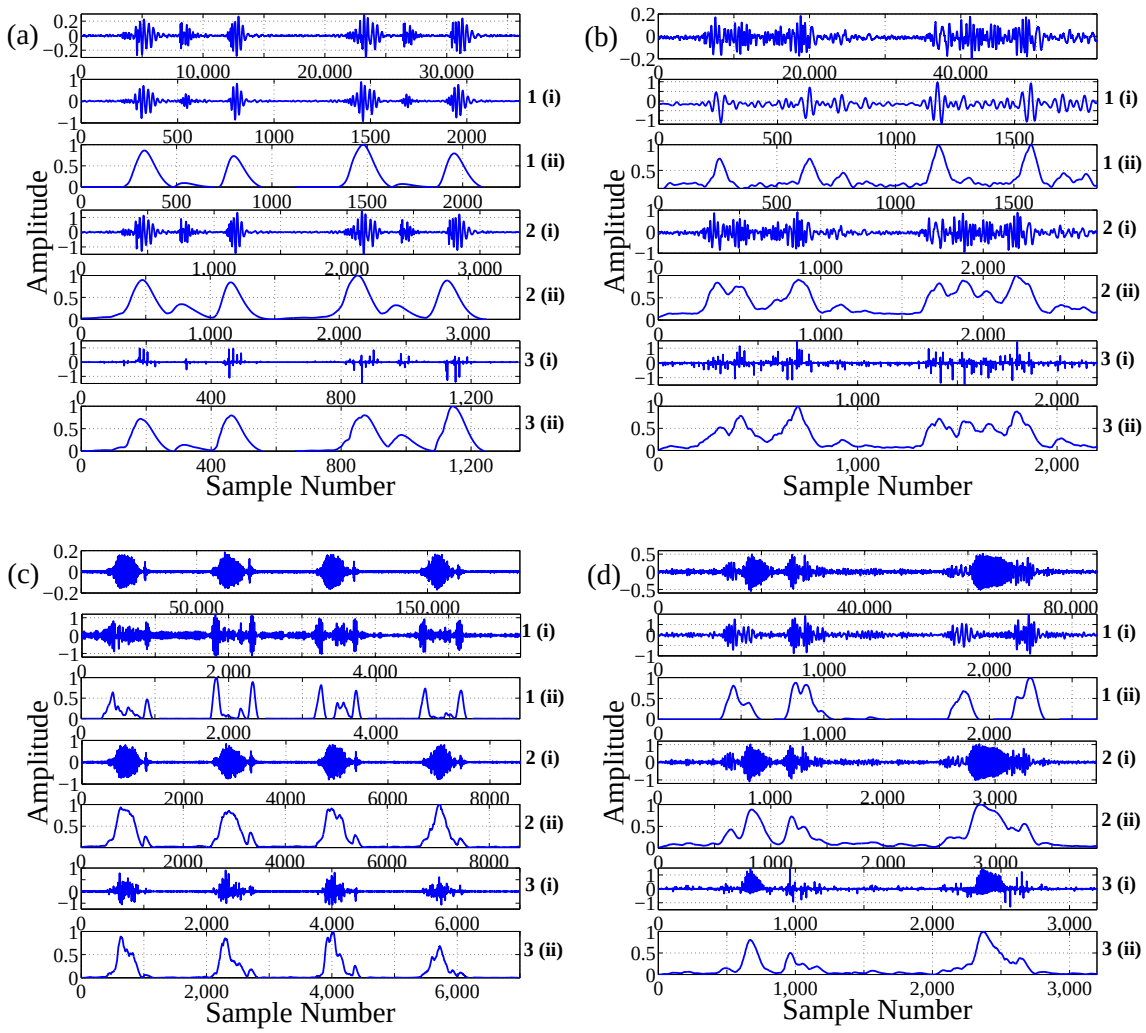

Figure 3.3. Comparison of results of proposed method with other methods in removing murmur for (a)-(d): Midsystolic click, Mitral regurgitation, Aortic stenosis and Tricuspid insufficiency. The numbers 1-3 represent the TQWT, WT, SSA based method respectively. The lower-case Roman numbers (i) and (ii) represent the reconstructed signal and its CSCW based envelope respectively.

the WT based method Daubechies-10 wavelet has been used to decompose input cardiac sound signals. The envelope is then extracted using CSCW after the reconstruction of the cardiac sound signals retaining the second level decomposed approximation coefficients. The details of the method are described in [83, 81]. The main limitation of the method is that the both the mother wavelet and number of levels of decomposition are kept fixed. Moreover, employing WT in the current proposed framework would not be as versatile as TQWT. This is due to the fact that WT cannot offer flexibility in varying sufficient number of input variables with respect to desired characteristics of reconstructed signal. On the other hand, constraining TQWT based decomposition and reconstruction provides effective enhancement of primary heart sounds because by varying the Q-factor the shape of wavelet can be matched with primary heart sounds and redundancy parameter can reduce the ringing effects in turn improving the localization of primary heart sounds with respect to murmurs. The adaptive SSA method is similar to the proposed method regarding adapting itself to the prior known statistical properties of the desired component in the reconstructed signal. In this method the sub-space size of the murmur free reconstructed cardiac sound signal is optimized using maximum kurtosis of the same as a constraint [91]. Even though the method uses statistical parameter to maximize the information regarding the primary heart sounds, it still lacks the parameter concerning its shape. Thus the main limitation of this method is that it does not take into account the shape of primary heart sounds and therefore it is unable to extract and localize primary heart sounds with respect to the overlapping murmurs as shown in Fig. 3.3. Another important fact is that both of these above methods lack exclusive study which considers more number of clinical cases. The constrained TQWT based decomposition and reconstruction on the other hand is found robust in removing all types of murmurs. It facilitates the integration of the main morphological characteristics of primary heart sounds along with statistical properties by varying its three input variables namely Q-factor which controls the shape of wavelet, redundancy which localizes the required information (or event) and the number of level of TQWT based decomposition which controls the frequency content. Altogether by adapting these input parameters, efficient extraction of the primary heart

sounds can be done from overlapping murmur even when the amplitude of the murmur is comparable to primary heart sounds. Table 3.1 shows the comparative study of the proposed method and methods based on adaptive SSA and conventional WT. In order to demonstrate the efficacy of the proposed method in removing murmur as compared with other popular methods, the four representative clinical cases which have been considered as examples are mid systolic click, mitral regurgitation, aortic stenosis and tricuspid insufficiency. For better comparison, the reconstructed signal and its CSCW based envelope of each approach are considered in the displayed results in Fig. 3.3. The examples are briefly described as follows:

I. Midsystolic Click

In midsystolic click, click may occur any time during systole. In general the click is high frequency sound with perceptible loudness. The proposed method with constrained TQWT based decomposition and reconstruction has been found to suppress this high frequency click more significantly than the other two popular methods as shown in Fig. 3.3 (a). The reconstructed signal is achieved with adaptively selected following values of parameter $r = 17$ and $j = 11$ at $Q = 1$. The suppression of click may help in reducing the interference of the click during establishing threshold and peak processing step thus giving better segmentation rate. This case is exceptional due to sampling frequency of 22.050 kHz therefore in order to obtain the desired sampling frequency of 1378.125 Hz the input signal is decimated by a factor of 16.

II. Mitral Regurgitation

The mitral regurgitation contains the holosystolic murmurs. The murmur goes into and obscures the S2 heart sound. The murmur is usually flat in intensity and blowing in pitch or timbre. When the regurgitation is of large magnitude, diastolic blood returns from the atrium to the ventricle producing a S3 heart sound and a diastolic flow rumble (FR). All of these features can be easily seen in the signal in Fig. 3.3 (b). In this case, the conventional WT and adaptive SSA based method are unable to discriminate between the primary heart sounds with overlapping murmurs. On the other hand, in spite of the flat nature of the murmur, it can be observed that the proposed method clearly identifies the primary heart

sounds and attenuates the murmurs which are of comparable in loudness to that of the primary heart sounds. The reconstructed signal is achieved with adaptively obtained $r = 17$ and $j = 19$ at $Q = 1$.

III. Aortic Stenosis

The cardiac sound signal associated with aortic stenosis contains consistent diastolic murmurs that have a diamond or kite like shape and they are referred to as crescendo-decrescendo murmurs. In this case, the performance of proposed method in suppressing the complex diastolic murmurs is encouraging. The other two compared methods are not able to separate S1 heart sound from overlapping murmurs. Moreover, the performance these methods in enhancing S2 heart sound, to ease its detection, are unsatisfactory. This can be judged by observing the differences in the envelope curves as shown in Fig. 3.3 (c). The reconstructed signal is achieved with adaptively selected $r = 14$ and $j = 18$ at $Q = 1$.

IV. Tricuspid Insufficiency

The soft holosystolic murmur characterizes the heart sounds of tricuspid insufficiency. The murmur may be high pitched in case if the regurgitation is trivial and it may be medium pitched if the regurgitation is severe. These murmurs are attenuated effectively by using the proposed method based on constrained TQWT based decomposition and reconstruction as shown in Fig. 3.3 (d). As with aortic stenosis case, in this case also, the other two methods are unsuccessful in identifying the primary heart sounds from the background murmurs. The reconstructed signal is achieved with automatically estimated $r = 12$ and $j = 20$ at $Q = 1$.

Table 3.1. The statistics of segmentation of the cardiac sound signals using constrained TQWT in comparison with other methods.

Method/Disease	TQWT based			SSA based			WT based		
	THV	SB/TB	SR (%)	THV	SB/TB	SR (%)	THV	SB/TB	SR (%)
Hypertrophic obstructive cardiomyopathy									
case 1	75	10/10	100	20	8/10	80.00	15	8/10	80.00
case 2	35	35/39	89.74	40	18/39	46.15	35	21/39	53.84
case 3	15	40/46	86.96	30	28/46	60.86	20	32/46	69.56
Opening snap of mitral stenosis									
case 1	15	11/11	100	50	10/11	90.90	25	9/11	81.82
case 2	25	15/15	100	60	15/15	100	70	15/15	100
case 3	20	14/14	100	25	12/14	85.71	15	12/14	85.71
Aortic regurgitation									
case 1	20	29/31	93.55	25	22/31	70.96	35	20/31	64.51
case 2	20	27/32	84.38	30	15/31	48.39	35	20/32	62.50
Aortic valve ejection sound									
case 1a	35	9/9	100	45	8/9	88.89	35	7/9	77.78
case 1b	30	9/9	100	50	6/9	66.67	35	8/9	88.89
case 1c	25	10/13	76.92	60	10/13	76.92	55	10/13	76.92
case 2a	25	10/16	62.50	50	10/16	62.50	70	10/16	62.50
Mitral valve stenosis									
case 1	35	15/16	93.75	50	12/16	75.00	75	14/16	87.50
case 2	30	14/14	100	15	11/14	78.57	25	13/14	92.86
case 3	15	9/12	75.00	45	9/12	75.00	65	12/12	100
case 4	15	11/12	91.67	15	10/12	83.34	15	11/12	91.67
Midsystolic click									
case 1a	20	17/17	100	15	13/17	76.47	20	16/17	94.11

Continued on next page

Table 3.1 *Continued*

Method/Disease	TQWT based			SSA based			WT based		
	THV	SB/TB	SR (%)	THV	SB/TB	SR (%)	THV	SB/TB	SR (%)
case 1b	20	6/6	100	15	3/6	50.00	25	5/6	83.34
case 2a	35	68/68	100	30	51/68	75.00	40	65/68	95.59
case 2b	15	34/35	97.14	20	26/35	74.29	40	34/35	97.14
case 3a	15	43/43	100	35	39/43	90.70	30	37/43	86.04
case 3b	15	27/27	100	35	23/27	85.19	35	21/27	77.78
case 3c	15	19/19	100	25	19/19	100	50	19/19	100
case 3d	15	27/27	100	50	24/27	88.89	30	21/27	77.78
case 3e	30	16/20	80.00	25	14/20	70.00	40	16/20	80.00
Mitral regurgitation									
case 1	15	16/18	88.88	50	9/18	50.00	60	12/18	66.67
case 2a	30	8/9	88.88	40	4/9	44.45	65	1/9	11.11
case 2b	35	13/16	72.23	50	13/16	81.25	45	5/16	31.25
Aortic stenosis									
case 1	15	21/25	84.00	55	21/25	84.00	75	21/25	84.00
case 2	15	40/46	86.96	20	40/46	86.96	40	40/46	86.96
Third heart sound									
case 1	30	10/11	90.90	35	9/11	81.82	30	10/11	90.90
case 2	30	29/30	96.66	20	13/30	43.34	20	10/30	33.33
Fourth heart sound									
case 1	45	29/29	100	50	24/29	82.76	35	18/29	62.07
case 2	45	30/30	100	50	24/30	80.00	35	18/30	60.00
Tricuspid valve insufficiency	25	26/27	96.29	40	2/27	7.40	20	19/27	70.37
Paradoxical split S2	20	39/41	95.12	25	25/41	60.98	30	27/41	65.85
Tumor plop	40	20/20	100	15	8/20	40.00	55	20/20	100
Pericardial knock									

Continued on next page

Table 3.1 *Continued*

Method/Disease	TQWT based			SSA based			WT based		
	THV	SB/TB	SR (%)	THV	SB/TB	SR (%)	THV	SB/TB	SR (%)
	30	18/18	100	15	9/18	50.00	30	18/18	100
Fixed splitting of S2	25	27/31	87.10	30	17/31	54.84	15	16/31	51.61
Wide splitting of S2	20	21/21	100	25	18/21	85.71	35	21/21	100
Flail mitral regurgitation									
case 1	20	13/13	100	25	2/13	15.38	65	13/13	100
case 2	20	12/12	100	20	8/12	75.00	25	4/12	75.00
Physiologic split of S2									
case 1	20	21/23	91.30	25	8/23	34.78	20	19/23	82.61
case 2	20	21/23	91.30	15	14/23	60.87	25	19/23	82.61
Austin flint rumble									
case 1	15	24/36	66.66	30	18/36	50.00	30	18/36	50.00
case 2	30	11/16	68.75	30	5/16	31.25	30	5/16	31.25
Pulmonary valve ejection sound									
case 1	15	15/16	93.75	40	12/16	75.00	45	14/16	87.50
case 2	15	26/28	92.86	35	22/28	78.57	30	26/28	92.86
Total			92.15			67.81			76.75

The computational complexity of the algorithms can be compared in terms of time complexity. In this study, the proposed method has been compared to other aforementioned methods with respect to the time complexity involved for murmur-free reconstruction of aortic stenosis signal having significant murmur. We have implemented all the main functions in Matlab using mfiles. The functions of the TQWT toolbox and genetic algorithm &

Table 3.2. The comparison of total execution time and speed up of proposed method with other existing methods for aortic stenosis signal.

	Run-times (seconds)			Speed up	
Signal length (N)	TQWT based method	SSA based method	WT based method	TQWT vs SSA	WT vs TQWT
44100	0.303831	3.705798	0.004793	12.20	63.39
88200	0.525625	7.009681	0.003339	13.34	157.42
176400	1.032956	14.061908	0.007810	13.61	132.26
352800	1.364058	27.970593	0.010920	20.51	124.91
705600	3.299968	56.173435	0.012764	17.02	258.32
1411200	5.559958	112.418065	0.030618	20.21	181.59
2822400	13.398961	225.619284	0.046962	16.84	285.32
5644800	27.908387	451.378124	0.105820	16.17	263.73
11289600	31.208611	917.718216	0.203534	29.41	153.34

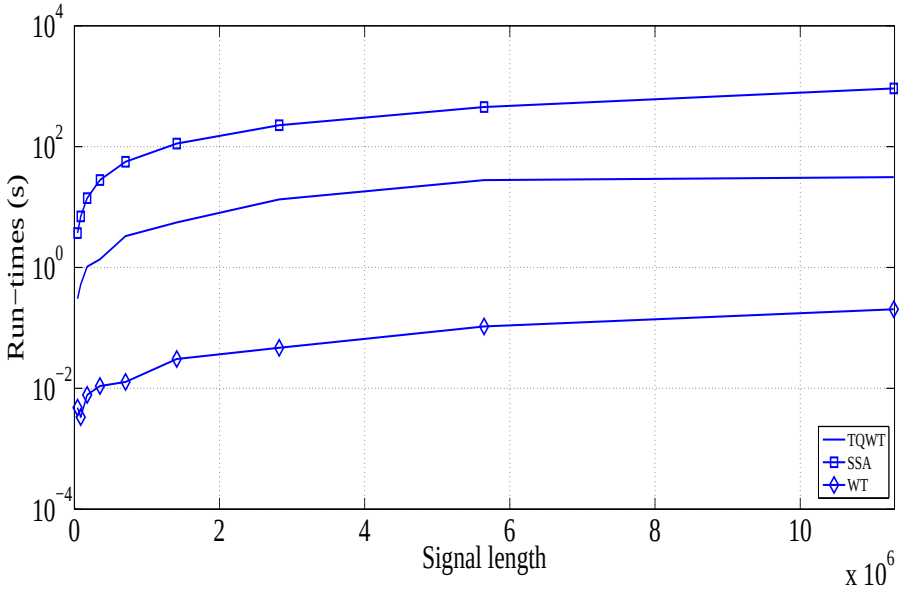

Figure 3.4. Run-times of murmur-free reconstruction of aortic stenosis signal for methods based on TQWT, SSA and WT. In case of proposed method, the timings are performed with adaptive values of parameter r and j at $Q = 1$.

direct search toolbox of Matlab have been used for implementing the proposed method. The Matlab software for TQWT toolbox is available at http://eeweb.poly.edu/iselesni/ TQWT/. The timings have been performed on a Dell personal computer with single CPU dedicated to Matlab version 7.7.0 (R2008b). The configuration of the computer which has been used for implementation is PCWIN with Intel (R) core (TM) i7 2600 CPU @3.40 GHz and system type 64 bit Windows 7 Professional operating system and 8.00 GB installed memory (RAM). The analysis for run-times and speed up is depicted in the Table 3.2 accompanied with a graph in Fig. 3.4. The speed up varies with signal length. For signal length, N $\leq$11289600 or 128 seconds the TQWT based method can run at most 20 times faster than SSA based method. For similar signal length, the WT based method is undoubtedly faster than the proposed method but it has its own limitations as described earlier in this chapter.

3.5 Summary

The TQWT is a useful and powerful transform for envelope based segmentation of oscillatory cardiac sound signals into heart beat cycles. The proposed method based on constrained TQWT based decomposition and reconstruction captures the required information in the reconstructed signal using sufficient number of adaptable input parameters of the TQWT. The experimental results reflect the capability of constrained TQWT based decomposition and reconstruction in perfectly identifying the primary heart sounds form the overlapping murmurs even when with they have comparable magnitude. A comparison of the proposed method in removing murmurs with other popular methods is also presented for various clinical cases. In comparison to these methods, the proposed method has been found to provide promising results. The future scope of work includes classification of heart valve disorders using the proposed segmentation method. The development of suitable features, the features selection process, and the classifier can further improve classification accuracy. The murmurs which are extracted by using constrained TQWT based decomposition and reconstruction can provide better classification of heart valve disorders with suitable features. Moreover, the murmurs which are extracted using constrained TQWT based decomposition and reconstruction can provide more insight into the modelling aspects of cardiovascular system. Finally, in order to establish the clinical use of the proposed method, it is necessary to test it on out-of-sample dataset.

Chapter 4

Diagnosis of Heart Valve Disorders using TQWT based Classification of Cardiac Sound Signals

4.1 Introduction

Heart disorders are the second major cause of mortality and morbidity worldwide, of which heart valve disorders are the most common in developing countries [101, 45]. Heart valve disorders cover a wide range of disorders including aortic stenosis, aortic regurgitation, mitral stenosis and mitral regurgitation and others [45]. Timely diagnosis of heart valve disorders is an important step in prevention, treatment and eradication of heart valve disorders. The cardiac sound signals can be used for the diagnosis of heart valve disorders. These signals are being produced by the mechanical action of the heart and can provide diagnostic information about the functioning of the cardiovascular system. The cardiac sound signals may consist of two types of components, the heart sounds and the murmur, which are low frequency and high frequency components respectively [12]. The heart beat cycles of the normal cardiac sound signals contain the S1 and S2 heart sounds which are referred to as primary heart sounds. On the other hand, the heart beat cycles of abnormal cardiac sound signals may

contain: murmur, S3 and S4 heart sounds, and other abnormalities associated with different pathologies of the cardiovascular system [12]. Thus, parameters extracted from cardiac sound signals can serve as valuable diagnostic features for detection and identification of the heart valve disorders [102, 8, 92, 103, 104].

In recent years, with the development of many advanced signal processing and medical artificial intelligence technologies, a huge potential exist for development of efficient, informative and accurate state of the art computer-aided diagnostic tool for heart valve disorders. Therefore, cardiac sound signals based expert system can be envisaged as a promising and cost effective technology for prompt, noninvasive, convenient and efficient diagnosis of heart valve disorders. Implementation of such systems involves analysis and extraction of suitable diagnostic features from the cardiac sound signals for final development of pattern classification process to classify a set of heart valve disorders. Moreover, for effective classification, the extracted features should represent similarity within the class along with differences among the classes [105].

In literature, a large number of studies have been focused on extracting effective diagnostic features for classification of cardiac sound signals using time-domain, frequency-domain, and time-frequency or scale domain. It is worth to note that the time-domain based analysis can discriminate between the normal and abnormal cardiac sound signals. However, it has shown difficulty in determining the type of murmur in cardiac sound signals [16, 106]. Therefore, in recent studies, a number of features have been defined in frequency-domain and time-frequency or scale domain to classify different types of cardiac sound signals. The automatic segmentation and support vector machine (SVM) based classification of cardiac sound signals using STFT and discrete cosine transform based features have been proposed in [45]. However, the method has shown lower classification accuracy in case of splitting of S2 heart sound. In [16], HMM based classification with the three feature extraction methods namely time-domain, STFT and Mel-frequency cepstral coefficient (MFCC) have been compared. The results show effective classification performance but inaccurate segmentation, in case of murmurs having large energy, may affect the diagnosis of heart valve disorders.

The maximum peak of the normalized autoregressive power spectral density curve and the frequency width between its crossed points on a selected threshold value have been used as features to represent the morphological characteristics of cardiac sound signals in frequency-domain in [106]. Then, SVM based classification of seven types of cardiac sound signals has been achieved with significant accuracies. However, in case of mitral regurgitation and splitting of S2 heart sound, the method has produced lower sensitivity.

In [107], the features based on singular value decomposition (SVD) and QR decomposition of the continuous wavelet transform (CWT) coefficient matrix have been extracted to classify innocent murmurs from pathological murmurs with classification and regression tree. However, this method has distinguished only innocent murmurs from pathological murmurs with manual segmentation. In order to characterize the cardiac murmur by their acoustic qualities, the acoustic properties of murmur have been analyzed in time-domain, frequency-domain as well as time-frequency domain in [108]. The features namely intensity, pitch, bandwidth, and signal structural simplicity have been used as input to k-nearest neighbors (KNN) classifier to classify the murmurs as music, blowing, coarse and non-coarse. However, this study was limited to the still's murmur and it needs further inclusion of pathological murmurs. The methodology in [109] describes artificial neural network (ANN) based classification of five different heart disorders with features based on a seven level of wavelet decomposition using Coifman fourth order wavelet. However, the study lacks automatic segmentation and broader range of clinical case under study. Daubechies (db)-2 wavelet detail coefficients at the second decomposition level have been used as feature vectors for ANN based classification of cardiac sound signals of type: normal, systolic murmur and diastolic murmur in [95]. The features obtained with detailed coefficients at sixth level of decomposition using db-2 wavelet have been used to classify seven types of cardiac sound signals in [110]. ANN based classification of cardiac sound signals using wavelet features that have been obtained as power of detail coefficients in all five sub-bands was performed for fourteen categories of heart disorders in [78]. The SVM based classification of five different pathological cases using wavelet features similar to [95] has been performed in [111].

The features based on envelope that is the number of peaks, the average distance in samples between consecutive peaks, the signal energy of the cardiac sound segment and that of wavelet coefficients have been used for detection of heart valve disorder in [69]. However, the method has not considered classification of murmurs. The features extracted using db-4 wavelet with five decomposition levels have been used for ANN based classification of three pathological and normal cardiac sound signals in [112]. The SVM based classification of four most usual heart disorders have been performed using wavelet based features in [113]. The four features namely, the maximum peak frequency, the position index of the wavelet packet coefficients corresponding to the maximum peak frequency, and the ratios of the wavelet energy and entropy information have been used for detection of regurgitation in [114]. The mean and standard deviation of wavelet packet energy has been used to classify normal and abnormal cardiac sound signals in [115]. The entropy of wavelet packet coefficients has been used in SVM based classification of normal, aortic stenosis, mitral regurgitation, and aortic regurgitation cardiac sound signals in [116, 117].

Recently, the TQWT has been proposed as a powerful technique for analysis and processing of oscillatory signals [1]. As compared to other wavelet architectures, the TQWT has the ability to tune itself with more input parameter according to the behavior of the signal under study. It can be concluded from the literature review that the capability of TQWT and Fourier-Bessel (FB) expansion in representing the cardiac sound signals has yet to be explored. In this article, we present a new method for classification of cardiac sound signals using feature based on time-domain representation, TQWT and FB expansion. In our previous study [118], constrained TQWT based removal of murmur for efficient segmentation of cardiac sound signals has been proposed.

In this work, the first main contribution is extraction of features during the separation of heart sounds and murmur from the segmented heart beat cycles. In fact, during separation optimized values of TQWT parameters are obtained that vary with nature and severity of murmurs in different clinical cases. These parameters are useful for representation of cardiac sound signals. Secondly, separation of heart sounds and murmur has been intended for ex-

tracting better and more diagnostic features with same parameters to eventually classify the cardiac sound signals. Finally, the features based on FB expansion can represent the spectral properties of segmented cardiac sound signals thus preventing undesired effect of windowing [119]. The features based on FB expansion can even model the perceptual hearing [120]. Therefore, the novel raw feature set has been created by the parameters that has been optimized during constraining the output of TQWT and that of extracted by using time-domain representation and FB expansion of separately reconstructed heart sounds and murmur. In order to improve classification accuracy, the adaptively selected features are then used for subsequent classification using LS-SVM with various kernel functions. The performance of the proposed method is validated with publicly available datasets and results have been compared with existing STFT based method. It is noteworthy that the proposed method uses well defined and lower dimensionality of feature vector that can reduce computational complexity as compared to STFT based method.

The rest of the chapter is being organized as follows: FB expansion is described in section 4.2. Section 4.3 presents the following subsections of the proposed methodology: Segmentation, constrained TQWT based reconstruction of heart sounds and murmur, feature extraction, adaptive feature selection and classification. Section 4.4 describes experimental results and comparison of proposed method with existing STFT based method. Finally, section 4.5 summarises the chapter.

4.2 Background

4.2.1 Fourier-Bessel Expansion

A continuous-time signal $s(t)$, over an arbitrary interval $(0, a)$, can be expressed with zero-order Bessel functions as basis functions in the form of Fourier-Bessel (FB) expansion as [119, 121]:

$$s(t) = \sum_{i=1}^{M} C_i J_0 \left(\frac{\lambda_i}{a} t \right) \tag{4.1}$$

where, C_i are the FB coefficients which can be computed by using following equation:

$$C_i = \frac{2\int_0^a ts(t)J_0(\frac{\lambda_i}{a}t)dt}{a^2[J_1(\lambda_i)]^2} \tag{4.2}$$

where, $J_0(\cdot)$ and $J_1(\cdot)$ are the zero-order and first-order Bessel functions respectively. For $i = 1, 2, ..., M$, the values of λ_i are M ascending order positive roots of $J_0(\lambda) = 0$. The roots of the Bessel function $J_0(\lambda) = 0$ can be obtained using the Newton-Raphson method [122, 123, 124]. These roots are computed in successive iteration. The iterations are stopped when the values of the roots no longer changes significantly. The FB coefficients C_i are unique for a given signal. The property of decaying of Bessel functions with respect to time makes the FB expansion of non-stationary signals like speech, electroencephalogram (EEG) signals, etc. suitable for analysis [26, 28-31][119, 121, 125, 126]. Generally, the order M is being kept same as the length of the signal so that the entire range of frequencies present in the given signal can be spanned. Here, throughout this study, the order M is set as length of the signal under study.

4.3 Methodology

The subsections of the proposed method for classification of cardiac sound signals are depicted in Fig. 4.1. The subsections include: segmentation, constrained TQWT based reconstruction of heart sounds and murmur, feature extraction, adaptive feature selection and classification. The details of each subsection are described as follows:

4.3.1 Segmentation

The automatic segmentation of cardiac sound signals into heart beat cycles can be performed by using constrained TQWT based method as presented in chapter 3. In this method, the parameters of the TQWT are adapted such that reconstruction occurs predominantly with heart sounds having relatively high kurtosis value as compared to that of murmur. As the heart sounds are low frequency component therefore murmur-free reconstructed signal is

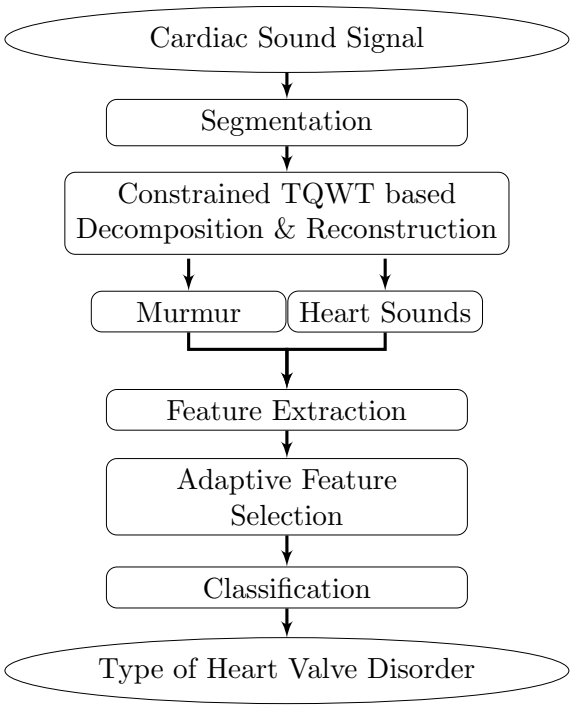

Figure 4.1. The schematic diagram of the proposed method for classification of the cardiac sound signals.

obtained by considering last stage low-pass sub-band signal of TQWT based decomposition. The envelope based on CSCW [81] is extracted after the removal of low energy components from murmur-free reconstructed cardiac sound signals. Finally, with the known clinical knowledge [79], the S1 and S2 heart sounds are identified and the timing information of the CSCW based envelope is used to derive the heart beat cycles of the original cardiac sound signals.

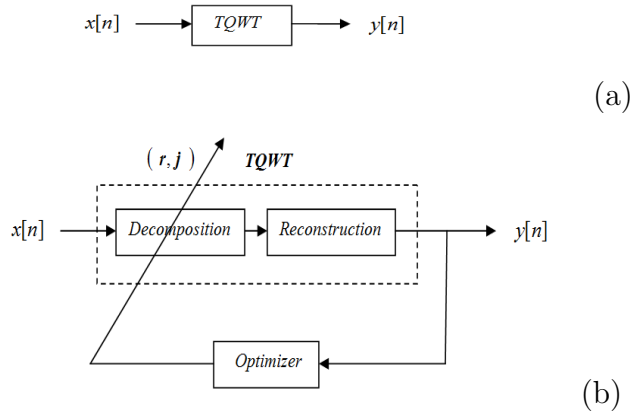

Figure 4.2. The block diagram of (a) TQWT and (b) the constrained TQWT with two adaptive parameters r and j, and a fixed value of Q.

4.3.2 Constrained TQWT based Reconstruction of Heart Sounds and Murmur

The amplitude distribution of primary heart sounds is super-Gaussian having sharper peak and often skewed toward left with relatively larger value of the kurtosis as compared to murmurs [91]. On the other hand, the amplitude distribution of murmurs is nearly Gaussian or sub-Gaussian. This knowledge about the statistical properties of primary heart sounds and murmurs can be used to constrain the output of the TQWT for separately reconstructing the heart sounds and murmur as follows. The block diagram of TQWT and constrained TQWT with two adaptive parameters r and j, and a fixed value of Q can be conceived as

shown in Fig. 4.2 (a) and 4.2 (b) respectively. The working of constrained TQWT based decomposition and reconstruction can be envisaged as working of TQWT with feedback mechanism involving optimizer or optimization method. The difference between the unconstrained and the constrained TQWT is that the later constrains the output of TQWT to be of certain desired statistical characteristics known a priory by optimally tuning the chosen input parameters during decomposition.

In order to separate the heart sounds, the input parameters of TQWT based decomposition have been adaptively selected such that the primary heart sounds having maximum kurtosis are obtained in the reconstructed signal. The heart sounds are low frequency component therefore the low-pass sub-band at last output stage of TQWT based decomposition has been used for signal reconstruction. It should be noted that while reconstruction with low-pass sub-band, other heart sounds also appear along with reconstructed primary heart sounds. For separation of murmur, only the high-pass sub-bands of each output stage of TQWT based decomposition have been considered during reconstruction. In order to constrain the output of the TQWT, the input parameters of TQWT can be adapted by using any suitable optimization method. As the genetic algorithms are more versatile in global optimization [93], therefore, in this study, genetic algorithm has been used as an optimization method. The kurtosis of the high-pass sub-band signal at the output stage of TQWT based decomposition has been minimized as an objective function.

From the previous experimental analysis, it has been found that Q close to unity provides better separation of heart sounds and murmur [118]. By considering a training set having five heart beat cycles of each clinical case in the dataset, the possible bounds of the parameters to be optimized have been obtained such that adaptive selection of these parameters results into adequate separation of heart sounds and murmurs. The murmurs exhibit relatively higher oscillations as compared to heart sounds. Therefore, low value of Q has been found to adequately enhance and localize the heart sounds from overlapping murmur for murmur-free reconstruction of heart sounds. Fig. 4.3(a) and 4.3(b) show the effect of increasing Q on constrained TQWT based reconstruction of heart sounds for two heart beat cycles of two

representative examples: aortic stenosis and tricuspid insufficiency respectively. However, these results have been accompanied usually with high value of r. It is evident from Fig. 4.3 that Q equals to unity provides better separation of heart sounds and murmur as compared to other higher values of Q. Another reason for this could be that the wavelet at this Q better matches with heart sounds. In Fig. 4.3, it should be noted that original signals have been decimated and normalized before constraining the output of TQWT.

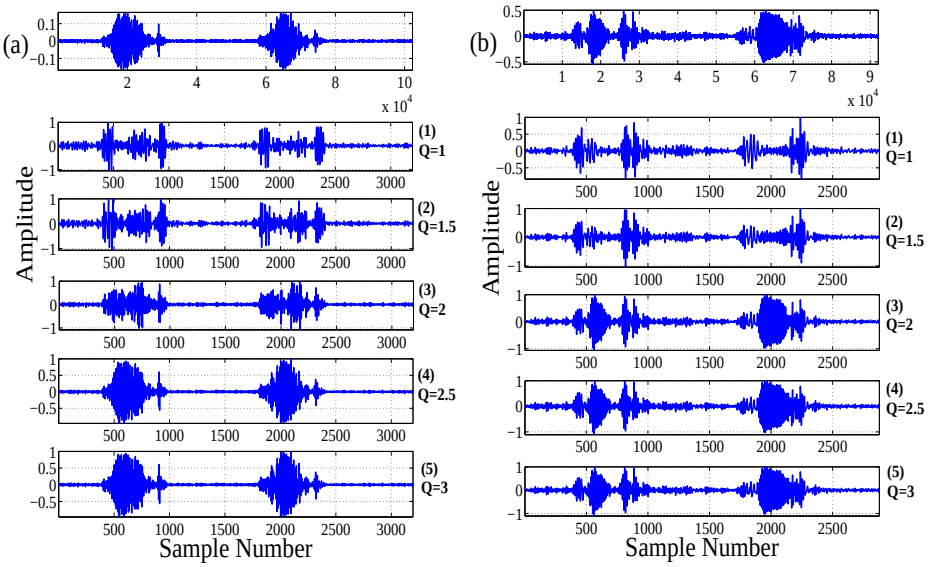

Figure 4.3. The effect of increasing Q on constrained TQWT based reconstruction of heart sounds for: (a) aortic stenosis and (b) tricuspid insufficiency. The number (1)-(5) represent the reconstructed heart sounds corresponding to different values of Q.

4.3.3 Feature Extraction

Feature extraction plays a vital role in detection and identification of heart valve disorders by deriving useful information accurately from the raw cardiac sound signals thereby reducing the dimensionality. The reduced feature set can avoid storage problem and improve computational speed. From the proposed experimental analysis, it has been observed that the optimized values of input parameters obtained while constraining output of TQWT vary

with nature and severity of murmurs in different clinical cases. Nevertheless, the distribution of FB coefficients with order of separately reconstructed heart sounds and murmur is also found to vary with the type of heart valve disorder. Therefore, in order to achieve better representation of various types of cardiac sound signals, the proposed novel raw feature set has been obtained by the parameters that has been optimized while constraining the output of TQWT and that of extracted by using time-domain representation and FB expansion of separately reconstructed heart sounds and murmur as described in Table 4.1. The expressions for CC, $RMSC$ and RVC have been derived from [127] to use with FB coefficients.

The feature namely $En_{heart\ sounds}$ has been computed for that of separated heart sounds. The values of the parameters: E_{left}, E_{right}, and En_{murmur} have been computed for that of separated murmurs. The $En_{heart\ sounds}$ and En_{murmur} have been measured with respect to total energy of corresponding segmented heart beat cycle. All other features were computed for both separated heart sounds and murmur to form a feature set containing twenty two features. In order to normalize the raw feature set for SVM based classification, the procedure of subtracting mean and dividing by its standard deviation has been applied for each feature.

4.3.4 Adaptive Feature Selection

The adaptive feature selection aims to obtain the final feature set of reduced dimension by selecting significant features that can corresponds to higher classification accuracy. In this study, Fisher's discriminant ratio (4.3) has been used to identify features that can provide the maximum contribution in discriminating the two classes as described in [45]. The feature selection procedure is adaptive because, for each hyperplane, the elements of final feature set depend on Fisher's discriminant ratio and classification accuracy as obtained using training and validation set. The procedure iteratively searches and adds the features in order of their significance to constitute final feature set that monotonously improves the classification accuracy between two classes during training. For a hyperplane $\Omega_{a,b}$, the elements of the raw feature set can be sorted by Fisher's discriminant ratio as follows. The training set containing n samples of considered two classes are created as $C_a = \{f_{a,1}, f_{a,2}, f_{a,3}, ..., f_{a,n}\}$

Table 4.1. The details of the proposed features for classification of cardiac sound signals.

Features	Expressions/definations
Optimal redundancy	r_o: It is obtained during constraining output of TQWT
Optimal decomposition levels	j_o: It is obtained during constraining output of TQWT
Center of FB coefficients	$CC = \sum_{k=2}^{N} \lvert\dot{C}_k\rvert\lvert C_k\rvert \Big/ \sum_{k=1}^{N} C_k^2$, where $\lvert\dot{C}\rvert = \lvert C_k\rvert - \lvert C_{k-1}\rvert$
Root mean square variance of coefficients	$RMSC = \sqrt{\sum_{k=2}^{N} \dot{C}_k^2 \Big/ \sum_{k=1}^{N} C_k^2}$
Root variance of coefficients	$RVC = \sqrt{RMSC^2 - CC^2}$
Order of the maximum peak value of coefficients	OC_{max}
The maximum peak value of coefficients	C_{max}
Band width obtained using coefficients	BWC: It is the range of order of coefficients that covers 95% of total signal energy (E)
Signal energy to the left of maximum of coefficients	E_{left}
Signal energy to the right of maximum of coefficients	E_{right}, where $E = \sum_{i=1}^{M} C_i^2 \frac{a^2}{2}[J_1(\lambda_i)]^2$
Kurtosis	$k = \frac{E(x-\mu)^4}{\sigma^4}$, where, μ and σ are the mean and standard deviation of x respectively
Skewness	$s = \frac{E(x-\mu)^3}{\sigma^3}$, and $E(y)$ represents the expected value of the quantity y
Relative energy of separated heart sounds	$En_{heart\ sounds}$: It is measured from separated heart sounds
Relative energy of separated murmur	En_{murmur}: It is measured from separated murmur

and $C_b = \{f_{b,1}, f_{b,2}, f_{b,3}, ..., f_{b,n}\}$ respectively. Initially, each sample vector $f_{i,j}$ contains 22 features which can be represented as $f_{i,j} = [f_{i,j,1}, f_{i,j,2}, ..., f_{i,j,22}]$. Then, for this hyperplane, the discriminant ratios of all features are calculated by using the following equation [45]:

$$I_{a,b,k} = \frac{(\mu_{a,k} - \mu_{b,k})^2}{\sigma_{a,k}^2 + \sigma_{b,k}^2} \tag{4.3}$$

where, $\mu_{i,k}$ and $\sigma_{i,k}$ denote the mean and standard deviation values of the k^{th} feature for all n samples in class i. The discriminant ratios obtained from (4.3) are arranged in an array as $I_{a,b} = [I_{a,b,1}, I_{a,b,2}, ..., I_{a,b,22}]$. The elements in this array are first sorted in the descending order to form the array $I_{a,b}^s = [I_{a,b,1}^s, I_{a,b,2}^s, ..., I_{a,b,22}^s]$ and the corresponding set of sorted features is obtained as $A^s = [u_1, u_2, ..., u_{22}]$, where, u_1 feature is the best feature selected for this hyperplane using (4.3). Then the classification procedure can be performed for selecting first k features of A^s, $1 \leq k \leq 22$ that provides the best classification accuracy between considered two classes.

4.3.5 Classification

SVMs are basically generalized linear classifiers that use supervised learning models for classification and regression analysis. However, they can be efficiently used for non-linear classification by using kernel functions that implicitly map the inputs into high-dimensional feature spaces. A SVM constructs a hyperplane in a input feature space, which can be used for classification. For better separation between involved two classes, the hyperplane that has the largest distance to the nearest training data samples is selected which is termed as functional margin. It is to be noted that, in general, larger the margin the lower the generalization error of the classifier. As the SVM works on the principle of structural risk minimization, it provides better generalization ability than that of traditional methods that use empirical risk minimization [128]. In [129], Suykens et al. have presented LS-SVM that uses a set of linear equations instead of quadratic programming to achieve faster and better classification performance.

The multi-class classification of cardiac sound signals can be efficiently performed by

using LS-SVM classifiers with one-against-one (OAO) approach [106]. The OAO approach achieves multi-class classification with two class LS-SVM classifiers such that the hyperplane of each of which discriminate between considered two-classes only. Therefore, for s classes, the total hyperplane being considered can be obtained as $C_2^s = s(s-1)/2$. However, the final decision is based on the principle of maximum likelihood of a class with majority votes among all these hyperplane as described in [45]. For a hyperplane, the LS-SVM classifier can be obtained as [129]:

$$y(x) = \text{sign}\left\{\sum_{i=1}^{N} y_i \alpha_i K(x, x_i) + b\right\} \tag{4.4}$$

where, $K(x, x_i)$ is the kernel function, x_i is the i^{th} input feature vector of d-dimension, y_i is the class label of x_i, which is either $+1$ or -1, b is the bias term, N represents the number of training input and output pairs and α_i denotes the Lagrange multipliers. The detail derivation of the LS-SVM is available in [129]. In this work the comparative performance of three kernel functions namely radial basis function (RBF), Mexican hat wavelet and Morlet wavelet kernel have been investigated. The RBF kernel can be defined as [130]:

$$K(x, x_i) = \exp\left[\frac{-\|x - x_i\|^2}{2\sigma^2}\right] \tag{4.5}$$

The Mexican hat wavelet kernel can be expressed as [131, 132]:

$$K(x, x_i) = \prod_{k=1}^{d}\left[1 - \frac{(x^k - x_i^k)^2}{a^2}\right]\exp\left[\frac{-\|x^k - x_i^k\|^2}{2a^2}\right] \tag{4.6}$$

The kernel function which is obtained by using Morlet wavelet can be expressed as [131, 132]:

$$K(x, x_i) = \prod_{k=1}^{d}\cos\left[\omega_0\frac{(x^k - x_i^k)}{a}\right]\exp\left[\frac{-\|x^k - x_i^k\|^2}{2a^2}\right] \tag{4.7}$$

where, in (4.5-4.7), x_i^k is the k^{th} element of the i^{th} training set. The kernel parameter σ controls the width of RBF kernel function and ω_0 controls the oscillations of Morlet wavelet function. Furthermore, a is the scaling parameter of the wavelet and d is the dimension of the feature set.

4.4 Experimental Results

The effectiveness of the proposed method for classification of cardiac sound signals has been validated with two online available datasets one of which can be freely downloaded as the heart sounds pod cast series (2011). This dataset has been produced by the Robert J. Hall Heart Sounds Laboratory of Texas Heart Institute at St. Luke's Episcopal Hospital. The dataset comprises of real clinical cases with 50 abnormal cardiac sound signals acquired from variety of subjects with relevant chest positions and patient maneuver. The sampling frequency of most of the data is 44.100 kHz except for few cases. For more information regarding the dataset, this series is available at [100]. The normal cardiac sound signals with sampling frequency of 44.100 kHz have been obtained from another dataset available at [133].

The proposed method has been implemented using Matlab. The cardiac sound signals have been segmented into heart beat cycles by using constrained TQWT based method. As shown in Table 4.2, the segmentation procedure has successfully segmented 1095 heart beat cycles out of 1180 heart beat cycles, yielding segmentation rate of 92.79%. In Table 4.2, TB represents the actual number of heart beat cycles. However, all the segmented beats have been used in the following part of the methodology. It should be noted that the reference actual number of heart beat cycles present in the dataset were manually annotated by an experienced cardiologist. The annotation procedure was carried out by combined audio and visual interpretation of the dataset.

Most of the murmurs exhibit higher frequency components in the range of 100 to 600 Hz [16]. Therefore, in order to reduce the time of execution of constrained TQWT, the decimation has been carried out before constrained TQWT based separation of heart sounds and murmur by a factor of 32 considering Nyquist-Shannon sampling theorem that provides highest expected frequency without affecting the murmurs. The decimation resamples the heart beat cycles from sampling frequency of 44.100 kHz to that of 1378.125 Hz. The separation of heart sounds and murmur has been achieved using constrained TQWT based approach. In order to highlight the significance of the proposed features based on FB coefficients in repre-

senting various abnormal clinical cases, four representative clinical cases namely midsystolic click, mitral regurgitation, aortic stenosis and tricuspid insufficiency have been described as follows:

4.4.1 Midsystolic Click

In case of midsystolic click, high frequency click may occur any time between S1 and S2 heart sounds. In general, the click is of perceptible loudness. The proposed method with constrained TQWT has been found effective in separating click and heart sounds as shown in Fig. 4.4.1 (b) and Fig. 4.4.1 (d). The reconstructed click and heart sounds have been obtained with adaptively selected following values of parameter: $r=17$ and $j=11$ at $Q=1$. This clinical case is exceptional because it has been recorded at sampling frequency of 22.050 kHz. Therefore, in order to obtain the desired sampling frequency of 1378.125 Hz, the input signal has been decimated by a factor of 16. The FB coefficients of separated click and heart sounds obtained using proposed method are shown in Fig. 4.4.1 (c) and Fig. 4.4.1 (e) respectively. As we know, the order is proportionally related to the frequency content of the signal. Therefore, the FB coefficients of click are clearly seen to be distributed across the whole range of order with maximum around the order of 250. However, the FB coefficients of heart sounds are dominating around lower range of order.

4.4.2 Mitral Regurgitation

The mitral regurgitation murmur is holosystolic in nature with flat intensity and obscured S2 heart sound. In case of severe mitral regurgitation, the murmur is accompanied with a S3 heart sound and a diastolic flow rumble. In spite of the flat nature of the murmur and loudness of murmur comparable with heart sounds, it can be observed that the proposed method has effectively separated the murmur and the heart sounds as shown in Fig. 4.4.2 (b) and Fig. 4.4.2 (d). The separation has been obtained with adaptively selected following values of TQWT parameters: $r=17$ and $j=19$ at $Q=1$. As with mid systolic click, for

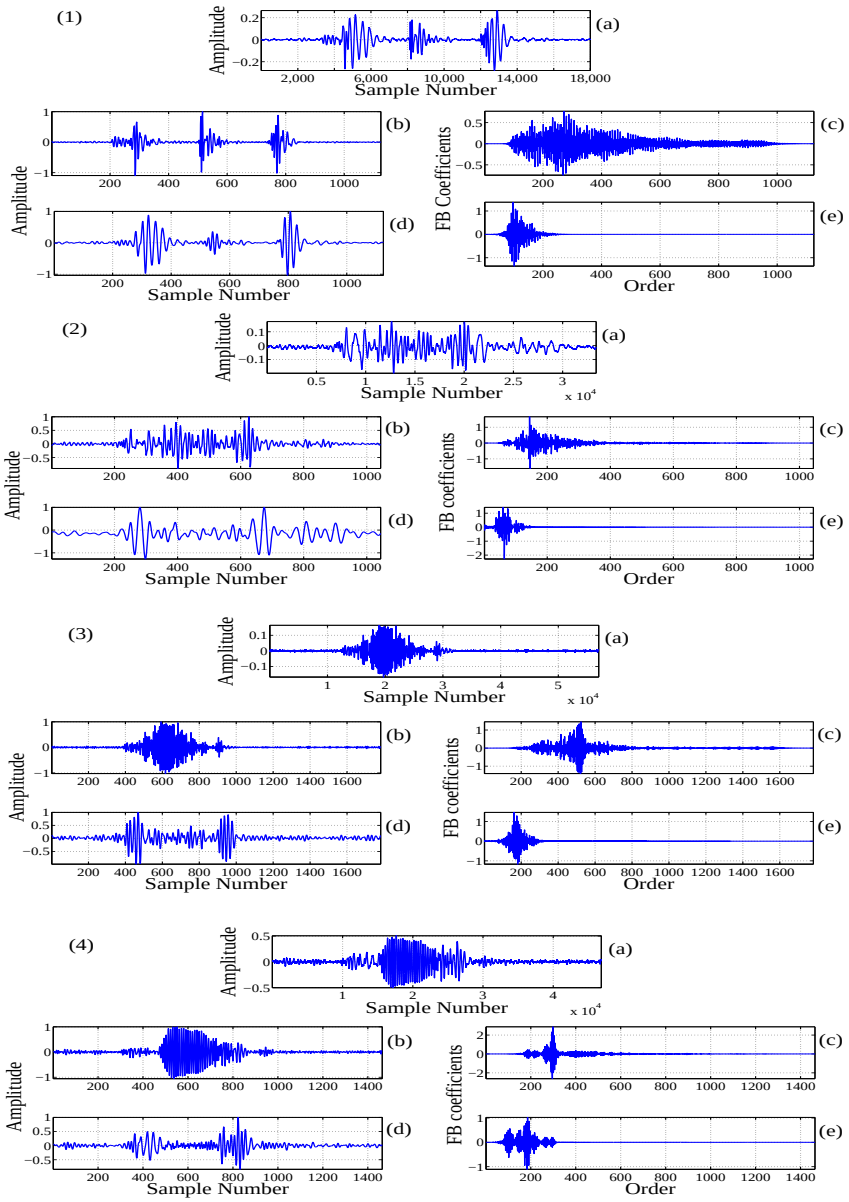

Figure 4.4. The FB coefficients of constrained TQWT based separated heart sounds and murmur of (1) midsystolic click, (2) mitral regurgitation, (3) aortic stenosis and (4) tricuspid insufficiency: (a) segmented heart beat cycle, (b) & (d) reconstructed murmur and heart sounds, (c) & (e) FB coefficients of murmur and heart sounds.

this case also, the information regarding the heart sounds are contained in the lower range of FB coefficients order. On the other hand, the scenario is significantly different for FB coefficients of separated murmur. In present case, non-zero range of the FB coefficients of separated murmurs exhibit narrower range and maximum at around the order of 150.

4.4.3 Aortic Stenosis

The cardiac sound signal associated with aortic stenosis contains regular diastolic, diamond or kite like shaped crescendo-decrescendo murmur. In this case, the performance of proposed method in separating the complex diastolic murmur and obscured heart sounds is encouraging. The method is capable to separate S1 from overlapping murmur. Moreover, the performance of the proposed method in enhancing S2 is also satisfactory as can be seen in Fig. 4.4.3 (d). The separately reconstructed murmur and heart sounds have been achieved with adaptively selected following values of parameters: $r=14$ and $j=18$ at $Q=1$.

4.4.4 Tricuspid Insufficiency

The soft holosystolic murmur features the cardiac sound signal associated with tricuspid insufficiency.

The murmurs and heart sounds have been effectively separated by using the proposed method based on constrained TQWT as shown in Fig. 4.4.4 (b) and Fig. 4.4.4 (d). As with aortic stenosis, in this case also, the proposed methods has been successful in identifying the heart sounds from the background murmur. The separation of heart sounds and murmur have been achieved with automatically estimated following TQWT parameters: $r=12$ and $j=20$ at $Q=1$. The FB coefficients of murmur are clearly seen to be distributed widely around upper range of order with maximum around the order of 300. However, the FB coefficients of heart sounds are around lower range of order.

After separation of heart sounds and murmur, the proposed novel raw features have been extracted for adaptive feature selection and LS-SVM based classification. For classification,

the dataset has been approximately partitioned into training, validation and testing set containing 60%, 20% and 20% of data respectively. The classification results are based on OAO approach employing 21 classes with 210 hyperplanes. For each hyperplane, a LS-SVM model has been created by adaptive feature selection along with classification using the training and validation set as follows. To begin with, the first feature subset corresponding to $k = 1$ has been created using sorted feature set A^s as obtained using equation(4.3). The regularization and kernel parameters were tuned by minimizing a cross-validation score function using procedure that combines coupled simulated annealing and a simplex method as described in [134]. The LS-SVM model corresponding to this hyperplane has been trained and validated. In search of feature subset that yields the highest overall accuracy, the above procedure is repeated sequentially for incremental values of k. Finally, the LS-SVM model for this hyperplane has been saved for the final feature subset that provided highest overall accuracy. The above procedure has been applied to all other hyperplanes till all the LS-SVM models were constructed. Eventually, these LS-SVM models were used for classification of cardiac sound signals using test set. It is noteworthy that the process of adaptive feature selection performs reordering and screening of the raw features by virtue of their significance. Table 4.2 shows the statistics related to the performance of LS-SVM based classification of the cardiac sound signals using different kernel functions. The classification performance of the proposed method has been determined by: computing classification accuracy (Acc) in percentage and the effective number of features (ENF) used. The parameter k indicates the first k significant features of the considered hyperplane. However, the ENF represents the average value of k of all the hyperplanes. It is noteworthy that for every hyperplane, final feature set was composed of finite integer number of elements k. But averaging the k for all the involved hyperplanes may lead to a non-integer value of ENF. In Table 4.2, Tr and Ts represent the training and testing accuracies respectively. From the experimental results, it was observed that the RBF kernel of LS-SVM classifier provides a better classification accuracy of 94.01% with effective number of features approximately 18. The experimental results show that the features based on time-frequency properties of constrained TQWT and

spectral properties of FB expansion are quite effective to represent the behavior of cardiac sound signals giving higher classification performance. In case of FB expansion, the decaying property of Bessel functions with respect to time makes it suitable for the analysis of non-stationary signals like cardiac sound signals. The subsequent part of this section describes the comparison of the proposed method with existing STFT based method.

Recently, Kao and Wei have presented automatic cardiac sound signal analysis for detecting heart valve disorders [45]. The procedure has been briefly described as follows. The method begins with preprocessing of cardiac sound signals that includes down sampling and histogram analysis based noise removal. The heart beat cycles were derived by using auto-correlation followed by energy analysis based timing offset adjustment. From each segmented heart beat cycles, time-frequency characteristics were extracted as raw features with STFT and two-dimensional discrete cosine transform (2D-DCT). The final feature set was formed by adaptively selected features. The final feature set serves as an input to SVM based classification using RBF kernel function with $\gamma = 1/9$. In comparison to STFT based method applied on same dataset, the proposed method was found to be more efficient in the following aspects. Firstly, the proposed constrained TQWT based method provides a well defined set of raw features containing 22 features. On the other hand, the STFT based method relies on whole values of coefficients of 2D-DCT. Due to high dimensionality of raw feature vectors, it is obvious that STFT based method needs more computational time as compared to the proposed method. Secondly, the proposed method has provided overall classification accuracy of 94.01% against 93.53% of STFT based method. In addition, the proposed method analyses LS-SVM based classification with robust data partitioning and three different kernels. The proposed method performs well for a wide range of clinical cases ranging in severity of murmur from moderate to extreme as comprised in the dataset. However, the segmentation of cardiac sound signals associated with Austin flint rumble poses serious restrictions on the performance of the proposed method as described in [118]. The other limitation of the proposed method is that it lacks the required number of patients for proper stratification of cross-validation procedure by patients. Before applying the proposed work for clinical use,

the performance of the method needs to be evaluated with out-of-sample data from adequate number of patients of each known clinical case of heart valve disorders.

4.5 Summary

In this chapter, we have proposed the representation of cardiac sound signals based on novel raw feature set. This feature set has been obtained by the parameters based on the constrained TQWT, time-domain representation, and FB expansion of cardiac sound signals. This work has suggested the extraction of features during the separation of heart sounds and murmur using the segmented heart beat cycles. It is noteworthy that the separation provides the optimized values of TQWT parameters that vary with nature and severity of murmurs in different cardiac sound signals. Moreover, the separation of heart sounds and murmur has been used for obtaining more diagnostic information with same features to successfully classify cardiac sound signals. Finally, the features based on FB expansion have been used to represent the spectral properties of segmented cardiac sound signals. The experimental results have shown that the proposed novel features are effective for classification of cardiac sound signals. The suggested feature set as an input to the LS-SVM classifier together with RBF kernel function has provided significant classification accuracy of 94.01%. The proposed classification method in this chapter requires less number of effective features that can lead to reduce computation complexity. This feature of the proposed method makes suitable for real time implementation of expert system for classification of heart valve disorders. Auscultation with an electronic stethoscope integrated with the proposed classification technique can be used as an expert system. This expert system may be helpful for clinicians to carry out investigations in the clinic, hospital and even at home.

In future, the research can be carried out for judicious choice and development of new time-domain and FB expansion based features which can further improve the classification accuracy for classification of cardiac sound signals in order to diagnose heart valve disorders. In this work, we have described the variation of the proposed features with respect to four

Table 4.2. The statistics of LS-SVM based classification of cardiac sound signals.

Method			TQWT		STFT
Type of disease	TB		Acc (%) Tr/Ts		Acc (%) Tr/Ts
		Mexican hat	Morlet	RBF	RBF ($\sigma = 2.121$)
Hypertrophic cardiomyopathy	95	80.66/80.76	81.72/80.81	100/83.33	93.75/80.71
Opening snap mitral stenosis	40	94.73/94.11	93.75/87.5	100/85.71	80/84.86
Aortic regurgitation	63	100/100	88.23/69.56	100/100	100/90.91
Aortic valve ejection sound	47	85.71/85	85/93.75	100/85.29	100/88
Mitral valve stenosis	54	88.89/80	92.30/78.57	100/85	80/80
Mid systolic click	262	95/85	86.47/78.46	85/83.33	100/83.97
Mitral regurgitation	43	100/85	100/86.10	100/100	100/96.77
Aortic stenosis	71	90.48/90.48	94.12/100	100/83.33	97.69/90.91
Third heart sound	41	100/94.74	100/100	100/100	100/100
Fourth heart sound	59	95.24/85	100/90.48	100/100	100/100
Tricuspid valve insufficiency	27	95/90	95/85	100/100	100/100
Paradoxical split S2	41	100/100	100/100	100/100	100/100
Tumor plop	20	100/100	100/100	100/100	100/100
Pericardial knock	18	100/100	100/100	100/100	100/100
Fixed splitting of S2	31	100/100	100/100	100/96	100/80
Wide splitting of S2	21	100/100	100/100	100/100	100/100
Flail mitral regurgitation	25	100/100	100/100	100/100	100/100
Physiological splitting of S2	46	100/97	94.12/99	100/100	100/100
Austin flint rumble	52	95/92.86	98/92.86	100/83.33	98.99/98
Pulmonary valve ejection sound	44	95/82.61	98/97	100/88.89	100/87
Normal sound	80	99/98	100/98	100/100	100/97
Total/Average	1180	95.94/92.40	95.56/92.24	99.28/94.01	97.64/93.53
ENF		11	12.31	17.97	65.92

representative cases namely midsystolic click, mitral regurgitation, aortic stenosis and tricuspid insufficiency. More rigorous quantitative and qualitative study can be performed with more cases to investigate the relationship between the proposed features and the underlying pathology which can help development of new diagnostic features. It would be of interest to investigate the effect of noise on the proposed methodology. In this work, categories of cardiac sound signals under study have been expanded to cover a broader range of diseases. However, future work is required to validate the proposed method with more number of patients for proper stratification of cross-validation procedure by patients. The k-fold cross-validation procedure can produce more effective classification performance for detection and identification of heart valve disorders. It might be interesting to find a best kernel function between every hyperplane instead of using one for all hyperplanes. In addition, the proposed methodology should be applied on out-of-sample data for its possible application in health care clinics. In order to measure reliable performance of proposed classification technique for diagnosis of heart valve disorders, more classification performance measures can be included. Moreover, the expert system based on the proposed framework can be further extended for detection and identification of cardiac devices especially the artificial heart valves in routine emergency check-ups at hospitals. Finally, it would be of great interest to study the expert system based on the proposed classification technique using features derived simultaneously from time-domain, TQWT and FB expansion as input to LS-SVM classifier for classification of other biomedical signals like EEG, ECG, electromyogram (EMG) signals corresponding to normal and abnormal conditions.

Chapter 5

Diagnosis of Septal Defects using TQWT based Classification of Cardiac Sound Signals

5.1 Introduction

The most common cardiac disorders result from defects in the wall of tissue separating the right and left chambers of the human heart. The wall is termed as the septum and the associated defects are referred to as septal defects. The wall of tissue between the right and left atria is called the atrial septum and that of between the ventricles is called the ventricular septum. Generally, the cardiac septal defects fall into two groups: ventricular septal defects (VSDs) and atrial septal defects (ASDs). The septal defects are congenital heart defects that can range from a small hole in the septum to a significant portion of the septum actually being absent. These defects can cause to shunting that enables undesired flow of blood between two compartments of the heart. Moreover, the septal defects can be categorized with the help of defect diameter as small, medium and large defects [51]. The early diagnosis of the septal defects is crucial to ensure sooner treatment in turn saving many lives. The septum defects can be easily diagnosed by prompt, accurate, convenient

and affordable medical diagnostic procedure based on analysis of cardiac sounds [12, 8]. The septal defects manifest themselves in the cardiac sounds with presence of murmurs that can be recognized by cardiac auscultation. Even features can be determined to characterize these murmurs in cardiac sound signals that are easily acquired using electronic stethoscope for computer-aided diagnosis [51, 102].

Septal defects, valvular defects and other defects like ventricular hypertrophy, constrictive pericarditis etc. can be analyzed with interpretations based on cardiac auscultation and that of phonocardiogram [135]. However, the auscultation and phonocardiography have not been widely recognized due to their limitations. Consequently, these non-invasive and cost effective investigations have been gradually superseded by other sophisticated modalities like echocardiography. Nevertheless, diagnosis with echocardiography is quite expensive and its presence is limited to health care centers in urban areas [107].

The recent advancement in the area of analog and digital electronics has paved the way for the development of effective portable medical devices like electronic stethoscope. The electronic stethoscope can facilitate the medical professional to apply both auscultation and phonocardiography more conveniently and in a more versatile way. Nevertheless, it has also opened the possibilities for the application of advanced signal processing and medical artificial intelligence technologies for convenient automatic diagnosis of cardiac disorders. In view of these, advanced signal processing techniques can be developed to use with electronic stethoscope or mobile technology for convenient computer-aided diagnosis of septal defects using cardiac sound signals.

The basic steps for diagnosis of cardiac abnormality using cardiac sound signals generally comprises the following process: segmentation, feature extraction and classification [136, 118, 137]. As the cardiac sound signals are non-stationary signals, therefore it is challenging to achieve the desired performance at each of these steps [79, 76, 69]. The inconsistent duration of the heart beat cycles, variation of the number of heart sounds, presence of various types of murmurs and the other noises can cause to inaccurate segmentation of cardiac sound signals [45, 92]. In need of successful segmentation, we have recently proposed constrained TQWT

based removal of murmur for easier automatic segmentation of cardiac sound signals [118]. In this approach, segmentation using time information from cardiac sound characteristic waveform (CSCW)[81] based envelope has been performed to achieve better segmentation performance. Recently, detection and boundary identification of S1, S2, S3 and S4 heart sounds in cardiac sound sounds using an expert frequency-energy based metric has been proposed in [138]. The segmentation of cardiac sound signals using moving window Hilbert transform (MWHT) has also been found to yield better segmentation performance [51]. A automatic method for cardiac sound moment segmentation using Viola integral based envelopes and detection of peak location of S1/S2 heart sounds using short-time modified Hilbert transform have been proposed for cardiac sound signals [139].

The process of feature extraction transforms the original cardiac sound signals into set of diagnostic features for analysis of cardiac abnormality. These features can be determined from time-domain, frequency-domain and time-frequency or scale domain. In time-domain, parameters related to the duration of the systole and diastole and the presence of murmurs in these durations have been used for detecting cardiac abnormality [81, 51, 108, 83]. In order to classify innocent and pathological murmurs, different spectral characteristics of murmurs in cardiac sound signals have been proposed in [106, 16]. The discrete energy spectrum based feature set has been used with the neural network for classification of innocent and pathological heart murmurs of VSD in [140]. With this method, the discrimination between innocent and VSD murmurs has achieved sensitivity of 93% and specificity of 90% with accuracy of 92.85%. In [141], VSDs were incorrectly classified as aortic stenosis/aortic regurgitation with a three-layered artificial neural network. One recent study has proposed diagnosis of three types of VSDs based on combination of features obtained from time-domain and frequency-domain envelope of segmented heart beat cycles [51]. In time-domain, the time intervals between primary heart sounds derived using envelope computed from Viola integral method have been extracted as features. Envelope based on MWHT has been used to extract feature in frequency-domain.

A new cardiac spectral segmentation method based on multi-Gaussian fitting was devel-

oped for discriminating between cardiac sound signals of normal and heart valvular diseases in [142]. The method considers clinical representative cases of aortic and mitral regurgitation murmurs. It uses five Gaussian profiles of multiple Gaussian peaks with spectral autoregressive power spectral density curve of preprocessed cardiac sound signals. This study has suggested that spectral parameters of these peaks were found suitable for diagnosis of heart valve disorders. In [143], a method for automated screening of congenital heart diseases in children has been developed using cardiac sound signals. The pathological murmurs have been identified by the cardiac sound energy over specific frequency bands named Arash-bands that provide the lowest error while clustering the two classes. The energy content of the Arash-bands has been used as feature for classification using a neural network. The results show more than 94% of correct identification of children with congenital heart diseases. The time growing neural network (TGNN) has been proposed for classification of short-duration heart sounds or clicks in [144]. The spectral power in adjacent frequency bands as computed in time windows of growing length have been used as input features for classification. The performance of the TGNN is compared to that of a time delay neural network and a multi-layer perceptron. The results show that the TGNN performs better than other compared method when frequency band power is used as classifier input with classification accuracy and sensitivity of 97.0% and 98.1% respectively.

In order to detect and identify cardiac abnormality using cardiac sound signals, various methods based on the short-time Fourier transform (STFT), wavelet transform (WT), wavelet packet decomposition and TQWT have been presented in [137, 92, 145, 95, 115, 111, 146, 147]. The S-transform based classification of S1 and S2 heart sounds has been presented in [147]. Recently, optimum multi-scale wavelet packet decomposition (OMS-WPD) based wavelet-time entropy was applied to extract features for classification of the normal and abnormal cardiac sound signals using support vector machines (SVM) [148]. The normal and five types of abnormal cardiac sounds were considered for this work. Moreover, the results were compared with methods based on STFT, wavelet packet transform, Hilbert Huang transform, and spectrogram, respectively. In this study, an accuracy of 88.98%, a sensitivity

of 85.29% and a specificity of 94% have been demonstrated. The work in [149] represents automatic detection of mitral valve prolapse based on a multifractal analysis. Several features including width and area under the curve, location of maxima etc. have been used for discriminating between subjects of the normal and mitral valve prolapse. This method achieves high accuracy of 96.91% in detecting the mitral valve prolapse. This method can also be used to indicate signal irregularities to users of electronic stethoscopes for apprentice avoiding the misinterpretation of cardiac sounds. The hidden Markov models have been used for classification of cardiac sound signals in [85]. The features based on empirical mode decomposition have been proposed for classification of cardiac abnormality in [150].

The classification is an important step for detection and identification of cardiac abnormality using cardiac sound signals. The detection of septal defect can be based on classification between four classes: one includes the septal defects and others include normal, valvular defects and other disorders. The classifiers which have been popularly and efficiently used for cardiac sound signals are neural network [95, 151, 78, 109, 152] and SVM [51, 45, 106, 113, 36].

The TQWT is a recently developed wavelet transform for analysis of oscillatory signals [1]. The cardiac sound signals are oscillatory signals and thus can be analyzed using TQWT. In our previous studies, the TQWT has been successfully deployed for segmentation and diagnosis of heart valve disorders in [118, 153]. The TQWT based fluctuation indices have been proposed for diagnosis of septal defects from cardiac sound signals in [146]. In this present work, we propose a new set of diagnostic features based on sum of average magnitude difference function (SAMDF) which can better represent the cardiac sound signals providing higher classification performance for the considered range of Q from 1 to 50 at certain level of decomposition.

The first main contribution of this work includes the use of SAMDF based feature set derived with TQWT. In fact, the correlation between sub-bands can characterize the various types of murmurs in cardiac sound signals associated with different clinical cases. Therefore, in order to represent the murmurs in cardiac sound signals, proposed feature set was created

with SAMDF that have been computed from reconstruction of decomposed sub-bands. It is noteworthy that the features are extracted after the process of segmentation that has been performed using the established constrained TQWT based approach. The feature set containing SAMDF as features has been used to classify cardiac sound signals for diagnosis of septal defects. Secondly, in search of effective feature set based on SAMDF that could provide significant classification performance, various decomposition levels have been examined. The classification has been performed using least squares support vector machine (LS-SVM) with various kernel functions namely, radial basis (RBF) kernel function, Morlet wavelet kernel function and Mexican wavelet kernel function. Finally, at each decomposition level under study, the effect of quality- factor (Q) of the TQWT from 1 to 50 on classification accuracy has been evaluated.

This chapter has been organized in five sections. Segmentation, TQWT, feature extraction, and LS-SVM based classification steps of the methodology have been described in section 5.2. Section 5.3 describes the experimental results and discussion on the proposed method. Comparison with other existing method is described in Section 5.4. Finally, Section 5.5 summarises the chapter.

5.2 Methodology

Fig. 5.1 presents the subsections of the proposed methodology for diagnosis of septal defects using cardiac sound signals. In Fig. 5.1., w_{J+1} represent the sub-band signal having lowest frequency and the sub-band signals from w_1 to w_J are high frequency signals obtained with TQWT based decomposition as described in section 2.3. The subsections of the proposed methodology include: segmentation, TQWT, feature extraction and LS-SVM based classification. The details of each subsection are described as follows.

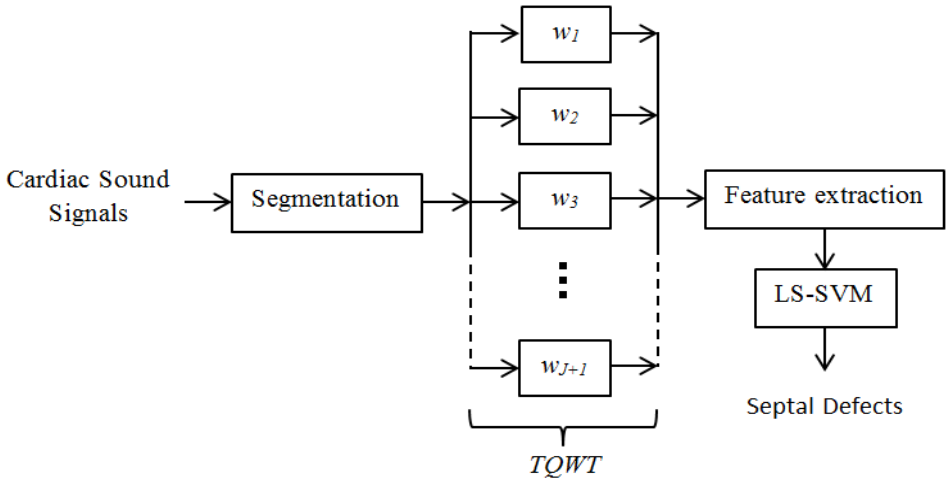

Figure 5.1. The proposed TQWT based automatic diagnosis of septal defects from cardiac sound signals.

5.2.1 Segmentation

The heart beat cycles forms the basic repeating segments of the cardiac sound signals. The heart beat cycles can provide stable features for revealing clinical information rather than that of any other arbitrary length of cardiac sound signals. Therefore, for accurate diagnosis, features need to be extracted from segmented cardiac sound signals. In view of this, the heart beat cycles can be obtained using the TQWT based segmentation procedure as described in chapter 3 [118]. After specified preprocessing, the TQWT based segmentation can be achieved with following main steps. In order to obtain the heart sounds in the output reconstructed cardiac sound signal, the parameters of the TQWT are adapted such that reconstruction occurs predominantly with heart sounds having relatively higher kurtosis value as compared with murmur. As the heart sounds are low -frequency components, therefore murmur-free reconstructed signal is obtained by considering last stage low-pass sub-band signal of TQWT based decomposition. The envelope based on CSCW is extracted after the removal of low energy components from these reconstructed cardiac sound signals. Subsequently, the S1 and S2 heart sounds are recognized and the timing information of the

CSCW based envelope is used to obtain the heart beat cycles from the original cardiac sound signals.

5.2.2 Feature extraction

The features can be extracted from segmented heart beat cycles of cardiac sound signals such that the obtained diagnostic features retain the similarities within the classes while reflecting differences among the classes. If raw cardiac sound signals are used directly as features then it may lead to storage problem and computational complexity. On the other hand, the reduced feature set containing significant diagnostic features can avoid the storage problem and can enhance the computational speed.

The cardiac sound signals are non-stationary in nature. Moreover, time-frequency or scale representation based methods like wavelet transform have been found to be suitable for analysing non-stationary cardiac sound signals [36, 107]. The correlation between sub-bands may contain significant information about the different types of murmur in various clinical cases. SAMDF can be used to measure the murmur induced changes in the cardiac sound signals. Therefore, in this study, we propose a novel feature set based on SAMDF derived using TQWT. The SAMDF can be computed from the reconstructed sub-bands of TQWT based decompositions as follows:

Considering the J-stage TQWT based decomposition, $J+1$ sub-band signals are obtained. These sub-band signals can be arranged in a cell array C as follows [1]:

$$C = \{w_1, w_2, w_3, ..., w_J, w_{J+1}\}, \tag{5.1}$$

where, w_{J+1} is the sub-band signal having lowest frequency and the sub-band signals from w_1 to w_J are signals having high frequencies. The number of samples in each of these sub-band signals depends upon the scaling parameters and can be arranged in the cell array C_l as follows [1]:

$$C_l = [\beta f_s N, \alpha\beta f_s N, \alpha^2\beta f_s N, ..., \alpha^{J-1}\beta f_s N, \alpha^J f_s N], \tag{5.2}$$

where, N is the number of samples in $s[n]$.

For any pair of reconstructed sub-bands as obtained from TQWT based decomposition, say wr_i and wr_j, the SAMDF φ_{wr_i,wr_j} can be measured using the following expression [154]:

$$\varphi_{wr_i,wr_j} = \frac{1}{M}\sum_{\tau=0}^{M-1}\sum_{k=0}^{l-\tau-1}|wr_i[k] - wr_j[k+\tau]|, \tag{5.3}$$

where, wr_m represent the reconstructed signals of sample length M for w_m with $1 \leq m \leq J+1$. $1 \leq i \leq J$, $2 \leq j \leq J+1$ and τ is the lag number. The expression (5.3) has been derived from [154] to use in the present context. In case, if $wr_i[k]$ and $wr_j[k+\tau]$ are similar then the value of φ_{wr_i,wr_j} would be lower. In [36], at the most, the sixth levels of WT based decomposition has been found useful for extraction of wavelet decomposition based features. In this study, in order to obtain the levels of TQWT based decomposition that can be useful for SAMDF based feature extraction for diagnosis of septal defects, various levels have been examined from 2 to 10. The pair-wise combinations of sub-bands can provide a set of SAMDF to form the proposed feature set to classify cardiac sound signals for diagnosis of septal defects. The Table 5.1 shows the summary of extracted features at various levels. For example, the sixth levels of TQWT based decomposition provides seven sub-bands that result into 21 pair-wise combinations or features.

5.2.3 LS-SVM based Classification

The diagnosis of septal defects can be considered as a multi-class problem which in turn can be formulated in terms of two class LS-SVM classifiers. In order to reduce the single multi-class classification problem into multiple binary classification problems, the two most common approaches that can be used are one-against-all (OAA) approach and one-against-one (OAO) approach [106]. In this study, the multi-class classification has been performed with OAO approach. The RBF, Morlet wavelet and Mexican hat wavelet kernel function have been used in this work as explained earlier in chapter 4.

5.2.3.1 Performance Evaluation Parameters

The classification performance of the LS-SVM based classification of cardiac sound signals can be evaluated by computing the sensitivity (Sen), specificity (Spe), accuracy (Acc) and Matthews correlation coefficient (Mcc). Sensitivity measures the proportion of actual positives which have been correctly identified as such. For example, the percentage of diseased people who have been correctly identified as having the disease. Specificity measures the proportion of negatives which have been correctly identified as such. For example, the percentage of healthy people who have been correctly identified as not having the disease. A perfect classifier would exhibit 100% sensitivity by detecting all diseased people as having diseased. Moreover, it would show 100% specificity by not claiming anyone from the healthy group as diseased. The Matthews correlation coefficient is basically a correlation coefficient between the actual and predicted outcomes. Its value lies between +1 and -1, where +1 represents a perfect prediction, 0 represents not better than random prediction and -1 indicates total disagreement between predicted and actual outcomes. These above mentioned classification parameters can be defined as [155, 156, 157, 158]:

$$Sen = \frac{TP}{TP + FN} \times 100 \tag{5.4}$$

$$Spe = \frac{TN}{TN + FP} \times 100 \tag{5.5}$$

$$Acc = \frac{TP + TN}{TP + TN + FP + FN} \times 100 \tag{5.6}$$

$$Mcc = \frac{TP \times TN - FP \times FN}{\sqrt{(TP + FN)(TP + FP)(TN + FN)(TN + FP)}} \tag{5.7}$$

where, TP and TN represent the total number of correctly detected true positive patterns and true negative patterns, respectively. The FP and FN represent the total number of erroneously positive patterns and erroneously negative patterns, respectively.

Along with the above mentioned classification evaluation parameters, the receiver operating characteristics (ROC) graphs are also commonly used in medical decision making for classifiers in order to visualize their performance [159]. ROC graphs are two-dimensional graphs that show relative tradeoffs between true positives rates (benefits) and false positives rates (costs). In case of multi-class classification problem having S classes, S different ROC graphs can be produced for each class [160, 161]. The ROC graph i shows the classification performance using class s_i as the positive class (P) and all other classes as the negative class (N) as [159]:

$$P_i = s_i \tag{5.8}$$

$$N_i = \bigcup_{j \neq i} s_j \in S \tag{5.9}$$

5.3 Experimental Results

A realistic cardiac sound signal classifier should learn about the similarity within the classes and differences among the classes mainly due to involved physiology or pathology irrespective of various other factors like (a) subjects of various ages (b) signal acquisition with various types of sensors/stethoscopes in tern having various components like filters, (c) in various modes covering bell, diaphragm and extended mode, (d) with various subjects posture and maneuver (e) different chest positions. In view of these, a more general heart sounds dataset has been formed with cardiac sound signals from five different heart sound sources [100, 162, 163, 164, 165] similar to as described in [113]. This dataset considers cardiac sound signals acquired under various conditions as described above. Some of the recordings in the dataset were corrupted by the human voice, rubbing sound due to stethoscope and other lung sounds. Also, the duration of the heart beat cycles are inconsistent. The sampling frequency of most of the data is 44.100 kHz with 16 bits except for few cases of mid systolic cases in [100].

In order to validate the usefulness of the proposed method for diagnosis of septal defects,

in spite of cardiac sound signals for septal defects and normal, signals to be detected for valvular defects and other defects like ventricular hypertrophy, constrictive pericarditis etc. have also been considered. Therefore, it results into four classes of cardiac sound signals for

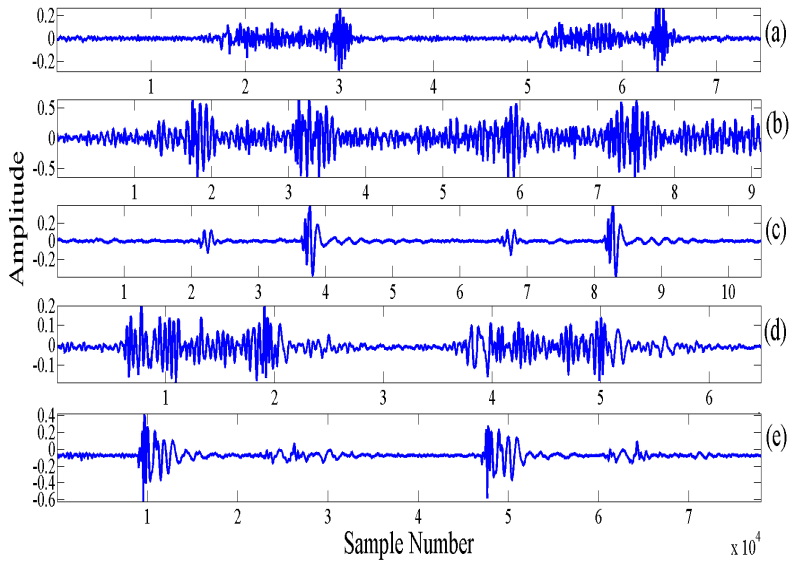

Figure 5.2. Illustrations of cardiac sound signals for (a) VSD, (b) ASD, (c) normal, (d) valvular defects (mitral regurgitation) and (e) other defect (pericardial knock).

evaluating the performance of the proposed method involving segmentation and classification of cardiac sound signals. Fig. 5.2. shows examples of cardiac sound signals corresponding to these clinical cases. Overall 163 cardiac sound signals with 4628 heart beat cycles have been used in this work. There are 15, 17, 101 and 30 cardiac sound signals of septal defects and normal, valvular defects and other defects respectively. The corresponding heart beat cycles are 444, 626, 2771 and 787 respectively. The cardiac sound signals have been segmented into heart beat cycles by using constrained TQWT based method. The TQWT based segmentation procedure has successfully segmented 4460 heart beat cycles out of 4628 heart beat cycles to provide segmentation rate of 96.37%. However, all the segmented heart beat cycles have been employed in the next stages of the methodology. The reference actual number of heart beat cycles present in the dataset has been pointed out by an experienced

cardiologist. The annotation procedure has been performed by combined audio and visual interpretation of the dataset.

Nyquist-Shannon sampling theorem can provide highest expected frequency without affecting the murmurs. In fact, the frequencies of most of the murmurs fall in the range of 100 to 600 Hz [16]. Therefore, in order to speed up the algorithm, the decimation of each segmented heart beat cycles has been performed before applying TQWT by a factor of 32 considering Nyquist-Shannon sampling. The decimation re-samples the heart beat cycles from sampling frequency of 44.100 kHz to that of 1378.125 Hz. The normalization is done to compensate amplitude variation among the heart beat cycles.

After decimation and normalization, the proposed novel feature set based on SAMDF derived from TQWT has been extracted. Each segmented heart beat cycles has been decomposed up to certain level using TQWT and SAMDF have been computed from reconstructed decomposed sub-bands to form the proposed feature set. The value of redundancy parameter of TQWT has been recommended to be higher than or equal to 3 [1]. Therefore, it has been set to 8 throughout this analysis. Then, this feature set has been used for LS-SVM based classification of cardiac sound signals for diagnosis of septal defects. For classification, randomly selected 926 (20%) heart beat cycles constitute the test set and rest of that forms the training and validation sets. In case of test set, there are 89, 125, 554 and 158 heart beat cycles of septal defects and normal, valvular defects and other defects respectively.

The classification results are based on OAO approach employing 4 classes with 6 hyperplanes resulting into six LS-SVM models. In this work, the three kernel functions have been used as mentioned previously. The regularization and kernel parameters were tuned by minimizing a cross-validation score function using procedure that combines coupled simulated annealing and a simplex method as described in [134]. For each hyperplane, a LS-SVM model has been created by proposed feature set with classification using the training and validation set. The above procedure of feature extraction and classification has been repeated sequentially for incremental values of Q from 1 to 50 in step of one. Moreover, each level from 2 to 10 has been examined for better classification performance. Finally, the LS-SVM

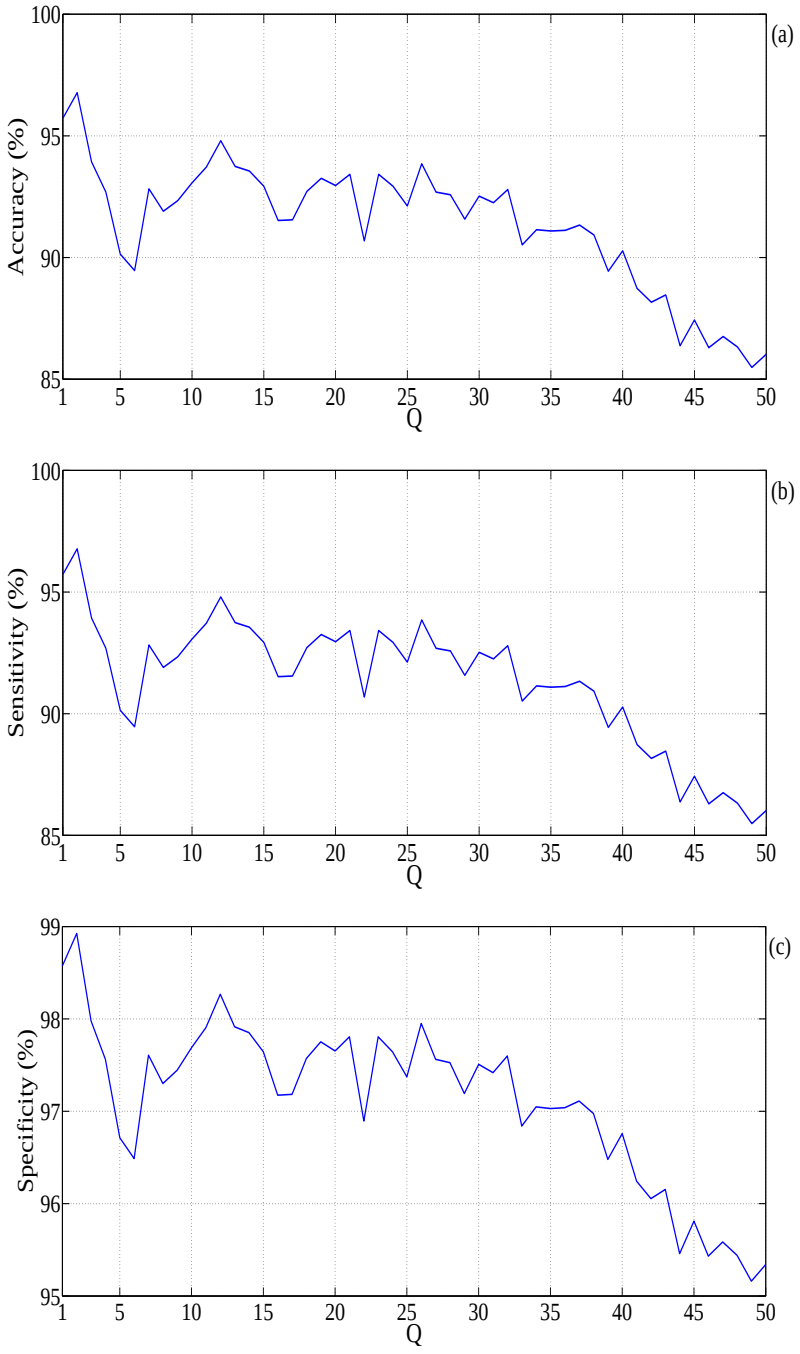

Figure 5.3. An illustration of the results obtained using proposed method with varying values of Q (a)-(c): accuracy as a function of Q, sensitivity as a function of Q and specificity as a function of Q respectively.

models that provide highest overall accuracy have been saved for the final test. Fig. 5.3 shows an example that depicts the effect of variation of Q on classification performance. The experimental results have been presented in Tables 5.1 to 5.4. In Tables 5.1 to 5.3, max, μ, and σ represent the maximum, mean, and standard deviation of the measured quantity for considered values of Q. The Q_b represents the value of Q corresponding to maximum value of accuracy. Table 5.2 shows that the proposed method has provided significant classification performance with tenth levels of decomposition for all the value of Q in the given range using Morlet wavelet kernel function. During training and validation at this level, the results as shown in Table 5.2 demonstrate classification accuracy of $99.03 \pm 0.29\%$ with sensitivity of $99.03 \pm 0.29\%$, specificity of $99.68 \pm 0.10\%$ and Matthews correlation coefficient of 0.9875 ± 0.0036 covering all the considered values of Q. Fig. 5.4 shows the ROC graphs of the four considered classes with following positive classes (a)-(d): septal, normal, valvular and others respectively. The corresponding area under ROC graphs are as follows: 0.99962, 1, 0.99689 and 0.99981 respectively. The ROC graphs depict significant classification performance. In Fig. 5.4, the results have been obtained for Morlet wavelet with optimized kernel and regularization parameters with test set. From the experimental results in Table 5.4 with test data, classification accuracy of 98.92% with sensitivity of 98.80%, specificity of 99.29% and Matthews correlation coefficient of 0.9684 have been obtained at tenth level of decomposition for $Q = 6$. The experimental results shows that features based on time-frequency properties of TQWT and SAMDF are quite effective to represent the behavior of cardiac sound signals giving higher classification performance.

The advantages of our proposed method can be stated as follows: Obtained the significant classification performance using a single type of feature. The overall diagnostic framework is automatic and therefore it can prevent inter/intra observer variability. This system can be used practically at manageable cost. The limitation of our work includes: Use of small dataset and therefore the system validation lacks rigorous k-fold cross validation for training and testing. Limited signals have been employed for this study. The system is digital therefore it cause to increased space complexity. The use of automation may weaken the

diagnostic skills of the medical professionals.

Table 5.1. Classification performance analysis of cardiac sound signals using training and validation set for RBF kernel function

J	F	Q_b	Acc			Sen			Spe			Mcc		
			max	μ	σ	max	μ	σ	max	μ	σ	max	μ	σ
2	3	1.00	78.03	39.67	5.91	78.03	39.67	5.91	92.68	79.89	1.97	0.7090	0.2017	0.0815
3	6	1.00	94.85	65.48	5.41	94.85	65.48	5.41	98.28	88.49	1.80	0.9331	0.5433	0.0713
4	10	1.00	98.30	89.49	2.33	98.30	89.49	2.33	99.43	96.50	0.78	0.9779	0.8612	0.0308
5	15	1.00	99.26	96.60	1.25	99.26	96.60	1.25	99.75	98.87	0.42	0.9902	0.9551	0.0165
6	21	3.00	99.59	97.84	1.09	99.59	97.84	1.09	99.86	99.28	0.36	0.9946	0.9715	0.0144
7	28	1.00	99.49	98.23	0.81	99.49	98.23	0.81	99.83	99.41	0.27	0.9933	0.9766	0.0108
8	36	18.00	99.77	98.60	0.67	99.77	98.60	0.67	99.92	99.53	0.22	0.9969	0.9816	0.0089
9	45	6.00	99.68	98.84	0.47	99.68	98.84	0.47	99.89	99.61	0.16	0.9958	0.9849	0.0061
10	55	18.00	99.68	98.97	0.29	99.68	98.97	0.29	99.89	99.66	0.10	0.9958	0.9865	0.0038

5.4 Comparison with other Existing Methodology

In this section, the performance of the proposed method has been compared with one recently presented fluctuation indices based method as described in [146]. This method uses the datasets and classes same as in the proposed method. The main steps of the compared method include segmentation followed by TQWT of heart beat cycles for subsequent feature extraction and LS-SVM based classification with RBF kernel. The TQWT based decomposition was performed up to sixth levels. The fluctuation indices were computed as features from reconstruction of decomposed sub-bands. Then, this feature set containing twenty one features was used to classify cardiac sound signals for detection of septal defects. In order to tune the Q of the TQWT to provide highest classification accuracy, the experiment was conducted with varying value of Q. The method has shown provided better classification

Table 5.2. Classification performance analysis of cardiac sound signals using training and validation set for Morlet wavelet kernel function

J	F	Q_b	Acc			Sen			Spe			Mcc		
			max	μ	σ	max	μ	σ	max	μ	σ	max	μ	σ
2	3	1.00	87.96	44.26	7.15	87.96	44.26	7.15	95.99	81.42	2.38	0.8396	0.2617	0.0970
3	6	1.00	99.63	91.98	2.40	99.63	91.98	2.40	99.88	97.33	0.80	0.8396	0.2617	0.0970
4	10	1.00	99.63	98.83	0.47	87.96	44.26	7.15	99.88	99.61	0.16	0.9951	0.9848	0.0060
5	15	41.00	99.72	98.96	0.43	99.72	98.96	0.43	95.99	81.42	2.38	0.9963	0.9866	0.0053
6	21	6.00	99.54	99.03	0.28	99.54	99.03	0.28	99.85	99.68	0.09	0.9940	0.9876	0.0035
7	28	41.00	99.86	98.96	0.44	99.86	98.96	0.44	99.95	99.65	0.15	0.9982	0.9867	0.0054
8	36	18.00	99.59	98.85	0.42	99.59	98.85	0.42	99.86	99.62	0.14	0.9946	0.9853	0.0051
9	45	32.00	99.72	98.99	0.42	99.72	98.99	0.42	99.91	99.66	0.14	0.9964	0.9871	0.0052
10	55	6.00	99.54	99.03	0.29	99.54	99.03	0.29	99.85	99.68	0.10	0.9940	0.9875	0.0036

Table 5.3. Classification performance analysis of cardiac sound signals using training and validation set for Mexican hat wavelet kernel function

J	F	Q_b	Acc			Sen			Spe			Mcc		
			max	μ	σ	max	μ	σ	max	μ	σ	max	μ	σ
2	3	1.00	70.82	38.67	5.04	70.82	38.67	5.04	90.27	79.56	1.68	0.6170	0.1938	0.0719
3	6	1.00	90.30	58.95	5.53	90.30	58.95	5.53	96.77	86.32	1.84	0.8711	0.4608	0.0710
4	10	1.00	96.05	79.46	3.75	96.05	79.46	3.75	98.68	93.15	1.25	0.9480	0.7273	0.0486
5	15	1.00	97.84	68.76	7.95	97.84	68.76	7.95	99.28	89.59	2.65	0.9715	0.5899	0.1029
6	21	1.00	98.58	67.75	8.50	98.58	67.75	8.50	99.53	89.25	2.83	0.9813	0.5749	0.1094
7	28	1.00	98.48	68.80	8.51	98.48	68.80	8.51	99.49	89.60	2.84	0.9800	0.5885	0.1117
8	36	1.00	98.76	83.36	6.70	98.76	83.36	6.70	99.59	94.45	2.23	0.9838	0.7867	0.0886
9	45	2.00	94.16	77.05	7.22	94.16	77.05	7.22	98.05	92.35	2.41	0.9246	0.7072	0.0912
10	55	1.00	95.96	86.11	7.21	95.96	86.11	7.21	98.65	95.37	2.40	0.9491	0.8292	0.0866

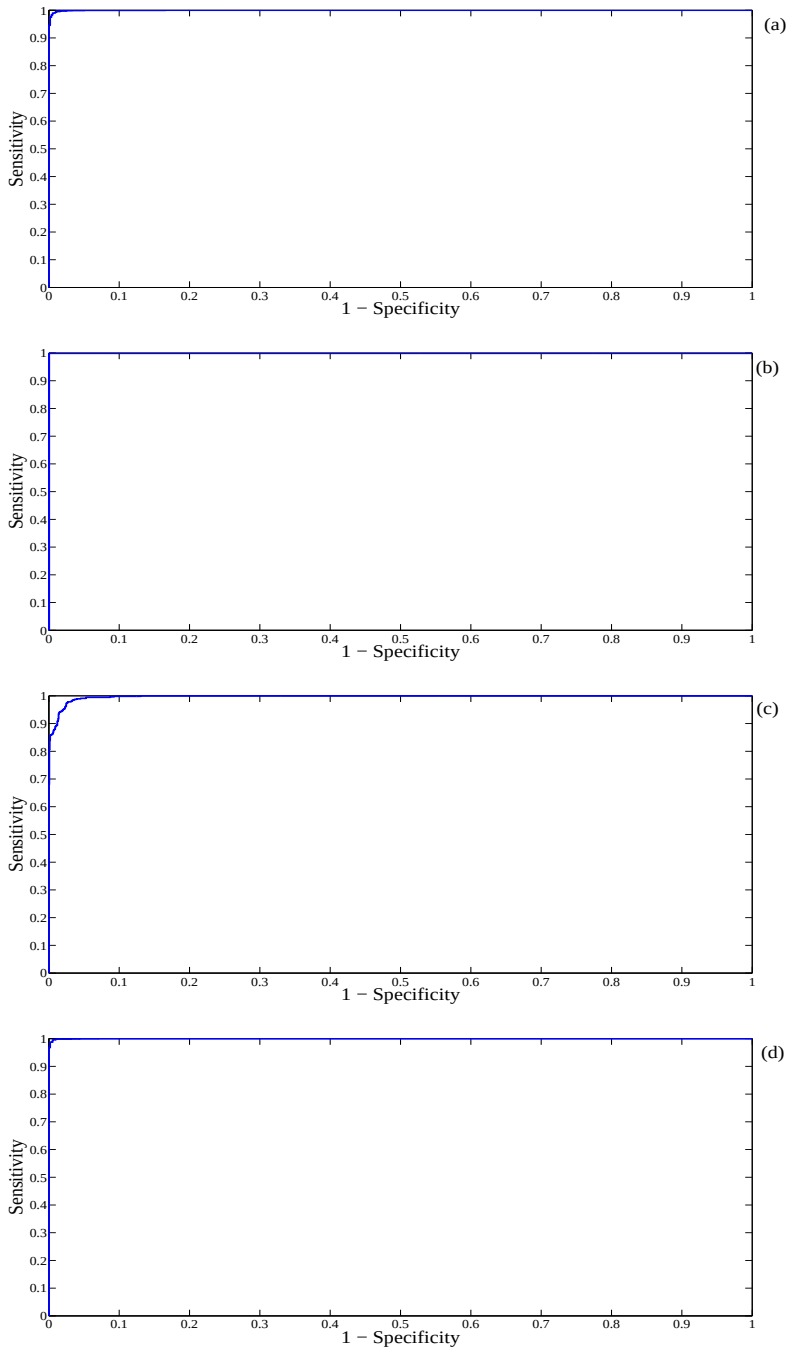

Figure 5.4. ROC graphs showing classification performance of the proposed method with following positive classes (a)-(d): septal, normal, valvular and others respectively.

Table 5.4. The confusion matrix showing classification performance using Morlet wavelet kernel function for test set

		Predicted classes			
		Normal	Valvular defects	Other defects	Septal defects
Actual classes	Normal	121	4	0	0
	Valvular defects	2	552	0	0
	Other defects	0	14	144	0
	Septal defects	0	0	0	89
	Acc	99.35	97.84	98.49	100
	Sen	98.37	96.84	100	100
	Spe	99.50	99.44	98.21	100
	Mcc	0.9721	0.9554	0.9460	1

performance at $Q = 2$ during the training and validation. The classification accuracy of 96.78% with sensitivity of 96.78% and specificity of 98.93% was obtained at $Q=2$.

As compared to fluctuation indices based method, the proposed method introduces new set of diagnostic features based on SAMDF that can better represent the considered classes of cardiac sound signals with following aspects. As shown in Table 5.1, significant results are obtained at sixth levels of TQWT based decomposition. At this levels, the classification accuracy of 99.59% with sensitivity of 99.59% and specificity of 99.86% was obtained for $Q = 3$. These results are better than fluctuation indices based method. Moreover, the proposed study explores more levels of decomposition form 2 to 10 with three different types of kernel functions. As described in earlier section, the salient feature of the proposed method is that its classification performance has been found to be higher and almost consistent for all the values of Q at tenth levels of decomposition.

5.5 Summary

In this work, we have presented the characterization of cardiac sound signals for diagnosis of septal defects based on novel raw feature set. This feature set has been obtained by the TQWT based SAMDF of segmented heart beat cycles derived from cardiac sound signals. The SAMDF based features can reveal information about different types of murmurs in cardiac sound signals considered in this study. Therefore, TQWT based SAMDF have been used as features to represent the time-frequency properties of murmurs in segmented cardiac sound signals. In order to show the effectiveness of the proposed method, cardiac sound signals for valvular defects and other defects have been considered for classification in addition to that of septal defects and normal. In search of appropriate level of TQWT based decomposition that can provide efficient features, the suggested feature sets have been formed and used to classify cardiac sound signals for different levels. The proposed features have been used as an input to the LS-SVM classifier together with different kernel functions. The experimental results have been found promising that reveals the capabilities of proposed feature set in characterization of different types of cardiac sounds signals for diagnosis of septal defects. The salient feature of the proposed method is that its classification performance has been found to be higher for all the values of Q at tenth level of decomposition. It has been found from this study that the proposed features at tenth level of decomposition with $Q = 6$ have provided significant classification accuracy of 98.92% with sensitivity of 98.80% specificity of 99.29% and Matthews correlation coefficient of 0.9684 using Morlet wavelet kernel function. The proposed method can be implemented as an expert system for classification of cardiac sound signals to diagnose septal defects. The computer-aided auscultation using electronic stethoscope or mobile technology with the proposed classification technique based on TQWT derived SAMDF can be used as an intelligent and affordable expert system that can automatically detect the septal defects. This expert system can reduce the health care expenses and avoid the challenges of mastering cardiac auscultation thereby helping the physicians to diagnose the septal defects in the clinic, hospital and even at home.

In our previous work [153] as presented in chapter 4, constrained TQWT, time-domain

representation and FB expansion based feature set have been proposed for classification of cardiac sound signals in a pursuit to detect and identify heart valve disorders. However, the current work is different in the sense that it explores the capability of a single type of feature namely SAMDF for less complex four class classification scheme dedicated to detect septal defects. It can be used to detect heart valve disorders but may not be quite helpful for identifying the types of the heart valve disorders. The work in [45, 36, 115, 81], also primarily aims to achieve detection of heart valve disorders. Moreover, the study in [51] can be used to detect and identify VSDs.

There are few aspects of this research that could be improved further or extended in nearest future. The performance of the proposed method can be evaluated using more clinical cases as out-of-sample data. In this study, integer values of Q have been considered. However, the real value of Q can be considered that can provide even better classification performance. It is to be noteworthy that inclusion of more clinical cases may affect the desired obtained value of Q. The effect of J have already been examined in this work. However, effect of r on classification performance is still needs to be addresses for further development of the feature extraction process. It would be of interest to compare the proposed methodology with other time-frequency methods to establish the significance of the proposed diagnostic framework. This methodology can be extended for identification of type and degree of septal defects.

Moreover, in future, the research can be carried out for screening of features that can reduce the computational burden of the algorithm with further improvement in the classification accuracy to diagnose septal defects. The study can be performed to reveal the relationship between the proposed features and the underlying pathology which can provide the basic understanding of the proposed TQWT based features. It can eventually help development of new diagnostic features.

Furthermore, the effect of noise on the proposed methodology is a topic of interest. In this work, cardiac sound signals associated with broader range of diseases have been used during classification. However, for practical implementation, future work is required to evaluate the usefulness of the proposed method with more number of patients. The classification

procedure should address proper stratification of cross-validation procedure by patients. The k-fold cross-validation procedure can produce more effective classification performance for diagnosis of septal defects. It would be of interest to search for a best kernel function between every hyperplane instead of using one for all hyperplanes.

Moreover, it would be of great interest to study the proposed classification technique using features derived from TQWT and SAMDF for classification of other biomedical signals like EEG, electrocardiogram (ECG), electromyogram (EMG) signals corresponding to normal and abnormal conditions. Finally, the proposed expert system can be further extended for detection and identification of cardiac devices especially the artificial heart valves in routine emergency check-ups at hospitals.

Chapter 6

Diagnosis of Coronary Artery Disease using TQWT of Heart Rate Signals

6.1 Introduction

In 2008, heart disorders were the leading cause of death around the globe causing about 17 million deaths or 48% of noncommunicable diseases (NCD) based deaths [166]. Most of the commonly occurring heart disorders result from coronary artery disease (CAD)[167]. It is mainly caused due to deposition of cholesterol and fatty deposits called plaque within the inner wall of the arteries, blocking the required flow of blood to the heart muscles [57]. Due to increased plaque deposition, the blood vessels become narrow and causing decreased amount of blood supply to the heart muscle thereby depriving adequate nutrients and oxygen. This condition becomes progressively worse affecting the metabolic activity of the heart muscles. Over a period of time, the heart muscles become weak and may lead to heart failure and arrhythmias [58]. Even more, often the deposited plaques erode or rupture resulting into thrombus formation that can restricts the flow of blood to the heart muscles causing sudden cardiac death. The other major causes of CAD but not limited to includes: tobacco smoking [59] and environmental pollution [60]. Timely diagnosis and treating of CAD is important to reduce the risk of occurrence of heart attack or stroke and save lives.

The physicians often evaluate the presence and extent of CAD by observing common symptoms, reviewing the medical history and risk factors, performing physical examination and diagnostic laboratory tests, including blood tests, an ECG and tread mill stress tests [61]. The imaging modalities like echocardiogram, coronary computed tomography angiogram (CTA) and coronary angiography or cardiac catheterization are also used to detect the presence of CAD. The ECG based diagnosis is quite promising and requires minor changes in the ECG recordings to detect specific heart disorders. However, in many cases, visual analysis of ECG recordings for detecting CAD is not reliable because it is difficult to notice the differences in recordings [62]. The presence of noises and artifacts like baseline wondering make it complex to accurately analyse the small morphological changes in the ECG recordings due to heart disorders. While undergoing tread mill stress tests, patients are at risk of developing tachycardia and eventual heart failure [63]. The cardiac catheterization is performed invasively and takes an average time of thirty minutes. However, overall time including the preparation and recovery time amounts to several hours. This leads to almost whole day for patients to do this test. Most of the imaging modalities can be operated only by trained physicians or radiologists. Some of the above mentioned diagnostic tools are quite expensive and their availability is limited to health care centers in urban areas.

Heart rate signals are nonlinear and non-stationary heart signals that carry a lot of information about the homeostasis of the human body [168, 169]. Other than heart disorders, the heart rate signals can be used for diagnosis of diseases like diabetic neuropathies, depression etc. [168, 170, 171, 172, 173]. They are cheap and readily acquirable signals from ECG signals. The CAD manifests in the heart rate signals in the form of subtle information that is difficult to notice by visual interpretation. The recent advancement in the field of signal processing, high performance computing and data mining techniques has helped the clinicians in their quality of diagnosis. It is tedious and time consuming to detect the minute changes in the ECG or heart rate by naked eye for the clinicians. Also, it is prone to inter/intra observer variability. Hence, a computer aided decision support system which is independent of human intervention can significantly improve the quality of decision making

[174]. Novel algorithms in the time, frequency and non-linear domain can be applied on the heart rate signals to decipher the subtle signatures of the diseases.

It is observed that value of power spectral density (PSD) of CAD heart rate signals is nearly half for very low frequency (VLF) and low frequency (LF) regions compared to normal group indicating lower thermoregulatory and sympathetic activities [175]. The PSD is similar in both groups in HF region indicating no change in parasympathetic activity [175]. Moreover, the reduction in low-frequency power with respect to severity of CAD is reported in [176]. While analyzing the heart rate signals in [177, 178], it is observed that CAD-affected subjects show lower circadian rhythm than normal subjects. The lower time and frequency domain parameters are shown for CAD patients in [179]. The statistical time-domain and frequency-domain based parameters do not perform well in the presence of noise [180]. Therefore, time-domain and frequency-domain based features are not appropriate for analysis of CAD [175]. The time-scale domain based method like WT outperforms these techniques in analyzing and deriving useful information about the structural changes in the heart rate signals for diagnosis of CAD [61, 181].

Due to non-linear nature of biomedical signals and physiological systems, non-linear methods are suitable for analysis [180, 182, 183, 153, 184, 137]. In recent past, many nonlinear methods such as Lyapunov exponents [168, 180], correlation dimension (D2) [168, 185, 186], fractal dimension [187, 188, 189, 190, 191], 1/f slope [192], approximate entropy [168], de-trended fluctuation analysis (DFA) [193, 194], Poincare geometry [195, 196, 197], recurrence quantification analysis (RQA)[198, 199, 200, 201], higher order spectrum (HOS) [202] are studied for diagnosis of CAD. In [194], it is shown that DFA and fractal dimension features exhibit lower values for CAD compared to normal heart rate signals. The poincare geometry based short and long term variability measures are also found to be lower for CAD patients. Reduced variation in CAD heart rate signals is indicated by higher values of RQA based four parameters [175]. Reduced value of entropy based parameters is registered for CAD cases. The value of correlation dimension is lower for CAD patients [175]. All the HOS parameters, except phase entropy decreases for CAD subjects as compared to normal group [175].

In this chapter, we have proposed a novel method for detection of CAD using centered correntropy (CCo) based feature set derived from TQWT. In recent years, the TQWT is proposed and successfully applied for analysis and processing of oscillatory signals in several problems [1, 118]. The TQWT can be used to extract the dynamical changes in the abnormal heart rate signals with respect to that of normal. The correntropy is proposed as a nonlinear parameter that measures the pairwise correlation of the feature vectors that are separated by a certain time delay in input space [203]. Moreover, it can measure the shape and size of the group of points in the feature space [203, 184]. The correntropy can characterize the heart rate signals by nonlinearly projecting the sub-band signals into high dimensional space using kernel function. The projected feature space can provide useful diagnostic features. Therefore, in this work, the proposed raw features are formed with CCo that are computed from particular decomposed detail sub-band. The principal component analysis (PCA) is applied to obtain the significant features. The transformed features are used to classify heart rate signals of normal and CAD subjects. The classification is performed using LS-SVM with various kernel functions namely RBF, Morlet and Mexican hat wavelet kernel functions. The effect of Q-factor (Q) on classification performance is studied to find the optimal value of Q. The proposed features at third level of decomposition for Q from 24 to 30 have provided significant classification performance using Morlet wavelet kernel function with optimized kernel and regularization parameters. The experimental results of this work has provided highest classification accuracy, sensitivity, specificity and Matthews correlation coefficient for $Q = 24$ using Morlet wavelet kernel function.

This chapter is organized in six sections. The dataset used in this work is described in Section 6.2. Pre-processing, feature extraction, PCA based feature selection, and LS-SVM based classification steps of the methodology are described in Section 6.3. Section 6.4 describes the experimental results of the proposed method. Discussion on the results is presented in Section 6.5 and finally chapter is summarised in Section 6.6.

6.2 Dataset

In this study, the heart rate signals were derived using ECG signals of twenty subjects. The ECG signals from CAD-affected subjects were obtained from Iqraa Hospital, Calicut, Kerela, India [175]. An experienced cardiologist assisted the screening of subjects and data acquisition procedure. The equal number (ten) of CAD patients and normal subjects had voluntarily contributed to the data acquisition. The participants aged in the range 40 to 70 years, (mean age of 55 years) participated in the study. The subjects having normal blood pressure, glucose level and ECG are considered as healthy volunteers. Only the CAD patients with similar medications were considered in this work. The subjects of this study were not suffering from any other diseases including left and right bundle branch block, ventricular hypertrophy, myopathy, congestive heart failure and atrial fibrilation. The ECG signals are acquired using Biopac^{TM} equipment with sampling frequency of 500 Hz as described at [204]. Overall, 143 ECG signals were obtained containing 61 from normal subjects and 82 from CAD patients. Each of these ECG signals have 1000 samples collected for 15 minutes recording interval.

6.3 Methodology

The proposed methodology for diagnosis of CAD using heart rate signals has been presented in Fig. 6.1. The heart rate signals can be obtained from raw ECG signals by adequate pre-processing which can be described as follows. The stage of pre-processing involves removal of low frequency baseline wander, unwanted high frequency noise and 50 Hz power line interference. In order to remove the baseline wander and unwanted high frequency noise, a band pass filter with lower and higher cut-off frequencies of 0.3 and 50 Hz is used. The notch filter is used to eliminate the power line interference. The Pan and Tompkins method is used to detect the R peaks in ECG signals [205, 206]. The RR peaks intervals (t_{RR}) between successive QRS complexes are computed to obtain RR-interval signals in seconds. The heart rate signals in beats per minute can be derived from RR-interval signals by using

the following expression:

$$HRate = \frac{60}{t_{RR}}(\text{bpm}) \tag{6.1}$$

After pre-processing the obtained heart rate signals are used for automatic diagnosis of CAD. The typical RR-interval signals and their corresponding heart rate signals for normal and CAD patient are shown in Figs. 6.2 and 6.3 respectively. The main subsections of the proposed methodology include: TQWT based decomposition, feature extraction, feature transformation and LS-SVM based classification. The details of each subsection are described as follows.

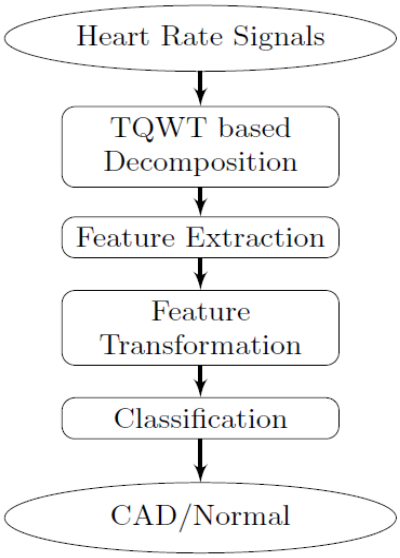

Figure 6.1. The proposed system.

6.3.1 Feature extraction

The effective diagnostic features can be extracted from heart rate signals such that the obtained diagnostic features retain the similarities within the classes while reflecting differences among the classes. If raw heart rate signals are used directly as features then they may lead to space and computational complexity. While the features containing definite significant

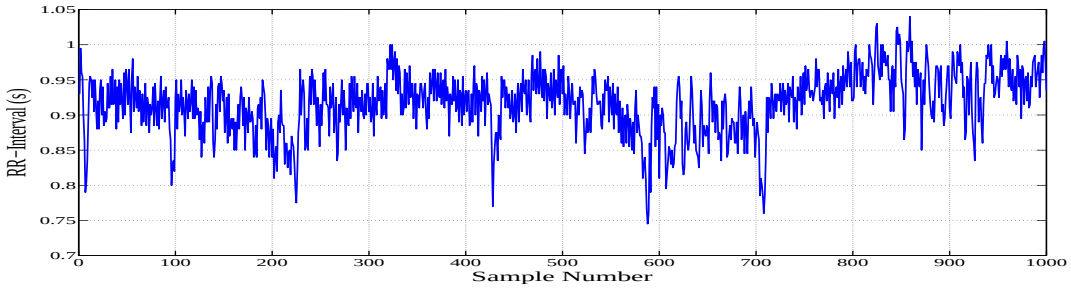

(a)

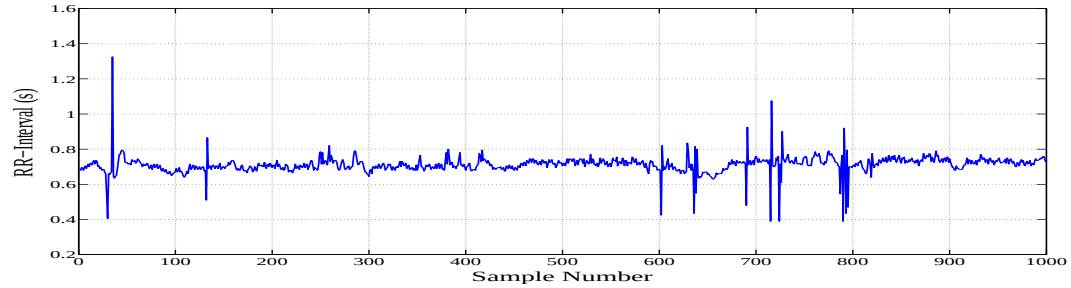

(b)

Figure 6.2. Typical RR-interval signals: (a) normal, (b) CAD subject.

diagnostic information can avoid the storage problem and can enhance the computational speed.

The heart rate signals are non-stationary in nature. In literature, time-frequency or scale representation methods like wavelet transform are found to be appropriate for analysing nonstationary signals [61]. The correntropy based nonlinear features can be used to measure the CAD induced changes in the heart rate signals. Therefore, in this study, we propose a novel feature set based on correntropy derived using TQWT. These features are computed from the considered sub-band of TQWT based decompositions.

The correntropy measures the correlation in nonlinear-domain for multiple delayed samples of the signal [203]. It uses the information theoretic learning in combination with kernel methods to capture the information in higher order moments [207]. It is sensitive to the time structure of the time-series/signals [203]. In feature space, it exhibits a lot of properties that can quantify the data probability density function directly [208]. It can be used to detect nonlinearities. In discrete-time domain, correntropy ($V[l]$) can be defined as follows [203, 208]:

$$V[l] = \frac{1}{N-l+1}\sum_{n=l}^{N}\kappa(x[n]-x[n-l]) \tag{6.2}$$

$$\widehat{V} = \frac{1}{N^2}\sum_{l=1}^{N}\sum_{n=l}^{N}\kappa(x[n]-x[n-l]) \tag{6.3}$$

Where, l represents the lag, $\widehat{V}$ is the mean correntropy and $\{x[1], x[2], ..., x[N]\}$ represent one realization of random process. In order to reduce the effect of DC bias, the mean value $\widehat{V}$ of the correntropy can be subtracted from the $V[l]$ to obtain the centered correntropy ($V_c[l]$) as:

$$V_c[l] = V[l] - \widehat{V} \tag{6.4}$$

In this study, Gaussian kernel function $\kappa(x[n], x[n-l])$ has been applied for computing $V_c[l]$. It can be defined as follows:

$$\kappa(x[n], x[n-l]) = \frac{1}{\sqrt{2\pi}\sigma}e^{\left\{-\frac{(x[n]-x[n-l])^2}{2\sigma^2}\right\}} \tag{6.5}$$

Where, σ is the Gaussian kernel parameter that controls the width. The matlab code for computing CCo [209, 210] is available in the form of ITL Toolbox at [211].

6.3.2 Feature Transformation

In this study, feature transformation is accomplished by PCA. PCA is a linear dimensional reduction technique that transforms the original features into features having more descriptive power. It replaces a group of features with a new feature vectors called principal components computed by linear combination of the original features. The principal components are orthogonal to each other therefore they do not contain any redundant information. The feature transformation using PCA involves calculating the covariance matrix of the raw features. Then matrix containing eigenvectors and eigenvalues of the obtained covariance matrix is obtained. The eigenvectors are arranged in the descending order of eigenvalues. The raw features are projected into the direction of sorted eigenvectors to obtain the transformed features. Finally, the first few significant features are selected for subsequent study. More in depth information about PCA can be obtained from [212, 213].

6.3.3 LS-SVM based classification

Recent advancements in the statistical learning theory has led to the development of SVMs. They are new generation machine learning and data mining systems based on supervised learning models that have successfully used in various real-world applications such as biomedical signal classification, image classification, text categorisation, hand-written character recognition, bioinformatics etc. The SVM is based on structural risk minimization therefore it renders more generalization than that of other traditional learning systems involving empirical risk minimization [129]. In recent years, LS-SVM has been proposed that solves linear equations instead of quadratic programming to get faster and better performance in machine learning and data mining tasks.

In this work, CAD and normal heart rate signals have been classified using the LS-

SVM classifier with the RBF, Morlet wavelet and Mexican hat wavelet kernel functions as described in chapter 4.

6.3.3.1 Classification performance measures

The classification performance of the LS-SVM based classification of heart rate signals of CAD and normal subjects can be analyzed by computing the following parameters [156, 157, 159]: sensitivity (Sen), specificity ($Spec$), accuracy (Acc) and Matthews correlation coefficient (Mcc). Sensitivity determines the probability of actual positives which have been correctly produced as such when used on the CAD affected population. In this work, it is the percentage of CAD-affected people who have been correctly diagnosed with the disease. Specificity measures the probability of negatives which have been correctly produced as such when used on the normal subjects. Here, it is the percentage of normal subjects who have been correctly identified as not having the CAD. A perfect classifier would exhibit 100% sensitivity by detecting all CAD patients as having disease. Moreover, it would show 100% specificity by not claiming anyone from the healthy group as CAD patient. The Matthews correlation coefficient (Mcc) measures correlation between the actual and predicted outcomes of the classifier. Its value fall in the range from +1 to -1. In case of perfect prediction, its value comes out to be +1. The value of Mcc is 0 for random prediction and -1 for total disagreement between predicted and actual outcomes. In order to generalize the results of proposed classification technique in terms of above parameters, three fold cross validation approach is used for classification of normal and CAD heart rate signals.

6.3.3.2 CAD index

The values of multiple significant features can be used and expressed in a single index for biomedical applications as suggested in [214, 215, 216, 217, 218, 219]. Such index can clearly depicts the difference between the consider classes. This kind of integrated index can be used for setting appropriate threshold to ease detection of events of interest. Here, in this work we propose CAD index that combines the significant features illustrated in Table 6.1

to form the mathematical expression as follows:

$$CADIndex = \alpha(PC_1 + \beta) - PC_2 \tag{6.6}$$

Where, PC_1 and PC_2 are the obtained principal components of the correntropy based two features. In order to generalize the above expression, we have used Genetic algorithm for optimizing the values of α and β. Their values are obtained as 0.1 and 55.

6.4 Results

The propose methodology for automated diagnosis of CAD by classification of heart rate signals of normal and CAD subjects is implemented in Matlab. The functions of the TQWT toolbox of Matlab and ITL toolbox are used. The Matlab software for TQWT toolbox is available at [220]. The Matlab codes for ITL toolbox are used from [211]. The pre-processing as described in Section 6.3 is applied on ECG signals to obtained the heart rate signals. The third level of wavelet decomposition are found to yield significant statistical difference between the features for normal and CAD heart rate signals [61]. Hence, the same level is considered in this study to decomposed the heart rate signals into sub-bands. It is noteworthy that unwanted excessive ringing of wavelets need to be prevented while performing TQWT by appropriately choosing the value of r greater than or equal to 3 [1]. Therefore, r is set to 8 throughout this analysis. The values of CCo are computed from third level detail wavelet coefficients to extract the proposed raw feature set. Fig. 6.3 shows the third level of TQWT based decomposition of heart rate signals for normal and CAD subjects with Q=30. The value of lag is empirically selected as two while computing the CCo, therefore two features are obtained for each detailed sub-band signal. The PCA is used to transform these two features. Table 6.1 shows the mean and standard deviation of the significant features obtained after PCA for normal and CAD heart rate signals. The transformed features are used as input feature set to perform classification using LS-SVM with three different kernel functions namely RBF, Morlet and Mexican hat wavelet. The regularization and kernel

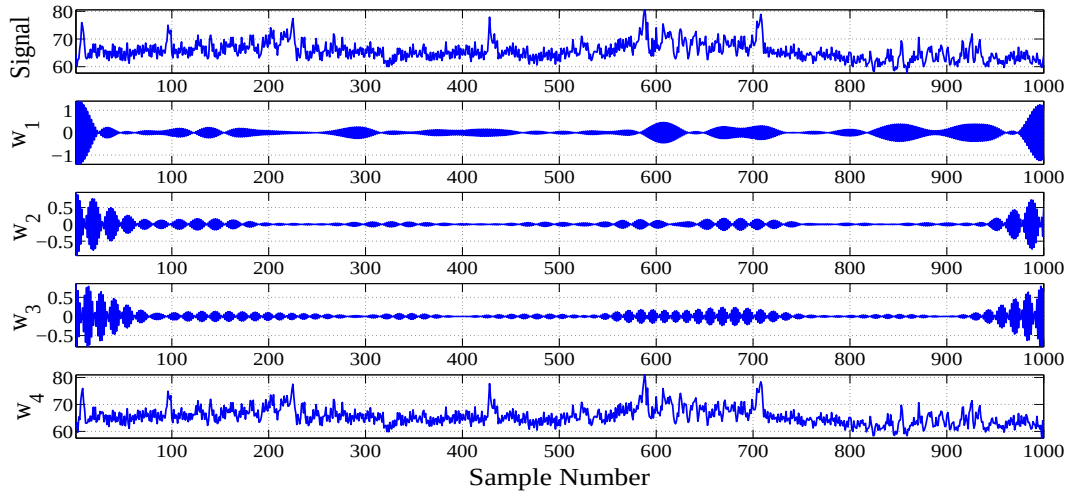

(a)

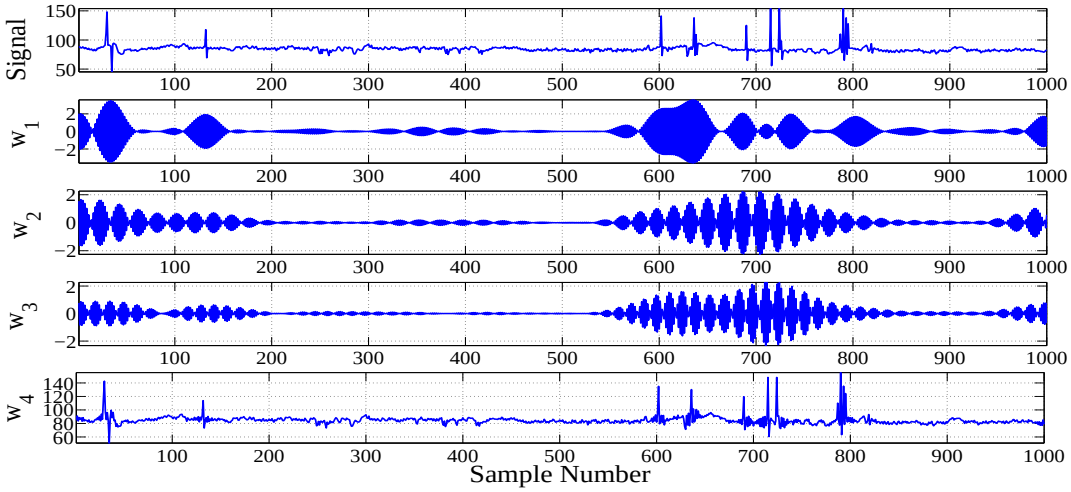

(b)

Figure 6.3. Third level of TQWT based decomposition of heart rate signals: (a) normal and (b) CAD subject.

parameters are tuned by minimizing a cross-validation score function using procedure that combines coupled simulated annealing and a simplex method as described at [134]. The training and testing of the proposed classification is done using three-fold cross validation approach. In all, 143 heart rate signals containing 61 from normal subjects and 82 from CAD patients are used for three-fold cross validation. Each of these heart rate signals have 1000 samples covering 15 minutes recording interval. The above mentioned procedure involving TQWT based decomposition, feature extraction, feature reduction and classification is repeated sequentially for incremental values of Q from 1 to 50 in step of one. For improved classification performance, best Q or underlying wavelets are sought at third level by conducting the experiment with various values of Q for the considered kernel functions. Figs. 6.4 shows the variation of performance of LS-SVM classifier for (a) RBF, (b) Morlet, and (c) Maxican hat wavelet kernel functions versus Q. It can be observed from Fig. 6.4 that, LS-SVM classifier kernels work better for Q from 24 to 30. Table 6.2 shows the LS-SVM classification results for Q from 24 to 30. It can be seen in Table 6.2 that the proposed method obtained a that the proposed method obtained a classification accuracy of $99.72 \pm 0.27\%$, sensitivity of $99.63 \pm 0.39\%$, specificity of $99.81 \pm 0.32\%$ and Matthews correlation coefficient of 0.9956 ± 0.0050 in the specified range of Q using Morlet kernel function. Moreover, Table 3 presents the maximum classification performance obtained for the kernel under study for a single selected value of Q. It is noteworthy that higher classification accuracy, sensitivity, specificity and Matthews correlation coefficient are obtained for $Q = 27$, 24 and 30 using RBF, Morlet, and Maxican hat wavelet kernel functions respectively. It should also be noted that three-fold cross validation is repeated ten times to produce the consistency in results shown in Fig. 6.4. and Table 6.2.

The experimental results shows that features based on time-frequency/scale properties of TQWT and CCo are quite effective to represent the behavior of heart rate signals for normal and CAD subjects giving higher classification performance for Q from 24 to 30.

Fig. 6.5 shows the distribution of CAD index that is measured for normal (7.2039 ± 0.5319) and CAD (5.0103 ± 0.3389) heart rate signals. The p-value is nearly zero for both

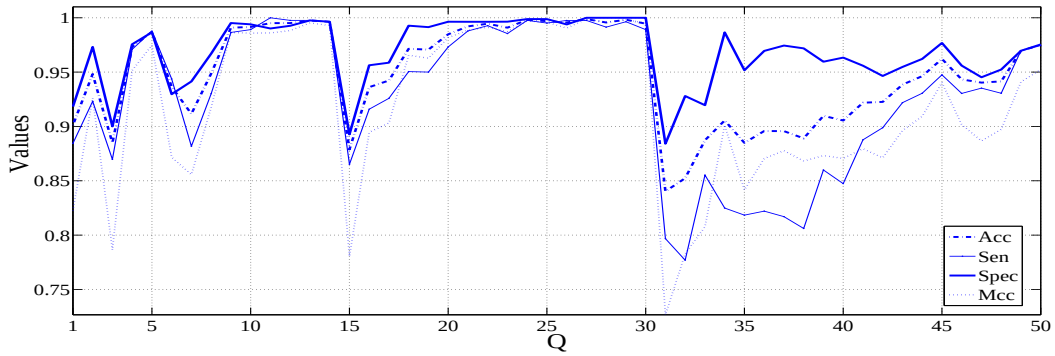

(a)

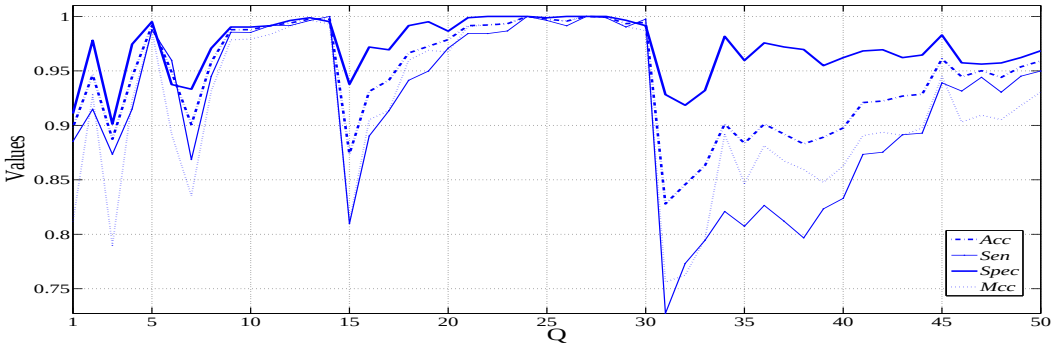

(b)

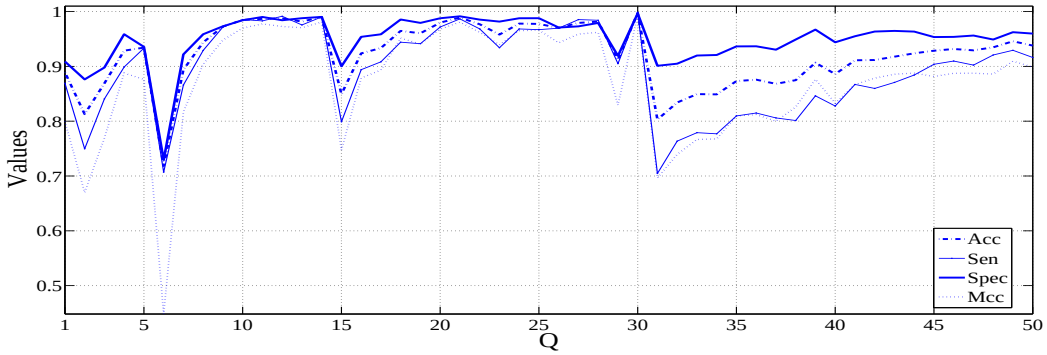

(c)

Figure 6.4. Variation of performance of LS-SVM classifier for (a) RBF, (b) Morlet, and (c) Maxican hat wavelet kernel functions versus Q.

Table 6.1. Results of principal components analysis (Mean± SD) for normal and CAD subjects after taking logarithm of absolute values of principal components.

Feature	Normal	CAD	p-value
	$\mu \pm \sigma$	$\mu \pm \sigma$	
PC_1	-3.7708 ± 1.003	-2.7814 ± 0.8023	7.4213 $\times 10^{-11}$
PC_2	-6.6915 ± 1.0920	-4.488 ± 0.8969	0

Table 6.2. Classification results for various kernel functions of LS-SVM classifier with respect to variation of Q between 24 to 30.

Kernel function	*Acc* (%)			*Sen* (%)			*Spec* (%)			*Mcc*		
	max	μ	σ	max	μ	σ	max	μ	σ	max	μ	σ
Morlet Kernel	100	99.72	0.27	100	99.63	0.40	100	99.81	0.32	1	0.9956	0.0051
RBF	99.88	99.69	0.16	99.76	99.49	0.34	100	99.88	0.22	0.9988	0.9959	0.0027
Mexican hat Kernel	99.76	97.09	2.73	99.88	96.83	3.03	99.64	97.35	2.56	0.9942	0.9455	0.0535

Table 6.3. Summary of the performance of the various automated methods used for diagnosis of CAD.

Authors	Features/Method	Classifiers	*Acc* (%)
Arafat et al. [221], 2005	ECG stress signals and Probabilistic Neural Networks	Fuzzy Interference Systems	80
Karimi et al. [181], 2005	DWT and cardiac sounds	Neural Networks	85
Kim et al. [222], 2007	Multiple Discriminant Analysis	Different classifiers	72.5-84.6
Lee et al. [223], 2007	Linear and nonlinear features	SVM	90
Lee et al. [224], 2008	Carotid arterial wall thickness	CPAR and SVM	85-90
Zhao and Ma [225], 2008	EMD-Teager Energy Operator	BPNN	85
Babaoglu et al. [226], 2010	BPSO with GA	SVM	81.46
Babaoglu et al. [227], 2010	PCA	SVM	79.71
Dua et al. [228], 2012	Linear and nonlinear features	MLP	89.5
Giri et al. [61] , 2013	Heart rate signals and ICA	GMM	96.8
The proposed work	**TQWT and Correntropy**	**LS-SVM**	**99.72**

the classes that reflects different ranges of this index for these two classes. The Fig. 6.5 clearly depicts that the CAD index is significantly different for the normal and CAD heart rate signals in turn can be effectively used for diagnosis of CAD subjects using a threshold.

As compared to published work in [61], the main contribution of this work is the development of new methodology that can provide highest possible classification accuracy in diagnosis of CAD. The proposed methodology suggests the use of just two features based on TQWT and correntropy that can provide significant differences between the considered two classes. It is noteworthy that after PCA based feature transformation, the CAD index has been measured by combining the values of both the principle components that is significantly different for normal and CAD with p-values nearly zero. Moreover, this study uses more classification performance parameters than that of earlier methods for detection of CAD. This work obtained the average classification accuracy of 99.7%, sensitivity of 99.6%, specificity of 99.8%, and Matthews correlation coefficient of 99.5% for Q varying between 24 to 30 using Morlet wavelet kernel function.

On the other hand, the method reported in [61] relies on ten features obtained from DWT coefficients using feature reduction techniques. The highest classification accuracy obtained using that method was 96.8% with sensitivity and specificity of 100% and 93.7%.

6.5 Discussion

Table 6.3 shows the summary of performance of the various methods used to automated diagnosis of CAD subjects using heart rate signals. In [181], DWT and wavelet packet decomposition (WPD) methods are applied on heart sound signals to diagnose the CAD. They have obtained an accuracy of 85% and 90% for DWT and WPD respectively using neural network classifier. Arafat et al. have compared the applicability of combined uncertainty model with fuzzy or probabilistic uncertainty model in computerised diagnosis of CAD using ECG stress signals [221]. The combined uncertainty model has provided better detection performance of CAD with an accuracy of 80%. Many linear and non-linear parameters have been extracted

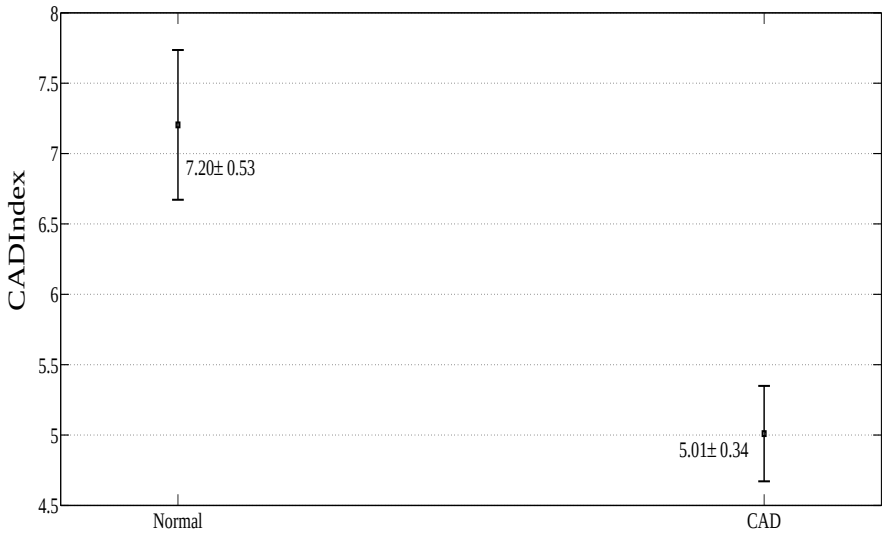

Figure 6.5. The ranges of CAD index for normal and CAD heart rate signals.

using heart rate signals to use as diagnostic features for classification intended to predict the subjects with CAD in [223]. Their experimental results show that classification using SVM performed better than other classifiers yielding the highest accuracy of 90%. Again in [224], the same features along with carotid arterial wall thickness are used for diagnosis of CAD. They have found that the classification using SVM and predictive association rules (CPAR) has provided better accuracies between 85% to 90%. Diagnosis of CAD using Empirical mode decomposition (EMD) and Teager energy operator based estimation of instantaneous frequency of diastolic murmurs have been performed in [225]. Their method yielded the diagnostic accuracy of 85% using back propagation neural network (BPNN). Various linear and nonlinear measures of heart rate signals are used for classification of control, angina pectoris and acute coronary syndrome in [222]. Multiple discriminant analysis coupled with the features yielded a classification accuracy of 75.0 % to classify three classes. The method demonstrated a sensitivity of 72.5% and specificity of 81.8% in the classification of angina pectoris, and sensitivity and specificity of 84.6 % and 91.5 %, respectively to detect acute coronary syndrome. The binary particle swarm optimization (BPSO) and genetic algorithm

(GA) techniques are used as feature selection models on exercise stress test data [226]. The eleven features coupled with SVM gave an accuracy of 81.46%. The effectiveness of PCA on the assessment of exercise stress test for SVM based diagnosis of CAD is studied in [227]. Their work obtained an accuracy of 79.71% using 18 principal components. In [228], the nonlinear features from the heart rate signals are extracted using recurrence plots, Poincare plots, DFA, Shannon entropy, approximation entropy, and sample entropy to automatically detect CAD patients. These features are fed to PCA. Their method yielded a classification accuracy of 89.5% using multilayer perceptron (MLP) classifier and eight principal components. In [61], the heart rate signals are decomposed by DWT upto third level. The detailed coefficients of DWT are reduced into lower dimensional feature set using PCA, independent component analysis (ICA) and linear discriminant analysis (LDA). The ICA coupled with gaussian mixture model (GMM) provided highest accuracy of 96.8%.

In this work, features were extracted from heart rate signals instead of ECG signals and cardiac sound signals. A new transform that is TQWT has been used for obtaining the desired sub-band signal for subsequent feature extraction. In fact, after TQWT based decomposition, we have extracted the correntropy based two features and applied PCA on the extracted features for transformation that can yield more discriminatory power to the input features. The transformed features were fed to the LS-SVM classifier that resulted in the highest classification performance for detecting CAD. It is worth to note that after PCA based feature transformation, both the principle components were used to measure CAD index for discriminating the normal and CAD subjects with p-values nearly zero. It can also be inferred that the CAD index derived using correntropy based features and TQWT exhibit relatively lower range for CAD subjects than that of normal. This inference has never been drawn in the literature and it reflects the novelty of this work. Moreover, this study uses more classification performance parameters than that of earlier methods for detection of CAD. This work obtained the average classification accuracy of 99.7%, sensitivity of 99.6%, specificity of 99.8%, and Matthews correlation coefficient of 99.5% for Q varying between 24 to 30 using Morlet wavelet kernel function. The proposed diagnostic frame work yield

significant classification performance than that of the previously published studies. However, we believe that the performance of our technique can be further evaluated and improved by considering more heart rate data. In a nut shell, the advantages and the disadvantages of our work can be summarized as described next.

The advantages of our proposed method are as follows:

(i) Obtained the highest performance using just two features.

(ii) There is no inter/intra observer variability as the system is completely automatic.

(iii) The cost of the system is only software. Hence can used installed in all hospitals and polyclinics for an affordable price.

(iv) System is more robust as we used ten times three-fold cross validation while training and testing.

The limitation of our work is as follows:

(i) We have used only ten normal and ten CAD subjects for this study.

(ii) System is completely digital. Hence may require more storage space.

(iii) Relying too much on the computer may bring down the discriminatory ability of the clinicians.

6.6 Summary

Accurate and early diagnosis of CAD can save the human life. In this paper, we have proposed a novel method based on TQWT and correntropy to detect CAD subjects using heart rate signals. Our method is able to capture the minute changes in the heart rate signals effectively using merely two correntropy based features extracted with TQWT to obtain the highest possible classification accuracy in diagnosis of CAD. In this work, we have defined CAD index that combines the significant features into a single-valued formulation

that can be used for deciding threshold to automatically detect CAD subjects using heart rate signals. It has been observed that this CAD index is significantly different for normal and CAD heart rate signals having relatively lower ranges for CAD. We have obtained the average classification accuracy of 99.7%, sensitivity of 99.6%, specificity of 99.8%, and Matthews correlation coefficient of 99.5% for Q varying between 24 to 30 using Morlet wavelet kernel function. Although the proposed diagnostic frame work yield significant classification performance, we believe that, as the future scope of this work, the performance of our work needs to be evaluated using proper stratification of cross-validation procedure by patients considering more heart rate data. The use of the CAD index needs to undergo rigorous clinical testing with adequate data in order to establish its efficient use for determining a stable threshold. After such successful validation with sufficient data, the proposed method can be used for mass screening of CAD patients accurately. This system is easy to use and can be installed in hospitals and polyclinics. This technique can be used to diagnose other healthcare applications.

Chapter 7

TQWT based Optimal Compression of Cardiac Sound Signals

7.1 Introduction

Heart disorders are the major cause of death worldwide. These cardiac abnormalities can be easily monitored, detected and identified by means of simpler and affordable diagnostic procedure based on acquiring cardiac sound signals using electronic stethoscope [12]. The compression of cardiac sound signals can improve the storage efficiency and the bandwidth for convenient diagnosis. Thus, compression and decompression methods for cardiac sound signals plays important role in data archiving and telemedicine.

The better compression is aimed at reducing the size of data while preserving the main morphological characteristics of signal after decompression [229, 230, 231]. The commonly used compression algorithm for biomedical signals are either lossy or lossless or combination of both. Generally, the compression using transform based methods such as WT leads to loss of information. The linear quantization can also cause to loss of original information. The Huffman and run length coding (RLC) have been used as traditional lossless techniques for compression.

The common transform based compression techniques use Fourier transform, Karhunen-

Loeve transform, Fast Walsh transform, Discrete cosine transform and WT. The WT based compression techniques such as embedded zero-trees wavelet, the set partitioning in hierarchical trees and the set partitioning embedded block have been found to provide promising compression performance [232, 233, 234, 235]. The first ever cardiac sound signal compression method using WT and WPT, together with Huffman coding and RLC has been proposed in [229]. Moreover, WT and WPT based compression algorithms similar to [236, 237, 238] have also been proposed for cardiac sound signals in [239, 240]. This compression algorithm has been found to yield better results for compression of cardiac sound signals than other existing standard audio compression techniques for music or speech like OGG Vorbis. The cardiac sound signals compression using this method depends on various parameters thus the optimization of these parameters have been carried out using GA as proposed in [241]. In order to encode the binary sequences resulting from WT, efficient and low-complexity compression technique has been presented in [242]. A quality driven cardiac sound signal coding for wireless cardiac patient monitoring has been developed in [243].

In this article, we present a new method for compression cardiac sound signals using TQWT having more parameters. Recently, the TQWT [1] has been found flexibly useful for analysis and processing of cardiac sound signals [118]. In the proposed method, the cardiac sound signals have been compressed using TQWT, linear quantization, Huffman coding and RLC. The proposed method decomposes the cardiac sound signals using TQWT and a dynamic threshold has been applied on the obtained wavelet coefficients to achieve target distortion error. On the one hand, the wavelet coefficients above the threshold have been compressed by steps involving zero removal, linear quantization and Huffman coding. On the other hand, the binary significant map of wavelet coefficients obtained after applying threshold have been compressed using last zero's block removal, RLC and Huffman coding. The optimized values of main compression parameters have been found using GA with a subset of dataset. The performance of these optimized values of compression parameters have been evaluated using a test set. The compression of cardiac sound signals by using proposed method have provided significant compression performance with lower distortion for various

clinical cases as comprised in the publicly available dataset. Moreover, the obtained results have been compared with other recent wavelet based method [241]. The comparative study shows better compression performance of the proposed method which can be attributed to the properties of TQWT and employment of more compression parameters for optimization. In addition, the effect of proposed compression/decompression on the diagnostic quality of signal for segmentation of cardiac sound signals into heart beat cycles has been studied. And it has been found that despite compression based malformations of cardiac sound signals, there occurs considerably lower distortion of cardiac sound signals for segmentation which is useful in performing diagnosis.

The rest of the chapter is organized as follows: The methodology for TQWT based compression of cardiac sound signals covering TQWT based compression, linear quantization, Huffman coding and RLC based additional compression, compression parameters and genetic algorithm (GA) based optimization of compression parameters have been presented in section 7.2. Section 7.3 describes the experimental results of the proposed method along with comparison of proposed method with one recent WT based method. Finally, section 7.4 summarises the chapter.

7.2 Methodology

The flowchart of the proposed method for compression of normal and abnormal cardiac sound signals has been presented in Fig. 7.1. The main steps involve: tunable-Q wavelet transform based decomposition (TQWD), application of threshold, zero removal, linear quantization / RLC and Huffman coding. The subsections of the proposed method can be described as follows.

7.2.1 TQWT based Compression

To begin with, the cardiac sound signals can be segmented into non-overlapping blocks containing N samples. Then, each of these segments can be decomposed into various sub-

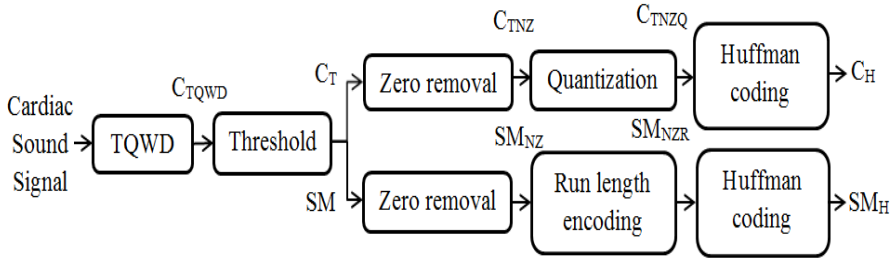

Figure 7.1. Flowchart of the proposed TQWT based compression of cardiac sound signals.

band signals by using TQWT. For a segment, $J+1$ sub-band signals are obtained considering J-levels of decomposition. The cell array containing these sub-band signals can be defined as [1]:

$$C_{\text{TQWD}} = \{w_1, w_2, w_3, ..., w_J, w_{J+1}\}, \tag{7.1}$$

where, w_{J+1} is the lowest frequency sub-band signal and from w_1 to w_J are the other high-pass sub-band signals. The number of samples in each of these sub-band signals can be obtained using the values of α and β as follows:

$$C_l = [\beta f_s N, \alpha\beta f_s N, \alpha^2\beta f_s N, ..., \alpha^{J-1}\beta f_s N, \alpha^J f_s N], \tag{7.2}$$

The order of the above obtained sub-band signals can be reversed for better screening before applying the threshold. The dynamic threshold can be computed to achieve the target distortion error of the original signal using percentage root mean square difference (PRD) as described in [244, 245]. After applying the threshold, two vectors can be formed such that one of these contains the thresholded wavelet coefficients (C_T) and other with significance map (SM). The later vector is a binary vector reflecting one's for nonzero wavelet coefficients. Then, nonzero thresholded coefficients (C_{TNZ}) and nonzero significance map without last block of zero's (SM_{TNZ}) can be derived using C_T and SM respectively.

7.2.2 Linear Quantization, Huffman and RLC based Compression

In order to perform the first stage of compression of C_{TNZ}, it can be linearly quantized in the range $[0, 2^b - 1]$ as follows [229]:

$$C_{\mathrm{TNZQ}} = \frac{2^b \left[C_{\mathrm{TNZ}} - \min(C_{\mathrm{TNZ}})\right]}{\max(C_{\mathrm{TNZ}}) - \min(C_{\mathrm{TNZ}})}, \tag{7.3}$$

where, C_{TNZQ} is the linearly quantized wavelet coefficient vector. The $\min(C_{\mathrm{TNZ}})$ and $\max(C_{\mathrm{TNZ}})$ are the minimum and maximum values of C_{TNZ} respectively.

7.2.3 Compression Parameters

The performance of the compression of cardiac sound signals can be measured in terms of compression rate (C_{rate}) and PRD by using following expressions [229, 245]:

$$C_{\mathrm{rate}} = \frac{Ln_s}{Ln_c}, \tag{7.4}$$

$$\mathrm{PRD} = \sqrt{\frac{\sum_{n=1}^{N}(s[n] - \widehat{s}[n])^2}{\sum_{n=1}^{N}(s[n] - \mu_s)^2}} \times 100, \tag{7.5}$$

where, Ln_s is the length of original signal $s[n]$ in bits having mean μ_s and Ln_c is the length of compressed signal formed with C_H and SM_H. The $\widehat{s}[n]$ represents the reconstructed signal.

7.2.4 GA based Optimization of Compression Parameters

The TQWT based compression of cardiac sound signals depends on many parameters. In this study, the compression performance depends on the type of mother wavelet or Q, J, the number of bits utilized for linear quantization (b), r, way of application of threshold. For each clinical case, the optimized value of these parameters can be found using GA by optimization of a objective function. The GA has been found to be versatile for solving both constrained and unconstrained optimization problems based on a natural selection process

Table 7.1. The optimized values of TQWT based cardiac sound signal compression parameters as obtained with GA

Method	TQWT					
Type of disease						
	Q	level (J)	r	b	N	Mean C_{rate}
Mitral regurgitation	4	22	4	7	8192	26.3421
Aortic stenosis	5	23	5	7	8192	15.2587
Mid systolic click	5	19	5	7	8192	13.2312
Aortic valve ejection sound	6	27	5	7	8192	13.5503
Third heart sound	3	14	4	7	8192	18.3300
Fourth heart sound	5	30	5	7	8192	16.2531
Normal heart sound	5	24	4	7	8192	28.4630
Average	5	23	5	7	8192	22.8416

of biological evolution [246]. The algorithm repeatedly modifies a population of individual solutions. At each step, the GA randomly chose individuals from the existing population and uses them as parents to create the children for the next generation. The procedure is repeated for successive generations such that population tends to be an optimal solution. The main advantage of employing GA for optimization of compression parameters is the faster execution covering entire search space as bounded by the ranges of the various compression parameters. In this chapter, the GA has been executed for 50 iterations with a population of 50 individuals. The parameters that have been optimized are Q, J, r, and b. Each of these parameters has a specific length in bits as determined using its possible range.

The objective function for optimization of cardiac sound signals using GA can be posed as [241].

$$\mathcal{L} = \left(\frac{1}{1 + k_1 \mathrm{PRD}}\right)^{\frac{1}{1+k_2 C_{\mathrm{rate}}}} \left(\frac{1}{1 + k_3 \mathrm{TPS}}\right)^{k_4}, \tag{7.6}$$

where, TPS is the time required to compress one second of cardiac sound signals. The value of objective function can vary in the range [0, 1]. The value of first exponential term varies in the range [0, 1]. In ideal situations this term takes value 1 for high values of C_{rate} and low values of PRD. The second exponential term accounts for variation in the time required for compression of one second of the cardiac sound signal. The values of the constant parameters k_1 to k_4 have been used to modify the relative significance of the PRD, C_{rate} and TPS. The values of these constant parameters have been found experimentally as follows: $k1 = k_3 = 5$, $k_2 = 0.2$, and $k_4 = 0.1$ [241].

7.3 Experimental Results

The proposed method for compression of cardiac sound signals has been validated with one online available dataset of abnormal cardiac sounds signals which can be freely downloaded as the heart sounds pod cast series (2011). This dataset has been produced by the Robert J. Hall Heart Sounds Laboratory of Texas Heart Institute at St. Luke's Episcopal Hospital. The

Table 7.2. The results of cardiac sound signal compression using test set

Method	C_{rate} ($\mu\pm\sigma$)	TPS ($\mu\pm\sigma$)
WT (db9)	8.4511±0.7021	0.3463±0.0731
WT (db10)	8.4274±0.7067	0.3660±0.0775
TQWT	13.5465±5.2175	0.3679±0.0716

dataset is composed of real clinical cases with 50 abnormal cardiac sound signals acquired from variety of subjects with relevant chest positions with different patient maneuver. The sampling frequency of most of the data is 44.100 kHz with 16 bits except for few cases. Some of the recordings in the dataset were corrupted by the human voice, rubbing sound due to stethoscope and other lung sounds. Also, the duration of the heart beat cycles are inconsistent. For more information regarding the dataset, this series is available at [100]. The normal cardiac sound signals with sampling frequency of 44.100 kHz with 16 bits have been obtained from [133].

The proposed compression has been implemented with Matlab using m-files. The functions of the TQWT toolbox and genetic algorithm & direct search toolbox of Matlab have been used for implementing the proposed method. The Matlab software for TQWT toolbox is available at [220]. A subset of dataset containing recordings of normal, mid-systolic click, aortic stenosis, mitral regurgitation, third heart sound and fourth heart sound have been used for optimization of compression performance. For initial 10 blocks of each recording, the results of GA based optimization of compression parameters have been shown in Table 7.1. During optimization, the tournament selection has been used to choose the individuals. The window length of 8192 samples has been used in this study in view of maximum samples allowed for Huffman coding. The dynamic threshold has been applied to achieve

target PRD of 3% as described in [245]. The final compression has been performed with average values of optimized parameters using the test set and the obtained results have been presented in Table 7.2. The test set consists of recordings from all the 20 clinical cases in the heart sounds pod cast series. The mean and standard deviation are denoted by μ and σ respectively. In Fig. 7.2, from (a), (c), (e), (g), (i), (k) and (m) shows the cardiac sound signals without compression for normal, third heart sound, aortic valve ejection sound, aortic stenosis, fourth heart sound, mitral regurgitation, mid-systolic click respectively. The corresponding decompressed cardiac sound signals after compression has been shown in Fig. 7.2 from (b), (d), (f), (h), (j), (l) and (n). Fig. 7.2 depicts lower distortion error in cardiac sound signals after compression/decompression than that of without compression. The experimental results in Table 6.2 show that maximum of C_{rate} for the proposed method and the WT based method with db10 wavelet have been 18.7215 and 9.1341 respectively. The proposed method outperforms the WT based method by providing higher value of C_{rate} with target PRD of 3% in turn ensuring better quality of reconstructed signal. The proposed method has provided comparatively better performance which can be attributed to the properties of TQWT. Moreover, the deployment of the TQWT provides more compression parameters for optimization.

The following part of this study shows the effect of compression/decompression on the diagnostic quality of signals for segmentation of cardiac sound signals into heart beat cycles. The automatic segmentation of cardiac sound signals into heart beat cycles is generally required for the detection and identification of heart disorders. The segmentation of the cardiac sound signals has been performed using TQWT as described in [118]. The murmurs from cardiac sound signals have been removed by suitably constraining TQWT based decomposition and reconstruction. The Q-factor, redundancy parameter and number of stages of decomposition of the TQWT have been adapted to the desired statistical properties of the murmur-free reconstructed cardiac sound signals. The envelope based on CSCW has been extracted after the removal of low energy components from the reconstructed cardiac sound signals. Then, the heart beat cycles have been derived from the original cardiac sound

signals by mapping the required timing information of CSCW which has been obtained using established methods. The experimental results on segmentation of cardiac sound signals have been shown in Table 7.3 with and without the proposed compression/decompression. The signals used for segmentation includes the normal and abnormal cardiac sound signals comprising six different pathological cases same as that have been used during optimization of compression of cardiac sound signals. In Table 7.3, the correct segmentation has been defined in terms of segmentation rate (SR) as the ratio of correctly segmented heart beat cycles (SB) to the actual total number of heart beat cycles (TB). From this study, it has been found that despite compression based malformations of cardiac sound signals, there occurs considerably lower distortion of cardiac sound signals for segmentation as applicable in diagnosis of heart disorders.

7.4 Summary

The TQWT is an important method for analysis and processing of cardiac sound signals. The compression of cardiac sound signals by using TQWT has been performed to improve the bandwidth and the storage efficiency for convenient diagnosis of heart disorders. The optimized values of the compression parameters have been obtained using GA for final evaluation of the proposed framework using test data. The proposed TQWT based method for compression of cardiac sound signals has been found more effective in ensuring diagnostic quality of signal after compression/decompression by virtue of more parameters for compression. The proposed compression method can be effectively used for data archiving and telemedicine for computer-aided diagnosis of heart disorders. It would be of interest to develop the compression method for ECG signals based on the proposed compression method in this chapter.

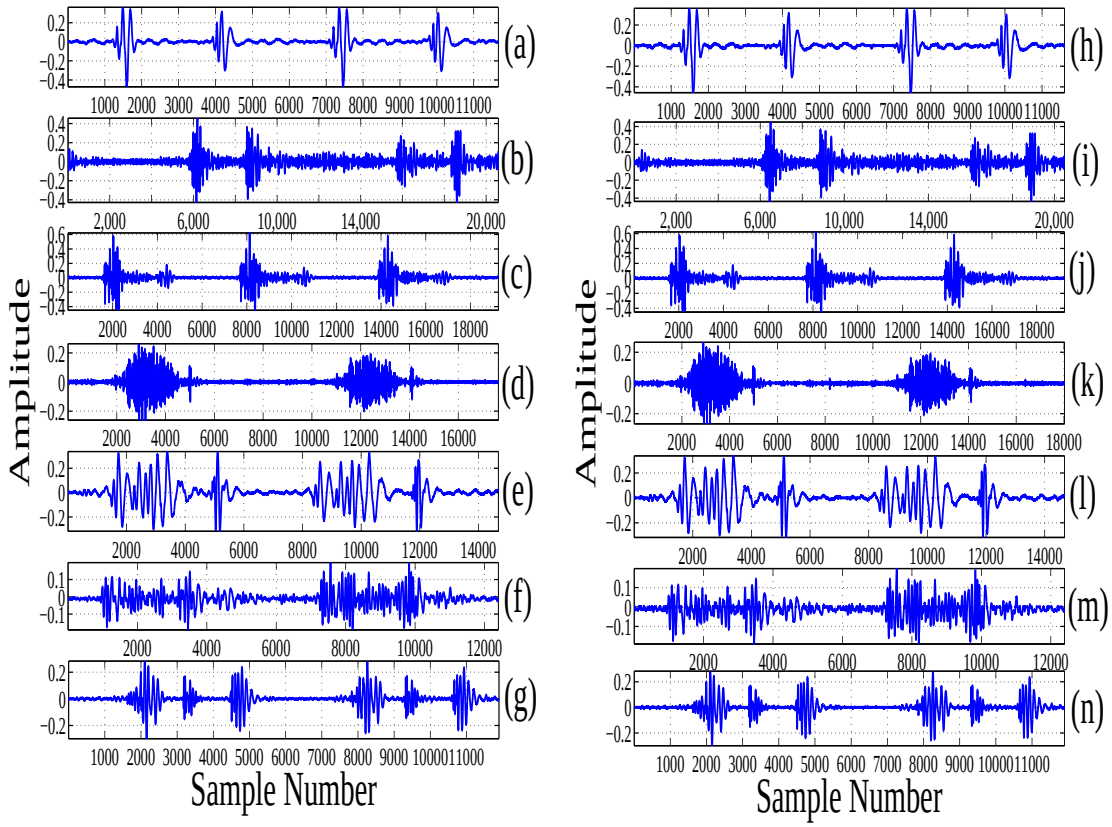

Figure 7.2. Examples of cardiac sound signals. (a), (c), (e), (g), (i), (k) and (m) shows signals without compression for normal, third heart sound, aortic valve ejection sound, aortic stenosis, fourth heart sound, mitral regurgitation, mid-systolic click respectively. The corresponding signals after compression/decompressed have been shown from (b), (d), (f), (h), (j), (l) and (n).

Table 7.3. The experimental results on segmentation of cardiac sound signals with and without the proposed compression/decompression compression

Method	Without Compression			With compression		
Type of disease						
	THV	SB/TB	SR(%)	THV	SB/TB	SR(%)
Mitral regurgitation	15	16/18	88.88	15	16/18	88.88
Aortic stenosis	15	40/46	86.96	10	40/46	86.96
Mid systolic click	15	27/27	100	15	27/27	100
Aortic valve ejection sound	25	10/13	76.92	25	10/13	76.92
Third heart sound	30	29/30	96.66	30	29/30	96.66
Fourth heart sound	45	29/29	100	40	29/29	100
Normal heart sound	10	50/50	100	10	50/50	100

Chapter 8

Conclusion and Future Scope of the Work

8.1 Conclusion

The cardiac signals can serve as useful means of diagnosis of heart disorders. The analysis, preprocessing, segmentation, feature extraction, feature selection and classification of cardiac signals are emerging areas of Biomedical signal processing for detection and identification of heart disorders. The advanced signal processing methods and medical artificial intelligence are of paramount significance to effectively carry out the medical decision making. Now a days, the need of application of health care services from a distance is growing. Due to this, the research in the area of telemedicine which use computerized or digital diagnostic equipment and incorporation of information systems for health care applications is developing tremendously. The application of telemedicine includes, among others, the following remotely executed processes: diagnosis, therapy and treatment, monitoring and rehabilitation of patients, prevention and education of patients, doctors and medical students.

This work explores the capability of TQWT for envelope based segmentation of oscillatory cardiac sound signals into heart beat cycles. The proposed method based on constrained TQWT based decomposition and reconstruction captures the required information in the re-

constructed signal using sufficient number of adaptable input parameters of the TQWT. The experimental results have reflected the capability of constrained TQWT based decomposition and reconstruction in perfectly identifying the primary heart sounds form the overlapping murmurs even when with they were having comparable magnitude.

The classification of cardiac sound signals for detection and identification of heart valve disorders using TQWT based novel feature set have been explored. This feature set has been obtained by the parameters based on the constrained TQWT, time-domain representation, and FB expansion of cardiac sound signals. This work has suggested the extraction of features during the separation of heart sounds and murmur using the segmented heart beat cycles. Nevertheless, the separation of heart sounds and murmur has been used for obtaining more diagnostic information with same features to successfully classify cardiac sound signals. Finally, the features based on FB expansion have been used to represent the spectral properties of segmented cardiac sound signals. The experimental results have shown that the proposed novel features are effective for classification of cardiac sound signals. The proposed classification method requires less number of effective features that can lead to reduce computation complexity. This feature of the proposed method makes suitable for real time implementation of expert system for classification of heart valve disorders. Auscultation with an electronic stethoscope integrated with the proposed classification technique can be used as an expert system. This expert system may be helpful for clinicians to carry out investigations in the clinic, hospital and even at home.

The diagnosis of septal defects by representation of cardiac sound signals with TQWT based features has been studied. This feature set has been obtained by the TQWT based SAMDF of segmented heart beat cycles derived from cardiac sound signals. In search of appropriate level of TQWT based decomposition that can provide efficient features, the suggested feature sets have been formed and used to classify cardiac sound signals for different levels. The proposed features have been used as an input to the LS-SVM classifier together with different kernel functions. The experimental results have been found promising that reveals the capabilities of proposed feature set in characterization of different types of cardiac

sounds signals for diagnosis of septal defects. The salient feature of the proposed method is that its classification performance has been found to be independent of the values of Q at tenth level of decomposition using Morlet wavelet kernel function. The proposed method can be implemented as an expert system for classification of cardiac sound signals to diagnose septal defects. The computer-aided auscultation using electronic stethoscope or mobile technology with the proposed classification technique based on TQWT derived SAMDF can be used as an intelligent and affordable expert system that can automatically detect the septal defects. This expert system can reduce the health care expenses and avoid the challenges of mastering cardiac auscultation thereby helping the physicians to conveniently diagnose the septal defects.

Accurate and early diagnosis of CAD can save the human life. In view of this, a novel method based on TQWT and CCo to detect CAD subjects using heart rate signals has been presented. Our method is able to capture the minute changes in the heart rate signal effectively. We have obtained the average classification accuracy of 99.7%, sensitivity of 99.6%, specificity of 99.8%, and Matthews correlation coefficient of 0.995% for Q varying between 24 to 30 using Morlet wavelet kernel function. The proposed method can be used for mass screening of CAD patients accurately. This system is easy to used and can be installed in hospitals and polyclinics. This technique can be used to diagnose other healthcare applications.

The compression of cardiac sound signals by using TQWT has been performed to improve the bandwidth and the storage efficiency for convenient diagnosis of heart disorders. The optimized values of the compression parameters have been obtained using GA for final evaluation of the proposed framework using test data. The proposed TQWT based method for compression of cardiac sound signals has been found more effective in ensuring diagnostic quality of signal after compression/decompression by virtue of more parameters for compression.

8.2 Future Scope of the Work

The proposed framework for analysis, segmentation, feature extraction, feature selection and classification of cardiac sound signals is effective for detection and identification of heart valve disorders and septal defects. The diagnosis of CAD by classification of ECG based heart rate signals can be used for routine medical check ups. The TQWT based optimal compression of cardiac sound signals is quite promising to be used for telemedicine purpose. However, to facilitate further development of the proposed methodologies in this thesis, the following highlighted issues can be addressed in the future.

The murmurs which are extracted using constrained TQWT based decomposition and reconstruction can provide more insight into the modelling aspects of cardiovascular system. In this work, categories of cardiac sound signals under study have been expanded to cover a broader range of diseases. It would be of interest to investigate the effect of noise on the proposed methodologies. For classification, the proposed methodologies need to be validated with more number of patients for proper stratification of cross-validation procedure by patients. The k-fold cross-validation procedure can produce more effective classification performance for detection and identification of heart valve and other disorders. It might be interesting to find a best kernel function between every hyperplane instead of using one for all hyperplanes. In order to measure reliable performance of proposed classification technique for diagnosis of heart valve disorders, more classification performance measures can be included. The proposed classification methodologies can be compared with other time-frequency methods to establish the significance of the proposed diagnostic framework. Moreover, in future, the research can be carried out for screening of features that can reduce the computational burden of the algorithm with further improvement in the classification accuracy in diagnosis. In addition, the proposed diagnostic framework should be applied on out-of-sample data for its possible application in health care clinics.

The part of this work can be further extended for detection and identification of cardiac devices especially the artificial heart valves in routine emergency check-ups at hospitals. The classification methodologies presented in this thesis can be extended for identification of type

and degree of septal defects. The proposed expert systems can be used for classification of other biomedical signals like EEG, ECG, EMG signals corresponding to normal and abnormal conditions.

The proposed compression method can be effectively used for data archiving and telemedicine for computer-aided diagnosis of heart disorders. It would be of interest to develop the compression method for ECG signals based on the proposed compression method in this chapter.

Bibliography

[1] I. W. Selesnick, Wavelet transform with tunable Q-factor, IEEE Transactions on Signal Processing 59 (8) (2011) 3560–3575.

[2] L. P. Feigen, Physical characteristics of sound and hearing, The American Journal of Cardiology 28 (2) (1971) 130–133.

[3] I. R. Hanna, M. E. Silverman, A history of cardiac auscultation and some of its contributors, The American Journal of Cardiology 90 (3) (2002) 259–267.

[4] L.-G. Durand, P. Pibarot, Digital signal processing of the phonocardiogram: review of the most recent advancements, Critical Reviews in Biomedical Engineering 23 (3-4).

[5] S. Lukkarinen, A.-L. Noponen, K. Sikio, A. Angerla, A new phonocardiographic recording system, in: Computers in Cardiology, 1997, pp. 117–120.

[6] S. Mangione, L. Z. Nieman, Cardiac auscultatory skills of internal medicine and family practice trainees. A comparison of diagnostic proficiency, Journal of the American Medical Association 278 (9) (1997) 717–722.

[7] A. Pease, If the heart could speak, Pictures of the Future (2001) 60–61.

[8] R. L. Watrous, Computer-aided auscultation of the heart: From anatomy and physiology to diagnostic decision support, in: Proceedings of 28th Annual International Conference of the IEEE Engineering in Medicine and Biology Society, New York, 2006, pp. 140–143.

[9] R. L. Watrous, W. R. Thompson, S. J. Ackerman, The impact of computer-assisted auscultation on physician referrals of asymptomatic patients with heart murmurs, Clinical cardiology 31 (2) (2008) 79–83.

[10] A. Gacek, W. Pedrycz, ECG Signal Processing, Classification and Interpretation, Springer, 2012.

[11] Z. Syed, D. Leeds, D. Curtis, F. Nesta, R. A. Levine, J. Guttag, A framework for the analysis of acoustical cardiac signals, IEEE Transactions on Biomedical Engineering 54 (4) (2007) 651–662.

[12] R. M. Rangayyan, R. J. Lehner, Phonocardiogram signal analysis: a review, Critical Reviews in Biomedical Engineering 15 (3) (1986) 211–236.

[13] R. Rushmer, Cardiovascular Dynamics (4th ed.) WB Saunders Company (1976).

[14] A. A. Luisada, F. Portaluppi, The heart sounds: New facts and their clinical implications, Praeger, New York, 1982.

[15] S. Ari, K. Sensharma, G. Saha, DSP implementation of a heart valve disorder detection system from a phonocardiogram signal, Journal of Medical Engineering & Technology 32 (2) (2008) 122–132.

[16] S. Chauhan, P. Wang, C. Sing Lim, V. Anantharaman, A computer-aided MFCC-based HMM system for automatic auscultation, Computers in Biology and Medicine 38 (2) (2008) 221–233.

[17] S. R. Messer, J. Agzarian, D. Abbott, Optimal wavelet denoising for phonocardiograms, Journal of Microelectronics 32 (12) (2001) 931–941.

[18] A. Almasi, M. Bagher Shamsollahi, L. Senhadji, Bayesian denoising framework of phonocardiogram based on a new dynamical model, IRBM 34 (3) (2013) 214–225.

[19] H. Naseri, M. Homaeinezhad, Computerized quality assessment of phonocardiogram signal measurement-acquisition parameters, Journal of medical engineering & technology 36 (6) (2012) 308–318.

[20] H. Pasterkamp, S. S. Kraman, G. R. Wodicka, Respiratory sounds: advances beyond the stethoscope, American Journal of Respiratory and Critical Care Medicine 156 (3) (1997) 974–987.

[21] K. M. Van de Graaff, R. W. Rhees, S. Palmer, Schaum's Outline of Human Anatomy and Physiology, McGraw-Hill Professional, 2010.

[22] S. R. Wiese, P. Anheier, R. D. Connemara, A. T. Mollner, T. F. Neils, J. A. Kahn, J. G. Webster, Electrocardiographic motion artifact versus electrode impedance, IEEE Transactions on Biomedical Engineering 52 (1) (2005) 136–139.

[23] T. Pawar, S. Chaudhuri, S. P. Duttagupta, Body movement activity recognition for ambulatory cardiac monitoring, IEEE Transactions on Biomedical Engineering 54 (5) (2007) 874–882.

[24] M. Fernández-Chimeno, M. Quílez, F. Silva, Understanding electrosurgical unit perturbations in order to address hospital operating room electromagnetic compatibility, IEEE Transactions on Biomedical Engineering 53 (6) (2006) 1206–1209.

[25] E. N. Bruce, Biomedical signal processing and signal modeling, Wiley-Interscience, New York, 2000.

[26] R. F. Santopietro, The origin and characterization of the primary signal, noise, and interference sources in the high frequency electrocardiogram, Proceedings of the IEEE 65 (5) (1977) 707–713.

[27] D. Jennings, A. Flint, B. C. H. Turton, L. D. M. Nokes, Introduction to medical electronics applications, Edward Arnold, a division of Hodder Headline PLC, London, 1995.

[28] S. Jesus, H. Rix, High resolution ECG analysis by an improved signal averaging method and comparison with a beat-to-beat approach, Journal of Biomedical Engineering 10 (1) (1988) 25–32.

[29] N. Ahmed, P. J. Milne, S. G. Harris, Electrocardiographic data compression via orthogonal transforms, IEEE Transactions on Biomedical Engineering (6) (1975) 484–487.

[30] E. J. Berbari, E. A. Bock, A. C. Cházaro, X. Sun, L. Sornmo, High-resolution analysis of ambulatory electrocardiograms to detect possible mechanisms of premature ventricular beats, IEEE Transactions on Biomedical Engineering 52 (4) (2005) 593–598.

[31] E. N. Marieb, K. Hoehn, The Cardiovascular System: The Heart, Human Anatomy & Physiology (2007) 677–712.

[32] R. Berne, M. Levy, Cardiovascular Physiology (4th ed), The C.V. Mosby Company, 1998.

[33] C. Ahlström, Nonlinear phonocardiographic signal processing (2008).

[34] R. M. Rangayyan, Biomedical Signal Analysis. A Case-Study Approach, IEEE Press, Piscataway, NJ, 2005.

[35] Y.-T. Zhang, G. Chan, X.-y. Zhang, L. Yip, Heart sounds and stethoscopes, Wiley Encyclopedia of Biomedical Engineering, Wiley Online Library, 2006.

[36] S. Ari, K. Hembram, G. Saha, Detection of cardiac abnormality from PCG signal using LMS based least square SVM classifier, Expert Systems with Applications 37 (12) (2010) 8019–8026.

[37] G. J. Tortora, B. H. Derrickson, Principles of anatomy and physiology (13th ed.), John Wiley & Sons, 2012.

[38] H. Nazeran, Electrocardiocarphy, Computer In, Vol. 3, Wiley Encyclopedia of Medical Devices and Instrumentation, Wiley Online Library, 2006.

[39] G.-X. Yan, R. S. Lankipalli, J. F. Burke, S. Musco, P. R. Kowey, Ventricular repolarization components on the electrocardiogramcellular basis and clinical significance, Journal of the American College of Cardiology 42 (3) (2003) 401–409.

[40] J. G. Webster, Medical Instrumentation: Application and Design (3rd ed.), John Wiley & Sons, New York, 1998.

[41] W. J. Tompkins, Biomedical digital signal processing, Prentice-Hall, Upper Saddle River, NJ.

[42] E. Grayden, Cardiopulmonary Resuscitation, Vol. 2, Wiley Encyclopedia of Medical Devices and Instrumentation, Wiley Online Library, 2006.

[43] E. Goldberger, Unipolar lead electrocardiography and vectorcardiography (ed. 3) lea & febiger, Publishers, Philadelphia (1954) 189.

[44] A. Leatham, Auscultation of the Heart and Phonocardiography (2nd ed.), J. & A. Churchill, London, UK, 1970.

[45] W.-C. Kao, C.-C. Wei, Automatic phonocardiograph signal analysis for detecting heart valve disorders, Expert Systems with Applications 38 (6) (2011) 6458–6468.

[46] A. C. Stasis, E. Loukis, S. Pavlopoulos, D. Koutsouris, A multiple decision trees architecture for medical diagnosis: The differentiation of opening snap, second heart sound split and third heart sound, Computational Management Science 1 (3-4) (2004) 245–274.

[47] V. Fuster, R. Alexander, R. O'Rourke, R. Roberts, S. King, I. Nash, E. Prystowsky, J. Hurst, Hurst's the Heart (11th ed.) (2004).

[48] K. Dumont, Experimental and numerical modeling of heart valve dynamics, Ph.D. thesis, Ghent University, Belgium (December 2005).

[49] S. of Cleveland Clinic, Diseases and conditions, `my.clevelandclinic.org` (2014).

[50] A. G. Tilkian, M. C. Boudreau, Understanding heart sounds and murmurs: With an introduction to lung sounds (4th ed.), Saunders, Philadelphia, 2001.

[51] S. Sun, H. Wang, Z. Jiang, Y. Fang, T. Tao, Segmentation-based heart sound feature extraction combined with classifier models for a VSD diagnosis system, Expert Systems with Applications 41 (4(2)) (2014) 1769–1780.

[52] C. A. Warnes, R. Liberthson, G. K. Danielson, A. Dore, L. Harris, J. I. Hoffman, J. Somerville, R. G. Williams, G. D. Webb, Task force 1: The changing profile of congenital heart disease in adult life, Journal of the American College of Cardiology 37 (5) (2001) 1170–1175.

[53] J. A. Finegold, P. Asaria, D. P. Francis, Mortality from ischaemic heart disease by country, region, and age: Statistics from World Health Organisation and United Nations, International Journal of Cardiology 168 (2) (2013) 934–945.

[54] D. P. Faxon, M. A. Creager, S. C. Smith, R. C. Pasternak, J. W. Olin, M. A. Bettmann, M. H. Criqui, R. V. Milani, J. Loscalzo, J. A. Kaufman, et al., Atherosclerotic vascular disease conference executive summary: Atherosclerotic vascular disease conference proceeding for healthcare professionals from a special writing group of the american heart association, Circulation 109 (21) (2004) 2595–2604.

[55] S. K. Bhatia, Biomaterials for clinical applications, Springer, 2010.

[56] D. M. L, O. T. G., Coronary Artery Disease. The Gale Encyclopaedia of Medicine (3rd ed.), L. Longe Jacqueline , Farmington Hills. MI. Thompson Gale, 2006.

[57] D. Steinberg, A. M. Gotto Jr, Preventing coronary artery disease by lowering cholesterol levels: fifty years from bench to bedside, Journal of the American Medical Association 282 (21) (1999) 2043–2050.

[58] P. D. Thompson, B. D. Levine, Protecting athletes from sudden cardiac death, Journal of the American Medical Association 296 (13) (2006) 1648–1650.

[59] J. K. Ockene, L. H. Kuller, K. H. Svendsen, E. Meilahn, The relationship of smoking cessation to coronary heart disease and lung cancer in the Multiple Risk Factor Intervention Trial (MRFIT), American Journal of Public Health 80 (8) (1990) 954–958.

[60] R. D. Brook, B. Franklin, W. Cascio, Y. Hong, G. Howard, M. Lipsett, R. Luepker, M. Mittleman, J. Samet, S. C. Smith, et al., Air pollution and cardiovascular disease: A statement for healthcare professionals from the expert panel on population and prevention science of the American Heart Association, Circulation 109 (21) (2004) 2655–2671.

[61] D. Giri, U. Rajendra Acharya, R. J. Martis, S. Vinitha Sree, T.-C. Lim, T. Ahamed VI, J. S. Suri, Automated diagnosis of coronary artery disease affected patients using LDA, PCA, ICA and discrete wavelet transform, Knowledge-Based Systems 37 (2013) 274–282.

[62] E. N. Silber, L. N. Katz, Heart Disease, Macmillan Publishing Co., New York, 1975.

[63] J. A. San Román, I. Vilacosta, J. A. Castillo, M. J. Rollán, M. Herńandez, V. Peral, Garcimartí, Selection of the optimal stress test for the diagnosis of coronary artery disease.

[64] M. Berman, A. Fenaughty, Technology and managed care: patient benefits of telemedicine in a rural health care network, Health Economics 14 (6) (2005) 559–573.

[65] N. Hjelm, Benefits and drawbacks of telemedicine, Journal of telemedicine and telecare 11 (2) (2005) 60–70.

[66] I. Sachpazidis, Image and medical data communication protocols for telemedicine and teleradiology, Ph.D. thesis, TU Darmstadt (2008).

[67] F. Kovacs, C. Horváth, M. Torok, G. Hosszu, Long-term phonocardiographic fetal home monitoring for telemedicine systems, in: Proceedings of Annual International

Conference of the Engineering in Medicine and Biology Society, IEEE, 2006, pp. 3946–3949.

[68] L. Cohen, Time-frequency distributions–A review, in: Proceedings of IEEE 77, 1989, pp. 941–981.

[69] S. Yuenyong, A. Nishihara, W. Kongprawechnon, K. Tungpimolrut, A framework for automatic heart sound analysis without segmentation, BioMedical Engineering Online 10 (13) (2011) 1–23.

[70] Y.-J. Chung, Using Kullback-Leibler distance in determining the classes for the heart sound signal classification, in: Intelligent Data Engineering and Automated Learning, 2008, pp. 49–56.

[71] Y.-H. Chen, H.-H. Chen, T.-C. Chen, L.-G. Chen, Robust heart rate measurement with phonocardiogram by on-line template extraction and matching, in: Proceedings of Annual International Conference of the IEEE Engineering in Medicine and Biology Society, IEEE, 2011, pp. 1957–1960.

[72] C. Papadaniil, L. Hadjileontiadis, Efficient heart sound segmentation and extraction using ensemble empirical mode decomposition and kurtosis features, IEEE Journal of Biomedical and Health Informatics 18 (4) (2014) 1138–1152.

[73] M. Malarvili, I. Kamarulafizam, S. Hussain, D. Helmi, Heart sound segmentation algorithm based on instantaneous energy of electrocardiogram, in: Computers in Cardiology, 2003, pp. 327–330.

[74] M. W. Groch, J. R. Domnanovich, W. D. Erwin, A new heart-sounds gating device for medical imaging, IEEE Transactions on Biomedical Engineering 39 (3) (1992) 307–310.

[75] R. J. Lehner, R. Rangayyan, A three-channel microcomputer system for segmentation and characterization of the phonocardiogram, IEEE Transactions on Biomedical Engineering (6) (1987) 485–489.

[76] A. Iwata, N. Ishii, N. Suzumura, K. Ikegaya, Algorithm for detecting the first and the second heart sounds by spectral tracking, Medical and Biological Engineering and Computing 18 (1) (1980) 19–26.

[77] S. Ari, G. Saha, On a robust algorithm for heart sound segmentation, Journal of Mechanics in Medicine and Biology 7 (2) (2007) 129–150.

[78] Z. Dokur, T. Ölmez, Feature determination for heart sounds based on divergence analysis, Digital Signal Processing 19 (3) (2009) 521–531.

[79] H. Liang, S. Lukkarinen, I. Hartimo, Heart sound segmentation algorithm based on heart sound envelogram, in: Computers in Cardiology, 1997, pp. 105–108.

[80] J. Vepa, P. Tolay, A. Jain, Segmentation of heart sounds using simplicity features and timing information, in: IEEE International Conference on Acoustics, Speech and Signal Processing, 2008, pp. 469–472.

[81] Z. Jiang, S. Choi, A cardiac sound characteristic waveform method for in-home heart disorder monitoring with electric stethoscope, Expert Systems with Applications 31 (2) (2006) 286–298.

[82] D. Kumar, P. Carvalho, M. Antunes, J. Henriques, L. Eugenio, R. Schmidt, J. Habetha, Detection of S1 and S2 heart sounds by high frequency signatures, in: Proceedings of 28th Annual International Conference of the IEEE Engineering in Medicine and Biology Society, 2006, pp. 1410–1416.

[83] S. Choi, Z. Jiang, Comparison of envelope extraction algorithms for cardiac sound signal segmentation, Expert Systems with Applications 34 (2) (2008) 1056–1069.

[84] Z. Dokur, T. Ölmez, Heart sound classification using wavelet transform and incremental self-organizing map, Digital Signal Processing 18(6) (6) (2008) 951–959.

[85] Y.-J. Chung, Classification of continuous heart sound signals using the ergodic hidden Markov model, in: Pattern Recognition and Image Analysis, 2007, pp. 563–570.

[86] S. Schmidt, C. Holst-Hansen, C. Graff, E. Toft, J. J. Struijk, Segmentation of heart sound recordings by a duration-dependent hidden Markov model, Physiological measurement 31 (4) (2010) 513–529.

[87] P. Wang, C. S. Lim, S. Chauhan, J. Y. A. Foo, V. Anantharaman, Phonocardiographic signal analysis method using a modified hidden Markov model, Annals of Biomedical Engineering 35 (3) (2007) 367–374.

[88] Z. Yan, Z. Jiang, A. Miyamoto, Y. Wei, The moment segmentation analysis of heart sound pattern, Computer Methods and Programs in Biomedicine 98 (2) (2010) 140–150.

[89] H. Tang, T. Li, T. Qiu, Y. Park, Segmentation of heart sounds based on dynamic clustering, Biomedical Signal Processing and Control 7 (5) (2012) 509–516.

[90] D. Gill, N. Gavrieli, N. Intrator, Detection and identification of heart sounds using homomorphic envelogram and self-organizing probabilistic model, in: Computers in Cardiology, 2005, pp. 957–960.

[91] S. Sanei, M. Ghodsi, H. Hassani, An adaptive singular spectrum analysis approach to murmur detection from heart sounds, Medical engineering & physics 33 (3) (2011) 362–367.

[92] S. Patidar, R. B. Pachori, A continuous wavelet transform based method for detecting heart valve disorders using phonocardiograph signals, in: Proceedings of Convergence and Hybrid Information Technology, Daejeon, Korea, 2012, pp. 513–520.

[93] J. Yuan, Z. He, Y. Zi, Gear fault detection using customized multiwavelet lifting schemes, Mechanical Systems and Signal Processing 24 (5) (2010) 1509–1528.

[94] M. Feldman, S. Braun, Description of free responses of SDOF systems via the phase plane and Hilbert transform: The concepts of envelope and instantaneous frequency,

in: Proceedings of SPIE, the International Society for Optical Engineering, Vol. 3089, Society of Photo-Optical Instrumentation Engineers, 1997, pp. 973–979.

[95] C. N. Gupta, R. Palaniappan, S. Swaminathan, S. M. Krishnan, Neural network classification of homomorphic segmented heart sounds, Applied Soft Computing 7 (1) (2007) 286–297.

[96] N. R. Pal, J. C. Bezdek, On cluster validity for the fuzzy c-means model, IEEE Transactions on Fuzzy Systems 3 (3) (1995) 370–379.

[97] H. Guldemır, A. Sengur, Comparison of clustering algorithms for analog modulation classification, Expert Systems with Applications 30 (4) (2006) 642–649.

[98] G. Amit, N. Gavriely, N. Intrator, Cluster analysis and classification of heart sounds, Biomedical Signal Processing and Control 4 (1) (2009) 26–36.

[99] S. Kofman, A. Bickel, A. Eitan, A. Weiss, N. Gavriely, N. Intrator, Discovery of multiple level heart-sound morphological variability resulting from changes in physiological states, Biomedical Signal Processing and Control 7 (4) (2012) 315–324.

[100] J. M. Wilson, Heart sound pod cast series, Retrieved April 6, 2014, from `www.texasheartinstitute.org` (2009).

[101] T. Gaziano, K. Reddy, F. Paccaud, S. Horton, V. Chaturvedi, Disease control priorities in developing countries (2nd ed.), World Bank, Washington (DC), 2006, Ch. Cardiovascular Disease, pp. 645–662.

[102] L. G. Gamero, R. Watrous, Detection of the first and second heart sound using probabilistic models, in: Proceedings of the 25th Annual International Conference of the IEEE Engineering in Medicine and Biology Society, Cancun,Mexico, 2003, pp. 2877–2880.

[103] H. Uğuz, A. Arslan, İ. Türkoğlu, A biomedical system based on hidden Markov model for diagnosis of the heart valve diseases, Pattern Recognition Letters 28 (4) (2007) 395–404.

[104] M. Rouhani, R. Abdoli, A comparison of different feature extraction methods for diagnosis of valvular heart diseases using PCG signals, Journal of Medical Engineering & Technology 36 (1) (2012) 42–49.

[105] C. Ahlstrom, P. Hult, P. Rask, J.-E. Karlsson, E. Nylander, U. Dahlström, P. Ask, Feature extraction for systolic heart murmur classification, Annals of Biomedical Engineering 34 (11) (2006) 1666–1677.

[106] S. Choi, Z. Jiang, Cardiac sound murmurs classification with autoregressive spectral analysis and multi-support vector machine technique, Computers in Biology and Medicine 40 (1) (2010) 8–20.

[107] Y. Chen, S. Wang, C.-H. Shen, F. K. Choy, Matrix decomposition based feature extraction for murmur classification, Medical Engineering & Physics 34 (6) (2012) 756–761.

[108] C.-H. Shen, F. K. Choy, Y. Chen, S. Wang, A modular approach to computer-aided auscultation: Analysis and parametric characterization of murmur acoustic qualities, Computers in Biology and Medicine 43 (6(1)) (2013) 798–805.

[109] T. R. Reed, N. E. Reed, P. Fritzson, Heart sound analysis for symptom detection and computer-aided diagnosis, Simulation Modelling Practice and Theory 12 (2) (2004) 129–146.

[110] T. Ölmez, Z. Dokur, Classification of heart sounds using an artificial neural network, Pattern Recognition Letters 24 (1) (2003) 617–629.

[111] S. Ari, G. Saha, In search of an optimization technique for artificial neural network to classify abnormal heart sounds, Applied Soft Computing 9 (1) (2009) 330–340.

[112] S. Babaei, A. Geranmayeh, Heart sound reproduction based on neural network classification of cardiac valve disorders using wavelet transforms of PCG signals, Computers in Biology and Medicine 39 (1) (2009) 8–15.

[113] I. Maglogiannis, E. Loukis, E. Zafiropoulos, A. Stasis, Support vectors machine-based identification of heart valve diseases using heart sounds, Computer Methods and Programs in Biomedicine 95 (1) (2009) 47–61.

[114] L. H. Cherif, S. Debbal, F. Bereksi-Reguig, Choice of the wavelet analyzing in the phonocardiogram signal analysis using the discrete and the packet wavelet transform, Expert Systems with Applications 37 (2) (2010) 913–918.

[115] S. Choi, Detection of valvular heart disorders using wavelet packet decomposition and support vector machine, Expert Systems with Applications 35 (4) (2008) 1679–1687.

[116] F. Safara, S. Doraisamy, A. Azman, A. Jantan, A. R. Abdullah Ramaiah, Multi-level basis selection of wavelet packet decomposition tree for heart sound classification, Computers in Biology and Medicine 43 (10) (2013) 1407–1414.

[117] F. Safara, S. Doraisamy, A. Azman, A. Jantan, S. Ranga, Wavelet packet entropy for heart murmurs classification, Advances in Bioinformatics Article ID 327269 (2012) 6 pages.

[118] S. Patidar, R. B. Pachori, Segmentation of cardiac sound signals by removing murmurs using constrained tunable-Q wavelet transform, Biomedical Signal Processing and Control 8 (6) (2013) 559–567.

[119] R. B. Pachori, P. Sircar, EEG signal analysis using FB expansion and second-order linear TVAR process, Signal Processing 88 (2) (2008) 415–420.

[120] K. Gopalan, T. R. Anderson, E. Cupples, A comparison of speaker identification results using features based on cepstrum and Fourier-Bessel expansion, Speech and Audio Processing, IEEE Transactions on 7 (3) (1999) 289–294.

[121] J. Schroeder, Signal processing via Fourier-Bessel series expansion, Digital Signal Processing 3 (2) (1993) 112–124.

[122] R. B. Pachori, Methods based on Fourier-Bessel representation for analysis of nonstationary signals, Ph.D. thesis, Department of Electrical Engineering, Indian Institute of Technology Kanpur, Kanpur, India (2007).

[123] E. Kreyszig, J. Wiley, Advanced Engineering Mathematics (9th ed.), John Wiley and Sons Inc., 1999.

[124] Tables of Bessel functions of fractional order, United States National Bureau of Standards Computation Laboratory, Columbia University Press, New York, 1948.

[125] R. B. Pachori, P. Sircar, A new technique to reduce cross terms in the Wigner distribution, Digital Signal Processing 17 (2) (2007) 466–474.

[126] R. B. Pachori, P. Sircar, Analysis of multicomponent AM-FM signals using FB-DESA method, Digital Signal Processing 20 (1) (2010) 42–62.

[127] V. T. Tran, F. AlThobiani, A. Ball, B.-K. Choi, An application to transient current signal based induction motor fault diagnosis of Fourier–Bessel expansion and simplified fuzzy ARTMAP, Expert Systems With Applications 40 (13) (2013) 5372–5384.

[128] E. Çomak, A. Arslan, A new training method for support vector machines: Clustering k-NN support vector machines, Expert Systems with Applications 35 (3) (2008) 564–568.

[129] J. A. K. Suykens, T. V. Gestel, J. D. Brabanter, B. D. Moor, J. Vandewalle, Least squares support vector machines, Vol. 4, World Scientific, 2002.

[130] L. Zhang, W. Zhou, L. Jiao, Wavelet support vector machine, IEEE Transactions on Systems, Man, and Cybernetics, Part B: Cybernetics 34 (1) (2004) 34–39.

[131] V. Bajaj, R. B. Pachori, Classification of seizure and nonseizure EEG signals using empirical mode decomposition, IEEE Transactions on Information Technology in Biomedicine 16 (6) (2012) 1135–1142.

[132] M. Zavar, S. Rahati, M.-R. Akbarzadeh-T, H. Ghasemifard, Evolutionary model selection in a wavelet-based support vector machine for automated seizure detection, Expert Systems with Applications 38 (9) (2011) 10751–10758.

[133] P. Bentley, G. Nordehn, M. Coimbra, S. Mannor, The PASCAL Classifying Heart Sounds Challenge 2011 (CHSC2011) Results, http://www.peterjbentley.com/heartchallenge/index.html.

[134] K. D. Brabanter, P. Karsmakers, F. Ojeda, C. Alzate, J. D. Brabanter, K. Pelckmans, B. D. Moor, J. Vandewalle, J. A. K. Suykens, LS-SVMlab Toolbox Users Guide (version 1.8), Retrieved from `http://www.esat.kuleuven.be/sista/lssvmlab/.` (August 2011).

[135] M. E. Tavel, Cardiac auscultation. A glorious past–but does it have a future?, Circulation 93 (6) (1996) 1250–1253.

[136] A. Haghighi-Mood, J. N. Torry, A sub-band energy tracking algorithm for heart sound segmentation, in: Computers in Cardiology, Vienna,Austria, 1995, pp. 501–504.

[137] S. Patidar, R. B. Pachori, Constrained tunable-Q wavelet transform based analysis of cardiac sound signals, AASRI Procedia 4 (2013) 57–63.

[138] H. Naseri, M. R. Homaeinezhad, Detection and boundary identification of phonocardiogram sounds using an expert frequency-energy based metric, Annals of Biomedical Engineering 41 (2) (2013) 279–292.

[139] S. Sun, Z. Jiang, H. Wang, Y. Fang, Automatic moment segmentation and peak detection analysis of heart sound pattern via short-time modified Hilbert transform, Computer Methods and Programs in Biomedicine 114 (3) (2014) 219–230.

[140] S. R. Bhatikar, C. DeGroff, R. L. Mahajan, A classifier based on the artificial neural network approach for cardiologic auscultation in pediatrics, Artificial Intelligence in Medicine 33 (3) (2005) 251–260.

[141] K. Higuchi, K. Sato, H. Makuuchi, A. Furuse, S. Takamoto, H. Takeda, Automated diagnosis of heart disease in patients with heart murmurs: application of a neural network technique, Journal of Medical Engineering & Technology 30 (2) (2006) 61–68.

[142] S. Choi, G. B. Jung, H.-K. Park, A novel cardiac spectral segmentation based on a multi-Gaussian fitting method for regurgitation murmur identification, Signal Processing 104 (2014) 339–345.

[143] A. A. Sepehri, J. Hancq, T. Dutoit, A. Gharehbaghi, A. Kocharian, A. Kiani, Computerized screening of children congenital heart diseases, Computer Methods and Programs in Biomedicine 92 (2) (2) (2008) 186–192.

[144] A. Gharehbaghi, T. Dutoit, P. Ask, L. Sörnmo, Detection of systolic ejection click using time growing neural network, Medical Engineering & Physics 36 (4) (2014) 477–483.

[145] I. Turkoglu, A. Arslan, E. Ilkay, An intelligent system for diagnosis of the heart valve diseases with wavelet packet neural networks, Computers in Biology and Medicine 33 (4) (2003) 319–331.

[146] S. Patidar, R. B. Pachori, N. Garg, Detection of septal defects from cardiac sound signals using tunable-Q wavelet transform, in: 19th Proceedings of IEEE International Conference on Digital Signal Processing, Kowloon, Hongkong, 2014, pp. 580–585.

[147] H. M. Hadi, M. Y. Mashor, M. Z. Suboh, M. S. Mohamed, Classification of heart sound based on S-Transform and neural network, in: 10th International Conference on Information Sciences Signal Processing and their Applications, Kuala Lumpur, 2010, pp. 189–192.

[148] Y. Wang, W. Li, J. Zhou, X. Li, Y. Pu, Identification of the normal and abnormal heart sounds using wavelet-time entropy features based on OMS-WPD, Future Generation Computer Systems 37 (2014) 488–495.

[149] A. Gavrovska, G. Zajić, I. Reljin, B. Reljin, Classification of prolapsed mitral valve versus healthy heart from phonocardiograms by multifractal analysis, Computational and Mathematical Methods in Medicine 2013, Article ID 376132, 10 pages.

[150] S. Ari, G. Saha, Classification of heart sounds using empirical mode decomposition based features, International Journal of Medical Engineering and Informatics 1 (1) (2008) 91–108.

[151] I. Cathers, Neural network assisted cardiac auscultation, Artificial Intelligence in Medicine 7 (1) (1995) 53–66.

[152] S. Patidar, R. B. Pachori, Classification of heart disorders based on tunable-Q wavelet transform of cardiac sound signals, in: A. T. Azar, S. Vaidyanathan (Eds.), Chaos Modeling and Control Systems Design, Springer International Publishing Switzerland, Switzerland, 2015.

[153] S. Patidar, R. B. Pachori, Classification of cardiac sound signals using constrained tunable-Q wavelet transform, Expert Systems with Applications 41(16) (2014) 7161–7170.

[154] T. Shimamura, H. Kobayashi, Weighted autocorrelation for pitch extraction of noisy speech, IEEE Transactions on Speech and Audio Processing 9 (7) (2001) 727–730.

[155] B. W. Matthews, Comparison of the predicted and observed secondary structure of T4 phage lysozyme, Biochimica et Biophysica Acta (BBA)-Protein Structure 405 (2) (1975) 442–451.

[156] A. T. Azar, S. A. El-Said, Performance analysis of support vector machines classifiers in breast cancer mammography recognition, Neural Computing and Applications 24(5) (5) (2014) 1163–1177.

[157] R. B. Pachori, S. Patidar, Epileptic seizure classification in EEG signals using second-order difference plot of intrinsic mode functions, Computer Methods and Programs in Biomedicine 113 (2) (2014) 494–502.

[158] R. Sharma, R. B. Pachori, Classification of epileptic seizures in EEG signals based on phase space representation of intrinsic mode functions, Expert Systems with Applications 42 (3) (2015) 1106–1117.

[159] T. Fawcett, An introduction to ROC analysis, Pattern Recognition Letters 27 (8) (2006) 861–874.

[160] T. Lane, Position paper: Extensions of ROC analysis to multi-class domains, in: Proceedings of ICML-2000 Workshop on Cost-Sensitive Learning, Stanford, 2000.

[161] A. Srinivasan, Note on the location of optimal classifiers in n-dimensional ROC space, in: Technical Report PRG-TR-2-99, Oxford University Computing Laboratory, Oxford, England, 1999.

[162] Stillman, ALDMD Clinical Cardiology Tools from Hennepin County Medical Center, Retrieved April 8, 2014, from `http://www.aldmd.com.` (2007).

[163] R. Lichtenberg, Heart sounds, Retrieved May 1, 2014, from `http://www.loyolauniversity.adam.com.` (n.d.).

[164] Retrieved March 16, 2014, from `http://www.med.umich.edu.` (n.d.).

[165] C. Cable, The aucultation assistant [Online], Retrieved April 3, 2014, from `www.med.ucla.edu/wilkes/intro.html` (1997).

[166] A. Alwan, et al., Global status report on noncommunicable diseases 2010, World Health Organization, 2011.

[167] National Heart, Lung and Blood Institute, What Is Coronary Heart Disease?, `http://www.nhlbi.nih.gov/health/health-topics/topics/cad/` (2014).

[168] U. R. Acharya, N. Kannathal, S. M. Krishnan, Comprehensive analysis of cardiac health using heart rate signals, Physiological measurement 25 (5) (2004) 1139–1151.

[169] F. Lombardi, Chaos theory, heart rate variability, and arrhythmic mortality, Circulation 101 (1) (2000) 8–10.

[170] Y. İşler, M. Kuntalp, Combining classical HRV indices with wavelet entropy measures improves to performance in diagnosing congestive heart failure, Computers in Biology and Medicine 37 (10) (2007) 1502–1510.

[171] A. Schumann, N. Wessel, A. Schirdewan, K. J. Osterziel, A. Voss, Potential of feature selection methods in heart rate variability analysis for the classification of different cardiovascular diseases, Statistics in Medicine 21 (15) (2002) 2225–2242.

[172] A. R. Gujjar, T. N. Sathyaprabha, D. Nagaraja, K. Thennarasu, N. Pradhan, Heart rate variability and outcome in acute severe stroke, Neurocritical Care 1 (3) (2004) 347–353.

[173] R. M. Carney, K. E. Freedland, P. K. Stein, J. A. Skala, P. Hoffman, A. S. Jaffe, Change in heart rate and heart rate variability during treatment for depression in patients with coronary heart disease, Psychosomatic Medicine 62 (5) (2000) 639–647.

[174] M. Malik, J. T. Bigger, A. J. Camm, R. E. Kleiger, A. Malliani, A. J. Moss, P. J. Schwartz, Heart rate variability standards of measurement, physiological interpretation, and clinical use, European Heart Journal 17 (3) (1996) 354–381.

[175] U. R. Acharya, O. Faust, V. Sree, G. Swapna, R. J. Martis, N. A. Kadri, J. S. Suri, Linear and nonlinear analysis of normal and CAD-affected heart rate signals, Computer Methods and Programs in Biomedicine 113 (1) (2014) 55–68.

[176] J. Hayano, Y. Sakakibara, M. Yamada, N. Ohte, T. Fujinami, K. Yokoyama, Y. Watanabe, K. Takata, Decreased magnitude of heart rate spectral components in coronary artery disease. Its relation to angiographic severity, Circulation 81 (4) (1990) 1217–1224.

[177] S. Nikolopoulos, A. Alexandridi, S. Nikolakeas, G. Manis, Experimental analysis of heart rate variability of long-recording electrocardiograms in normal subjects and patients with coronary artery disease and normal left ventricular function, Journal of Biomedical Informatics 36 (3) (2003) 202–217.

[178] K. L. Lavoie, R. P. Fleet, C. Laurin, A. Arsenault, S. B. Miller, S. L. Bacon, Heart rate variability in coronary artery disease patients with and without panic disorder, Psychiatry research 128 (3) (2004) 289–299.

[179] J. T. Bigger, J. L. Fleiss, R. C. Steinman, L. M. Rolnitzky, W. J. Schneider, P. K. Stein, RR variability in healthy, middle-aged persons compared with patients with chronic coronary heart disease or recent acute myocardial infarction, Circulation 91 (7) (1995) 1936–1943.

[180] U. R. Acharya, K. P. Joseph, N. Kannathal, C. M. Lim, J. S. Suri, Heart rate variability: a review, Medical and Biological Engineering and Computing 44 (12) (2006) 1031–1051.

[181] M. Karimi, R. Amirfattahi, S. Sadri, S. A. Marvasti, Noninvasive detection and classification of coronary artery occlusions using wavelet analysis of heart sounds with neural networks, in: Proceedings of the 3rd IEE International Seminar on Medical Applications of Signal Processing, (Ref. No. 2005-1119 2005), IET, 2005, pp. 117–120.

[182] U. Rajendra Acharya, P. Subbanna Bhat, S. S. Iyengar, A. Rao, S. Dua, Classification of heart rate data using artificial neural network and fuzzy equivalence relation, Pattern Recognition 36 (1) (2003) 61–68.

[183] A. L. Goldberger, B. J. West, Applications of nonlinear dynamics to clinical cardiologya, Annals of the New York Academy of Sciences 504 (1) (1987) 195–213.

[184] A. Garde, L. Sörnmo, R. Jané, B. F. Giraldo, Correntropy-based spectral characterization of respiratory patterns in patients with chronic heart failure, IEEE Transactions on Biomedical Engineering 57 (8) (2010) 1964–1972.

[185] U. R. Acharya, N. Kannathal, O. W. Sing, L. Y. Ping, T. Chua, Heart rate analysis in normal subjects of various age groups, Biomedical Engineering Online 3 (1) (2004) 24.

[186] P. Persson, C. Wagner, General principles of chaotic dynamics, Cardiovascular Research 31 (3) (1996) 332–341.

[187] U. R. Acharya, P. S. Bhat, N. Kannathal, A. Rao, C. M. Lim, Analysis of cardiac health using fractal dimension and wavelet transformation, Innovation and Technology in Biology and Medicine 26 (2) (2005) 133–139.

[188] K. Antanavičius, A. Bastys, J. Blužas, L. Gargasas, S. Kaminskienė, G. Urbonavičienė, A. Vainoras, Nonlinear dynamics analysis of electrocardiograms for detection of coronary artery disease, Computer Methods and Programs in Biomedicine 92 (2) (2008) 198–204.

[189] G. Manis, S. Nikolopoulos, A. Alexandridi, C. Davos, Assessment of the classification capability of prediction and approximation methods for HRV analysis, Computers in Biology and Medicine 37 (5) (2007) 642–654.

[190] T. T. Laitio, H. V. Huikuri, T. H. Mäkikallio, J. Jalonen, E. S. Kentala, H. Helenius, O. Pullisaar, J. Hartiala, H. Scheinin, The breakdown of fractal heart rate dynamics

predicts prolonged postoperative myocardial ischemia, Anesthesia & Analgesia 98 (5) (2004) 1239–1244.

[191] K. Qtsuka, G. Cornélissen, F. Halberg, Circadian rhythmic fractal scaling of heart rate variability in health and coronary artery disease, Clinical Cardiology 20 (7) (1997) 631–638.

[192] M. Kobayashi, T. Musha, 1/f fluctuation of heartbeat period, IEEE Transaction on Biomedical Engineering 29(6) (1982) 456–457.

[193] C.-K. Peng, S. Havlin, J. M. Hausdorff, J. E. Mietus, H. E. Stanley, A. L. Goldberger, Fractal mechanisms and heart rate dynamics: long-range correlations and their breakdown with disease, Journal of Electrocardiology 28 (Supplement 1) (1995) 59–65.

[194] K. Karamanos, S. Nikolopoulos, K. Hizanidis, G. Manis, A. Alexandridi, S. Nikolakeas, Block entropy analysis of heart rate variability signals, International Journal of Bifurcation and Chaos 16 (07) (2006) 2093–2101.

[195] M. A. Woo, W. G. Stevenson, D. K. Moser, R. B. Trelease, R. M. Harper, Patterns of beat-to-beat heart rate variability in advanced heart failure, American Heart Journal 123 (3) (1992) 704–710.

[196] P. W. Kamen, H. Krum, A. M. Tonkin, Poincare plot of heart rate variability allows quantitative display of parasympathetic nervous activity in humans, Clinical Science 91 (2) (1996) 201–208.

[197] M. P. Tulppo, T. H. Makikallio, T. E. Takala, T. Seppanen, H. Huikuri, Quantitative beat-to-beat analysis of heart rate dynamics during exercise, American Journal of Physiology-Heart and Circulatory Physiology 271 (1) (1996) H244–H252.

[198] C. L. Webber Jr, J. P. Zbilut, Dynamical assessment of physiological systems and states using recurrence plot strategies, Journal of Applied Physiology 76 (2) (1994) 965–973.

[199] N. Marwan, N. Wessel, U. Meyerfeldt, A. Schirdewan, J. Kurths, Recurrence-plot-based measures of complexity and their application to heart-rate-variability data, Physical Review E 66 (2) (2002) 026702.

[200] J. P. Zbilut, C. L. Webber Jr, Embeddings and delays as derived from quantification of recurrence plots, Physics letters A 171 (3) (1992) 199–203.

[201] J. P. Zbilut, N. Thomasson, C. L. Webber, Recurrence quantification analysis as a tool for nonlinear exploration of nonstationary cardiac signals, Medical engineering & physics 24 (1) (2002) 53–60.

[202] K. C. Chua, V. Chandran, U. R. Acharya, C. M. Lim, Cardiac state diagnosis using higher order spectra of heart rate variability, Journal of Medical Engineering & Technology 32 (2) (2008) 145–155.

[203] I. Santamaría, P. P. Pokharel, J. C. Principe, Generalized correlation function: definition, properties, and application to blind equalization, IEEE Transactions on Signal Processing 54 (6) (2006) 2187–2197.

[204] ECG Electrocardiogram Amplifier, Retrieved from `www.biopac.com` (2013).

[205] J. Pan, W. J. Tompkins, A real-time QRS detection algorithm, IEEE Transactions on Biomedical Engineering 32 (3) (1985) 230–236.

[206] R. Warlar, C. Eswaran, Integer coefficient bandpass filter for the simultaneous removal of baseline wander, 50 and 100 Hz interference from the ECG, Medical and Biological Engineering and Computing 29 (3) (1991) 333–336.

[207] J.-W. Xu, J. C. Principe, A pitch detector based on a generalized correlation function, IEEE Transactions on Audio, Speech, and Language Processing 16 (8) (2008) 1420–1432.

[208] W. Liu, P. P. Pokharel, J. C. Principe, Correntropy: properties and applications in non-Gaussian signal processing, IEEE Transactions on Signal Processing 55 (11) (2007) 5286–5298.

[209] M. Rao, S. Seth, J. Xu, Y. Chen, H. Tagare, J. C. Príncipe, A test of independence based on a generalized correlation function, Signal Processing 91 (1) (2011) 15–27.

[210] S. Seth, J. C. Principe, On speeding up computation in information theoretic learning, in: IEEE International Joint Conference on Neural Networks, 2009, pp. 2883–2887.

[211] S. Seth, Codes:ITL toolbox, Retrieved April 6, 2014, from `www.sohanseth.com/Home/codes` (2012).

[212] R. O. Duda, P. E. Hart, D. G. Stork, Pattern classification, John Wiley & Sons, 2001.

[213] L. I. Smith, A tutorial on principal components analysis, Cornell University, USA 51 (2002) 52.

[214] U. R. Acharya, S. V. Sree, M. Muthu Rama Krishnan, N. Krishnananda, S. Ranjan, P. Umesh, J. S. Suri, Automated classification of patients with coronaryartery disease using grayscale features from leftventricle echocardiographic images, Computer Methods and Programs in Biomedicine 112 (3) (2013) 624–632.

[215] U. Acharya, O. Faust, V. Sree, F. Molinari, R. Garberoglio, J. Suri, Cost-effective and non-invasive automated benign and malignant thyroid lesion classification in 3D contrast-enhanced ultrasound using combination of wavelets and textures: a class of ThyroScane algorithms, Technology in Cancer Research & Treatment 10 (4) (2011) 371–380.

[216] U. R. Acharya, E. Ng, J. Tan, V. Sree, N. KH, An integrated index for the identification of diabetes retinopathy stages, Journal of Medical Systems 36 (3) (2012) 2011–2020.

[217] D. N. Ghista, Nondimensional physiological indices for medical assessment, Journal of Mechanics in Medicine and Biology 9 (4) (2009) 643–669.

[218] D. N. Ghista, Applied biomedical engineering mechanics, CRC Press, Wayland, Massachusetts, USA, 2009.

[219] D. N. Ghista, Physiological systems numbers in medical diagnosis and hospital cost effective operation, Journal of Mechanics in Medicine and Biology 4 (4) (2004) 401–418.

[220] I. Selesnick, TQWT Toolbox Guide, Retrieved February 3, 2014, from `http://eeweb.poly.edu/iselesni/TQWT/` (October 6 2011).

[221] S. Arafat, M. Dohrmann, M. Skubic, Classification of coronary artery disease stress ECGs using uncertainty modeling, in: Proceedings of Congress on Computational Intelligence Methods and Applications, 2005, p. 4.

[222] W.-S. Kim, S.-H. Jin, Y. Park, H.-M. Choi, A study on development of multiparametric measure of heart rate variability diagnosing cardiovascular disease, in: R. Magjarevic, J. Nagel (Eds.), World Congress on Medical Physics and Biomedical Engineering 2006, Vol. 14 of IFMBE Proceedings, Springer Berlin Heidelberg, 2007, pp. 3480–3483.

[223] H. Lee, K. Noh, K. Ryu, Mining Biosignal Data: Coronary Artery Disease Diagnosis Using Linear and Nonlinear Features of HRV, in: T. Washio, Z.-H. Zhou, J. Huang, X. Hu, J. Li, C. Xie, J. He, D. Zou, K.-C. Li, M. Freire (Eds.), Emerging Technologies in Knowledge Discovery and Data Mining, Vol. 4819 of Lecture Notes in Computer Science, Springer Berlin Heidelberg, 2007, pp. 218–228.

[224] H. G. Lee, K. Y. Noh, K. H. Ryu, A data mining approach for coronary heart disease prediction using HRV features and carotid arterial wall thickness, in: Proceedings of International Conference on Biomedical Engineering and Informatics, Vol. 1, 2008, pp. 200–206.

[225] Z. Zhao, C. Ma, An intelligent system for noninvasive diagnosis of coronary artery disease with EMD-TEO and BP neural network, in: International Workshop on Educa-

tion Technology and Training and International Workshop on Geoscience and Remote Sensing, Vol. 2, IEEE, 2008, pp. 631–635.

[226] İ. Babaoglu, O. Findik, E. Ülker, A comparison of feature selection models utilizing binary particle swarm optimization and genetic algorithm in determining coronary artery disease using support vector machine, Expert Systems with Applications 37 (4) (2010) 3177–3183.

[227] I. Babaoğlu, O. Fındık, M. Bayrak, Effects of principle component analysis on assessment of coronary artery diseases using support vector machine, Expert Systems with Applications 37 (3) (2010) 2182–2185.

[228] S. Dua, X. Du, S. V. Sree, T. A. Vi, Novel classification of coronary artery disease using heart rate variability analysis, Journal of Mechanics in Medicine and Biology 12 (04) (2012) 1240017–1–19.

[229] J. Martínez-Alajarín, R. Ruiz-Merino, Wavelet and wavelet packet compression of phonocardiograms, Electronics Letters 40 (17) (2004) 1040–1041.

[230] J. Martínez-Alajarín, J. López-Candel, R. Ruiz-Merino, ASEPTIC: Aided system for event-based phonocardiographic telediagnosis with integrated compression, in: Computers in Cardiology, 2006, pp. 537–540.

[231] W.-C. Kao, W.-H. Chen, C.-K. Yu, C.-M. Hong, S.-Y. Lin, Portable real-time home-care system design with digital camera platform, IEEE Transactions on Consumer Electronics 51 (4) (2005) 1035–1041.

[232] J. M. Shapiro, Embedded image coding using zerotrees of wavelet coefficients, IEEE Transactions on Signal Processing 41 (12) (1993) 3445–3462.

[233] G. Tohumoglu, K. E. Sezgin, ECG signal compression by multi-iteration EZW coding for different wavelets and thresholds, Computers in Biology and Medicine 37 (2) (2007) 173–182.

[234] Z. Lu, D. Y. Kim, W. A. Pearlman, Wavelet compression of ECG signals by the set partitioning in hierarchical trees algorithm, IEEE Transactions on Biomedical Engineering 47 (7) (2000) 849–856.

[235] S. M. Ahmed, A. Al-Shrouf, M. Abo-Zahhad, ECG data compression using optimal non-orthogonal wavelet transform, Medical engineering & physics 22 (1) (2000) 39–46.

[236] B. Bradie, Wavelet packet-based compression of single lead ECG, IEEE Transactions on Biomedical Engineering 43 (5) (1996) 493–501.

[237] M. L. Hilton, Wavelet and wavelet packet compression of electrocardiograms, IEEE Transactions on Biomedical Engineering 44 (5) (1997) 394–402.

[238] B. A. Rajoub, An efficient coding algorithm for the compression of ECG signals using the wavelet transform, IEEE Transactions on Biomedical Engineering 49 (4) (2002) 355–362.

[239] M. S. Manikandan, S. Dandapat, Wavelet energy ased compression of phonocardiogram (PCG) signal for telecardiology, in: Proceedings of IET-UK International Conference on Information and Communication Technology in Electrical Sciences, 2007, pp. 650–654.

[240] F. Toledo-Moreo, A. Legaz-Cano, J. Martinez-Alvarez, J. Martinez-Alajarin, R. Ruiz-Merino, Compression system for the phonocardiographic signal, in: Proceedings of International Conference on Field Programmable Logic and Applications, 2007, pp. 770–773.

[241] J. Martínez-Alajarín, J. Garrigós-Guerrero, R. Ruiz-Merino, Optimization of the compression parameters of a phonocardiographic telediagnosis system using genetic algorithms, in: Bio-inspired Modeling of Cognitive Tasks, 2007, pp. 508–517.

[242] J. Martinez-Alajarin, J. Martinez-Rosso, R. Ruiz-Merino, Encoding technique for binary sequences using vector tree partitioning applied to compression of phonocardiographic signals, Electronics Letters 44 (2) (2008) 84–86.

[243] M. S. Manikandan, K. Soman, S. Dandapat, Quality-driven wavelet based pcg signal coding for wireless cardiac patient monitoring, in: Proceedings of the 1st International Conference on Wireless Technologies for Humanitarian Relief, 2011, pp. 519–526.

[244] M. Blanco-Velasco, F. Cruz-Roldán, J. I. Godino-Llorente, J. Blanco-Velasco, C. Armiens-Aparicio, F. López-Ferreras, On the use of PRD and CR parameters for ECG compression, Medical engineering & physics 27 (9) (2005) 798–802.

[245] M. Blanco-Velasco, F. Cruz-Roldan, J. Godino-Llorente, K. Barner, ECG compression with retrieved quality guaranteed, Electronics Letters 40 (23) (2004) 1466–1467.

[246] D. A. Coley, An introduction to genetic algorithms for scientists and engineers, Vol. 31, World scientific Singapore, 1999.

List of Publications

International Journals

1. S. Patidar, R.B. Pachori, and N. Garg, "Diagnosis of septal defects using tunable-Q wavelet transform of cardiac sound signals," *Expert Systems with Applications*, vol. 42(7), pp. 3315-3326, May 2015.

2. S. Patidar, R.B. Pachori, and U. R. Acharya, "Automated diagnosis of coronary artery disease using tunable-Q wavelet transform applied on heart rate signals," *Knowledge Based Systems*, vol. 82, pp. 1-10, July 2015.

3. R.B. Pachori and S. Patidar, "Epileptic seizure classification in EEG signals using second-order difference plot of intrinsic mode functions," *Computer Methods and Programs in Biomedicine*, vol. 113, no. 2, pp. 494-502, February 2014.

4. S. Patidar and R.B. Pachori, "Classification of cardiac sound signals using constrained tunable-Q wavelet transform," *Expert Systems with Applications*, vol. 41 (16), 7161-7170, November 2014

5. S. Patidar and R.B. Pachori, "Segmentation of cardiac sound signals by removing murmurs using constrained tunable-Q wavelet transform," *Biomedical Signal Processing and Control*, vol.8, no. 6, pp. 559-567, November 2013.

6. S. Patidar and R.B. Pachori, "Constrained tunable-Q wavelet transform based analysis of cardiac sound signals," *AASRI Procedia*, vol. 4, pp. 57-63, June 2012.

7. S. Patidar and R.B. Pachori, "Tunable-Q wavelet transform based optimal compression of cardiac sound signals," *IRBM*, Under review.

International Conferences

1. S. Patidar, R.B. Pachori, and N. Garg, "Detection of septal defects from cardiac sound signals using tunable-Q wavelet transform, "In *Proceedings of* 19^{th} *IEEE International Conference on Digital Signal Processing*, 20-23 August, 2014, Hong Kong.

2. S. Patidar and R.B. Pachori, "A continuous wavelet transform based method for detecting heart valve disorders using phonocardiograph signals, "In *Proceedings of International Conference on Hybrid Information Technology*, 23-25 August, 2012, Daejeon, Korea.

Book Chapters

1. R. B. Pachori, R. Sharma, and S. Patidar, "Classification of normal and epileptic seizure EEG signals based on empirical mode decomposition, " *Complex System Modeling and Control through Intelligent Soft Computations*, Springer International Publishing Switzerland, Chapter 13, ISBN: 978-3-319-12882-5.

2. S. Patidar and R. B. Pachori, "Classification of heart disorders based on tunable-Q wavelet transform of cardiac sound signals, " *Chaos Modeling and Control Systems Design*, Springer International Publishing Switzerland, Chapter 10, ISBN: 978-3-319-11016-5.